AD_____

Award Number: W81XWH-10-1-0194

TITLE: MicroRNA regulation of $CD44^+$ prostate tumor stem/progenitor cells and prostate cancer development/metastasis

PRINCIPAL INVESTIGATOR: Can Liu, B.S.

CONTRACTING ORGANIZATION: The University of Texas MD Anderson Cancer Center
Smithville, TX 78957

REPORT DATE: May 2013

TYPE OF REPORT: Annual Summary

PREPARED FOR: U.S. Army Medical Research and Materiel Command
Fort Detrick, Maryland 21702-5012

REPORT DOCUMENTATION PAGE

Form Approved
OMB No. 0704-0188

1. REPORT DATE	2. REPORT TYPE	3. DATES COVERED
May 2013	Annual Summary	1 April 2010 - 31 March 2013

4. TITLE AND SUBTITLE

MicroRNA regulation of CD44$^+$ prostate tumor stem/progenitor cells and prostate cancer development/metastasis

5a. CONTRACT NUMBER

5b. GRANT NUMBER
W81XWH-10-1-0194

5c. PROGRAM ELEMENT NUMBER

6. AUTHOR(S)
Can Liu

E-Mail: canliu@mdanderson.org

5d. PROJECT NUMBER

5e. TASK NUMBER

5f. WORK UNIT NUMBER

7. PERFORMING ORGANIZATION NAME(S) AND ADDRESS(ES)

The University of Texas MD Anderson Cancer Center
Smithville, TX 78957

8. PERFORMING ORGANIZATION REPORT NUMBER

9. SPONSORING / MONITORING AGENCY NAME(S) AND ADDRESS(ES)
U.S. Army Medical Research and Materiel Command
Fort Detrick, Maryland 21702-5012

10. SPONSOR/MONITOR'S ACRONYM(S)

11. SPONSOR/MONITOR'S REPORT NUMBER(S)

12. DISTRIBUTION / AVAILABILITY STATEMENT
Approved for Public Release; Distribution Unlimited

13. SUPPLEMENTARY NOTES

14. ABSTRACT

During the last year of the grant period, we carried out in vitro and in vivo work to further understand the role of miR-141 in regulating PCa stem/progenitor cells and PCa development. We validated the under-expression of miR-141 in the purified CD44+ populations from 21 primary patient PCa samples. We also confirmed that miR-141 is a negative regulator of EMT and suppresses migration and invasion of PCa cells. We observed that miR-141 promotes tumorigenicity of bulk PCa cells, but suppresses the stem cell properties of CD44$^+$ PCa cells. By studying the role of several different miRNA in PCa cells, we have proved our original hypothesis, which is miRNA play important role in regulating prostate cancer stem cells and PCa development and different miRNAs regulate different aspects of tumor development and distinct CSC properties, and together, they coordinately control the tumor progression.

15. SUBJECT TERMS
microRNA, prostate cancer stem cells, miR-141, miR-34a, let-7, miR-301

16. SECURITY CLASSIFICATION OF:			17. LIMITATION OF ABSTRACT	18. NUMBER OF PAGES	19a. NAME OF RESPONSIBLE PERSON
a. REPORT	b. ABSTRACT	c. THIS PAGE			USAMRMC
U	U	U	UU	102	19b. TELEPHONE NUMBER *(include area code)*

Table of Contents

Department of Defense PCRP Predoctoral Award (W81XWH-10-1-0194)

'MicroRNA regulation of CD44$^+$ prostate tumor stem/progenitor cells and prostate cancer development/metastasis'

PI: Can Liu

FINAL REPORT (April 1, 2010 to March 31, 2013)

INTRODUCTION

Most human tumors contain a subset of cancer cells with certain stem cell properties, called cancer stem cells (CSC), that are thought to be responsible for tumor maintenance, progression, therapeutic resistance, relapse and metastasis (1, 2). Previous work from our lab has identified several populations of human prostate cancer (PCa) stem/progenitor cells including the side population (SP), the CD44$^+$ and CD44$^+\alpha2\beta1^+$ PCa cells, which possess high tumorigenic and metastatic ability (3-8). Despite their potential clinical importance, how CSCs are regulated at the molecular level is not well understood. MicroRNAs (miRNAs), small non-coding RNAs that play critical roles in modulating normal stem cell functions during development, have emerged as important regulators of many cancers and CSCs as well (9, 10). Based on our preliminary miRNA profiling data, in which we identified several miRNAs including miR-34a, let-7b, miR-301 and miR-141 differentially expressed in several prostate CSC populations, i.e., the LAPC9, LAPC4, Du145 CD44$^+$ cells, Du145 $\alpha2\beta1^+$ and LAPC4 CD133$^+$ cells, we proposed that **miRNAs such as miR-34a play an important role in regulating prostate tumor stem/progenitor cells as well as PCa development and metastasis**. To test this hypothesis, we proposed three Specific Aims:

1) *To further study the role of miR-34a in regulating PCa stem/progenitor cells and tumor development;*
2) *To test the hypothesis that CD44 and Nanog represent two critical downstream targets of miR-34a in PCa stem/progenitor cells;*
3) *To investigate the role of miR-141 and miR-301 in regulating PCa stem/progenitor cell properties and tumor development/metastasis.*

During the first year of grant period (April 1, 2010 to March 31, 2011), we focused on Aim 1 and part of Aim 2 and generated convincing evidence showing that miR-34a was a critical negative regulator of PCa stem/progenitor cells and prostate tumor development. We also demonstrated that CD44 was a direct and functional downstream target of miR-34a in PCa stem/progenitor cells that mediated the suppression of PCa metastasis (11).

In the second year (April 1, 2011 to March 31, 2012), we further characterized our original miRNA expression profiling results in PCa stem/progenitor cells and identified distinct and common miRNA expression patterns in different PCa stem/progenitor subpopulations. We also investigated the role of two other commonly differentially expressed miRNAs, i.e., let-7b and miR-301 in regulating PCa development (12).

In the last year of the grand period (April 1, 2012 to March 31, 2013), we mainly focused on Aim 3 and have shown that miR-141 plays an important role in regulating PCa development and metastasis. We confirmed miR-141 under-expression in the $CD44^+$ cells of 21 primary PCa samples, and over-expression of miR-141 suppressed migration/invasion abilities of PCa cells. Unlike miR-34a and let-7b, miR-141, unexpectedly, promoted proliferation and tumor development in bulk PCa cells, but suppresses stem cell related properties and tumor growth in the purified $CD44^+$ PCa cells.

BODY

Material and Methods

Most basic methodologies have been described in our earlier publications (11,12).

Quantification of mature miRNA by qRT-PCR: Total RNA was purified using mirVana Paris miRNA isolation kit (Ambion). The miRNA levels were quantified using Taqman miRNA assay (Applied Biosystems).

miRNA mimics/anti-sense oligo transfection: Du145 cells were transfected with 30 nM of miR-141 miRNA mimics or non-targeting negative control (NC) oligos (Life Technologies) using Lipofectamine RNAiMax (Life Technologies) according to the manufacturer's instructions. After culturing for overnight to 48 h, transfected cells were harvested for further studies.

Migration and invasion assays: Cell invasion assays were performed using Matrigel Invasion Chamber (8 μm pore size, BD). Du145 cells were transfected with NC and miR-141 oligos. Cells (5×10^4) were seeded in the upper chamber of the insert. Medium with 20% FBS in the lower chamber served as chemo-attractant. After 22 h, non-invading cells were removed by a cotton swab and invaded cells were stained with HEMA3 stain (Fisher) and counted under a microscope.

Clonal and sphere formation assays: For holoclones assays, transfected Du145 cells were plated at a clonal density (i.e., 100 cells/well in a 6-well dish). The number of holoclones was counted after 2 weeks. For sphere formation assays, cells were suspended in serum free epithelial basal medium (PrEBM) supplemented with 4 μg/ml insulin, B27 (Invitrogen), 20 ng/ml EGF and 20 ng/ml bFGF. Single-cell suspension was plated (1,000 cells/well) in Ultra-Low Attachment (ULA) plates and floating spheres that arose in 1-2 weeks counted. For all these experiments, a minimum of triplicate wells was performed for each condition.

Results and Discussion

1. Background & Summary

The whole project was originated from our microRNA expression profiling in PCa stem/progenitor cell populations. We identified four miRNAs that were commonly under-expressed in the stem/progenitor cell populations, which were miR-34a, let-7b, miR-106a and miR-141, and two commonly over-expressed miRNAs, i.e., miR-452 and miR-301.

In the first 2 years (April 2010 to March 2012), we focused on experiments proposed in Specific Aims 1 and 2 and published two papers on the subject. In the first paper (11), we provided ample evidence that miR-34a represented a critically important tumor-suppressive miRNA that functioned to restrict the prostate CSC activity, which, in turn, inhibited the tumorigenic potential of prostate CSCs. By directly targeting CD44, miR-34a, when exogenously administered to PCa-bearing animals, significantly inhibited PCa metastasis and extended the survival of the tumor-bearing animals. This paper covers all experiments initially proposed in Aim 1 and the first part of Aim 2 (i.e., CD44 being the target of miR-34a). Regarding the second part of Aim 2, i.e., Nanog also as a potential, biologically relevant target of miR-34a, in regulating prostate CSC activity, despite our conscientious efforts and multiple lines of experiments, we could not obtain concrete evidence that the endogenous Nanog gene in prostate cancer cells represents an authentic downstream target of miR-34a. Hence, we have stopped exploring this line of research.

In the second paper (12), we investigated the roles of let-7 and miR-301 in regulating tumorigenic PCa cells and we showed that let-7 possessed very similar tumor-inhibitory effects to miR-34a although with different mechanisms of action. On the other hand, miR-301 displayed cell type-specific effects in different PCa models. This paper satisfies the second part of Aim 3.

In the last year of the grant period (April 2012 to March 2013), I have been focusing on experiments on miR-141 (i.e., the first part of Specific Aim 3). I have obtained some preliminary results on the interesting behavior of this miRNA, which will be presented below.

2. Under-expression of miR-141 in PCa stem/progenitor cells

In our miRNA library screening experiments, we first purified a total of 5 populations of PCa stem/progenitor cells from 3 xenografts (i.e., LAPC9, LAPC4, and Du145), including $CD44^+$ PCa cells from all 3 xenografts, $\alpha2\beta1^+$ cells from Du145, and $CD133^+$ cells from LAPC4. Comparisons of the miRNA expression in these stem/progenitor cell populations (with their corresponding marker-negative cells) reveal that 4 miRNAs, i.e., let-7b, miR-34a, miR-106a, and miR-141, are consistently under-expressed, and only two miRNAs, i.e., miR-301 and miR-452, are over-expressed, in all 5 PCa stem/progenitor cell populations (Fig. 1A).

To confirm the under-expression of miR-141 in clinical samples, we obtained 21 prostatectomy tumors (IRB-LAB-04-0498). Epithelial cancer cells were purified, and CD44 positive and negative cells were further purified by MACS (magnetic affinity-based cell sorting) or FACS. We subsequently measured the expression of miR-141 and the other five commonly differentially expressed miRNAs in these $CD44^+$ and $CD44^-$ HPCa cells. Indeed, miR-141 is significantly under-expressed in 20 of the 21 HPCa-purified $CD44^+$ cells (Fig. 1B).

3. Over-expression of miR-141 suppresses migration and invasion in PCa cells.

There is strong evidence that miR-141/miR-200 miRNAs regulate cell migration and invasion and cancer metastasis via the suppression on EMT (Epithelia-Mesenchymal Transition) (13-16). Among the reported miR-141 targets are TGFβ2, ZEB1 (zinc-finger E-box binding homeobox1), SIP1 (Smad Interacting Protein 1; also called ZEB2), Dlx5 (distal-less homeobox 5), MKK4 (mitogen-activated protein kinase kinase 4), PTEN and UBAP1 (ubiquitin-associated protein 1),

most of which are well known EMT mediators. To understand whether the under-expression of miR-141 in CSC populations observed in both prostate xenograft models and primary PCa patient samples possesses any biological consequence, we first explored the miR-141 functions in regulating EMT by performing the migration and Boyden Chamber invasion assays. Du145 cells were transfected with miR-141 mimicking oligonucleotides (oligos) or non-targeting negative control (NC) oligos and plated for Matrigel invasion assay (BD). I observed that over-expression of miR-141 inhibited Du145 cell migration and invasion (Fig. 2).

4. miR-141 affects PCa cells proliferation, clonal and sphere formation abilities.

We then tried to determine whether miR-141 would affect the stem cell related properties of PCa cells by performing clonal and sphere-formation assay. miR-34, let-7 and miR-200 are well established tumor suppressive miRNA families, and indeed, my own work has confirmed the PCa- inhibitory effects of both miR-34a and let-7a/b (11, 12; also see previous Progress Reports). Might miR-141 also possess PCa-suppressive functions? To answer this question, we first transfected miR-141 oligos into Du145 cells, and performed proliferation, clonal and sphere formation assays. To our surprise, I observed that enforced expression of miR-141 into Du145 cells promoted cell proliferation (Fig. 3A). Du145 cells also forms more holoclones when transfected with miR-141 in clonal assay that represents the proliferative ability of the cells (Fig. 3B). On the other hand, over-expression of miR-141 seems to suppress the sphere formation of Du145 (Fig. 3C), which implies that miR-141 might negatively regulate the CSC properties, as observed in breast CSCs (17).

In contrast, when we performed similar clonal and sphere-formation experiments in other PCa cell lines including PC3, and PPC-1, we observed that over-expression of miR-141 inhibited clonal expansion in PC3 and PPC-1 (Fig. 3D), and promoted sphere formation in PC3 cells, but not in PPC-1 cells (Fig. 3E and data not shown). We suspect that since PTEN is one of the miR-141 targets, in Du145 cells with wild type PTEN, PTEN might be the primary downstream target that mediates promotion of proliferation and related properties. By contrast, in PC3 and PPC-1 cells with null PTEN, miR-141's effects on proliferation might be attenuated by the impact of miR-141 on other downstream targets; consequently, the effect of miR-141 on PCa cells seems to be cell type dependent.

5. Enforced expression of miR-141 promoted tumor regeneration of PCa cells.

To determine the effect of miR-141 on tumor formation ability of PCa cells, we then performed tumor development experiments using bulk Du145, PC3 and LAPC9 cells. We first manipulated miR-141 levels by transfecting miR-141 oligos and then implanted the Du145 cells subcutaneously in NOD/SCID mice. We were expecting to observe similar tumor-inhibitory effects to those of miR-34a and let-7 (since all of them are reported as tumor suppressive miRNAs). However, enforced expression of miR-141 showed a trend in promoting tumor development in the bulk Du145 cells (Fig. 4A, B), although the difference is not statistically significant. Similar results were observed in PC3 (Fig. 4C, D) and LAPC9 (data not shown).

6. miR-141 affects the stem cell related properties of CD44$^+$ PCa cells.

Since miR-141 was under-expressed in the CD44$^+$ populations of PCa xenograft and primary

patients samples, we then decided to evaluate whether miR-141 may directly regulate the CSC populations. We first performed in vitro clonal and sphere formation experiments in purified $CD44^+$ Du145 cells, and observed that over-expression of miR-141 in $CD44^+$ Du145 cells suppressed colony formation (Fig.5A). On the other hand, knocking down miR-141 using antisense oligo in $CD44^-$ Du145 cells promoted clonal and sphere formation (Fig.5B).

Consistent with the in vitro results, When I over-expressed miR-141 into $CD44^+$ Du145 cells, I observed that these cells formed fewer and smaller tumor than the NC (control) transfected $CD44^+$ Du145 cells (Fig. 5C).

Personnel Paid on this Project:

Can Liu, Principal Investigator

KEY RESEARCH ACCOMPLISHMENTS

Over the three-year course of the award, I have made several research accomplishments.

1. We are the first to identify distinct miRNA expression patterns in different PCa stem/progenitor subsets from our original miRNA expression profiling of a library of 310 miRNAs in several PCa stem/progenitor cell populations including $CD44^+$, $CD133^+$, $\alpha2\beta1^+$ and side population cells.

2. Multiple commonly and differentially expressed miRNA in the PCa stem/progenitor cell populations were identified including four commonly under-expressed miRNAs, namely miR-34a, let-7b, miR-106a and miR-141, as well as two commonly over-expressed miRNAs, namely miR-301 and miR-452.

3. We performed experiments to validate the six commonly and differentially expressed miRNAs, i.e., miR-34a, let-7b, miR-106a, miR-141, miR-301 and miR-452 in $CD44^+$ populations purified from 21 primary patient prostate tumor samples. Four miRNAs, miR-34a, let-7b, miR-141 and miR-301 showed consistent differential expression in the stem/progenitor subpopulations between xenograft model and primary patient samples.

4. We have, for the first time, provided strong experimental evidence that miR-34a under-expression in the $CD44^+$ prostate CSC population is important for regulating PCa stem cells and PCa development and metastasis. We also confirmed that CD44 itself is a direct and functional target of miR-34a that mediates the miR-34a suppression of metastasis in PCa.

5. Functional studies of let-7 in PCa cells revealed that, similar to miR-34a, let-7 negatively regulates CSC properties of PCa cells and consequently regulates tumorigenic ability of PCa cells.

6. Let-7 and miR-34a exert differential effect on cell cycle in PCa cells, where miR-34a prominently induces G1 cell cycle arrest followed by cell senescence and let-7 mainly induces G2/M cell cycle and did not induce cell senescence.

7. miR-301 exerts differential biological effect on different PCa cells. Manipulation of miR-301 level in $CD44^+/CD44^-$ Du145 and PC3 cells did not affect their sphere formation and tumor regeneration abilities. In contrast, in LAPC9 cells, miR-301 could promote clonal and sphere formation.

8. miR-141 plays an important role in several biological aspects in regulating PCa development/metastasis. We have confirmed that miR-141 negatively regulates migration and invasion in PCa cells. Meanwhile, miR-141 regulates proliferation, clonal, sphere formation and tumor development of PCa cells in a cell type dependent manner. Enforced expression of miR-141 suppresses the stem cell related properties of $CD44^+$ PCa cells. Further investigations will elucidate the intricate biological functions of miR-141 in regulating tumorigenic PCa cell populations and PCa development and metastasis.

REPORTABLE OUTCOMES

This DOD pre-doctoral fellowship has greatly facilitated my scientific training as a graduate student and an independent scientist. It supported me to attend the 2010, and 2011 International Society of Stem Cell Research (ISSCR) annual meetings, the 2012 AACR meeting in Chicago and 2013 Keystone Symposia on noncoding RNA in Toronto. I have also been honored with the Travel Award in the 2010 ISSCR meeting. By attending these meetings, I have had the opportunities to present my research work and also to interact with and learn about the other scientists' work on the miRNAs and CSCs. In our department, I have also been selected several times to present my work in graduate student seminars and retreats.

Other reportable outcomes are:

Liu C, Kelnar K, Liu B, Chen X, Calhoun-Davis T, Li H, Patrawala L, Yan H, Jeter C, Honorio S, Wiggins J, Bader AG, Fagin R, Brown R, and Tang DG. The microRNA miR-34a inhibits prostate cancer stem cells and metastasis by directly repressing CD44. *Nature Med,* **17**:211-215 (2011).

Liu C and Tang DG. microRNA regulation of cancer stem cells. *Cancer Res,* **71**:5950-5954 Review (2011).

Liu C, Kelnar K, Vlassov AV, Brown D, Wang J, Tang DG. Distinct microRNA expression profiles in prostate cancer stem/progenitor cells and tumor suppressive functions of let-7. *Cancer Res,* **72**:3393-3404 (2012).

Meeting abstracts:

2013 Keystone microRNA Symposia
MicroRNA expression profiling in prostate cancer stem/progenitor cells reveals tumor suppressive microRNAs that negatively regulate prostate cancer stem cells and prostate cancer development

Most human tumors contain a population of cells with stem cell properties, called cancer stem cells (CSCs), which are believed to be responsible for tumor establishment, metastasis, and resistance to clinical therapy. It's crucial to understand the regulatory mechanisms unique to CSCs, so that we may design CSC-specific therapeutics. Recent discoveries of microRNA (miRNA) have provided a new avenue in understanding the regulatory mechanisms of cancer. However, how miRNAs may regulate CSCs is still poorly understood. Here, we present miRNA expression profiling in six populations of prostate cancer (PCa) stem/progenitor cells that possess distinct tumorigenic properties. Six miRNAs were identified to be commonly and differentially expressed, namely, four miRNAs (miR-34a, let-7b, miR-106a and miR-141) were under-expressed, and two miRNAs (miR-301 and miR-452) were over-expressed in the tumorigenic subsets compared to the corresponding marker-negative subpopulations. Among them, the expression patterns of miR-34, let-7b, miR-141 and miR-301 were further confirmed in the $CD44^+$ human primary prostate cancer (HPCa) samples. Functional assays of miR-34a revealed miR-34a as a critical negative regulator in prostate CSCs and PCa development and metastasis. Over-expression of miR-34a in either bulk or $CD44^+$ PCa cells significantly suppressed clonal expansion, tumor development and metastasis. Systemic delivery of miR-34a in tumor-bearing mice demonstrated a potent therapeutic effect against tumor progression and metastasis, leading to extended animal survival. Like miR-34a, let-7 manifests similar tumor suppressive effects in PCa cells. In addition, we observed differential mechanisms between let-7 and miR-34a on cell cycle, with miR-34a mainly inducing G1 cell-cycle arrest followed by cell senescence and let-7 inducing G2/M arrest. MiR-301, on the other hand, exerted a cell type dependent effect in regulating prostate CSC properties and PCa development. In summary, our work reveals that the prostate CSC populations display unique miRNA expression signatures and different miRNAs distinctively and coordinately regulate various aspects of CSC properties. Altogether, our results lay a scientific foundation for developing miRNA-based anti-cancer therapy.

2012 AACR

Distinct microRNA expression profiles in prostate cancer stem/progenitor cells and tumor suppressive functions of let-7

microRNAs (miRNAs) regulate cancer cells but their potential effects in cancer stem/progenitor cells is still being explored. In this study we used quantitative RT-PCR to define miRNA expression patterns in various stem/progenitor cell populations in prostate cancer (PCa), including CD44+, CD133+, integrin α2β1+ and side population cells. We identified distinct and common patterns in these different tumorigenic cell subsets. Multiple tumor suppressive miRNAs were downregulated coordinately in several PCa stem/progenitor populations, namely, miR-34a, let-7b, miR-106a and miR-141, whereas miR-301 and miR-452 were commonly overexpressed. let-7 overexpression inhibited PCa cell proliferation and clonal expansion in vitro and tumor development in vivo. In addition, let-7 and miR-34a exerted differential inhibitory effects in PCa cells, with miR-34a inducing G1 phase cell cycle arrest accompanied by cell senescence and let-7 inducing G2/M phase cell cycle arrest without senescence. Taken together, our findings define distinct miRNA expression patterns that coordinately regulate the tumorigenic prostate cancer cells.

2010 ISSCR

Identification of miR-34a as a potent inhibitor of prostate cancer progenitor cells and metastasis by directly repressing CD44

Human tumors contain cancer stem cells (CSCs) or tumor progenitor cells that are involved in tumor progression and metastasis. MicroRNAs (miRNAs) regulate both normal stem cell and CSC properties and altered miRNA expression has been implicated in tumorigenesis. CSCs in many tumors, including those in the breast, pancreas, head and neck, colon, liver, and stomach are identified using surface adhesion molecule CD44, either individually or in combination with other marker(s). Prostate cancer (PCa) stem/progenitor cells with enhanced clonogenic and tumor-initiating and metastatic capacities are also harbored in the CD44+ cell population, but whether miRNAs regulate the CD44+ PCa progenitor cells and PCa metastasis remains unclear. Here we show, through expression analysis, that miR-34a, a direct p53 target was under-expressed in CD44+ PCa cells purified from xenograft as well as primary patient tumors. Enforced expression of miR-34a in bulk PCa cells inhibited clonogenic expansion and tumor development and miR-34a re-expression in CD44+ PCa cells completely blocked tumor regeneration. Furthermore, systemically delivered miR-34a inhibited PCa metastasis and extended the survival of tumor-bearing animals. Of significance, CD44 was identified and validated as a direct and functional target of miR-34a and CD44 knockdown phenocopied miR-34a over-expression in inhibiting PCa regeneration and metastasis. Our study reveals miR-34a as a critical negative regulator of CD44+ tumorigenic PCa cells by targeting CD44 and establishes a strong rationale for developing miR-34a as a novel therapeutic against prostate CSCs.

CONCLUSIONS

By now we have accomplished all the scientific goals proposed in the original application. During the first year of grant period, I have finished the experiment proposed in Aim 1 and part of Aim 2 and have shown that miR-34a is significantly under-expressed in CD44+ PCa xenograft cells as well as in primary human patient cells. Enforced expression of miR-34a in bulk and CD44+ PCa cells suppressed prostate tumor development and metastasis. miR-34a inhibits stem cell properties of PCa cells, as evidenced by in vitro clonal and sphere assays. Notably, miR-34a possesses therapeutic efficacy against established prostate tumors. CD44 itself is a direct and functional target of miR-34a.

During the second year of the grant period, we further characterized the miRNA expression profiling process and identified common and distinct miRNA expression patterns in several PCa stem/progenitor cell populations. We also investigated the role of let-7 in regulation PCa cells and revealed its tumor suppressive function in regulating PCa development. We have also explored the biological function of miR-301 in regulating PCa stem/progenitor cells and PCa development.

In the last year of the grant period, we carried out in vitro and in vivo work to further understand the role of miR-141 in regulating PCa stem/progenitor cells and PCa development. We confirmed the under-expression of miR-141 in the purified CD44+ populations from 21 primary patient PCa samples. Unlike miR-34a, which exerts potent tumor suppressive function in PCa cells, miR-141 seems to be involved in several biological processes in prostate cancer development. We confirmed that miR-141 is a negative regulator of EMT and suppresses migration and invasion of PCa cells. We also observed that miR-141 promotes tumorigenicity of bulk PCa cells, but suppresses the stem cell properties of $CD44^+$ PCa cells.

By studying the role of several different miRNA in PCa cells, we have proved our original hypothesis, which is miRNA play important role in regulating prostate cancer stem cells and PCa development and different miRNAs regulate different aspects of tumor development and distinct CSC properties, and together, they coordinately control the tumor progression.

REFERENCES

1. J. E. Visvader, G. J. Lindeman, Cancer stem cells in solid tumours: accumulating evidence and unresolved questions. Nat. Rev. Cancer 8, 755-768 (2008).
2. J. M. Rosen, C.T. Jordan, The increasing complexity of the cancer stem cell paradigm. Science 324, 1670-1673 (2009).
3. L. Patrawala, et al., Side population (SP) is enriched in tumorigenic, stem-like cancer cells whereas ABCG2+ and ABCG2- cancer cells are similarly tumorigenic. Cancer Res. 65: 6207-6219 (2005).
4. L. Patrawala, et al., Highly purified CD44+ prostate cancer cells from xenograft human tumors are enriched in tumorigenic and metastatic progenitor cells. Oncogene 25: 1696-1708 (2006).
5. D. G. Tang, et al., Prostate cancer stem/progenitor cells: Identification, characterization, and implications. Mol. Carcinogenesis 46: 1-14 (2007).
6. L. Patrawala, T. Calhoun-Davis, R. Schneider-Broussard, D. G. Tang, Hierarchical organization of prostate cancer cells in xenograft tumors: The CD44+a2b1+ cell population is enriched in tumor-initiating cells. Cancer Res. 67: 6796-6805 (2007).
7. H. Li, X. Chen, T. Calhoun-Davis, K. Claypool, D. G. Tang, PC3 human prostate carcinoma cell holoclones contain self-renewing tumor-initiating cells. Cancer Res.; 68: 1820-1825 (2008).
8. H. Li, et al., Methodologies in assaying prostate cancer stem cells. Methods Mol. Biol.; 569: 85-138 (2009).
9. D.P. Bartel, MicroRNA: genomics, biogenesis, mechanism, and function. Cell; 116: 281-297 (2004).
10. G. A. Calin, C. M. Croce, MicroRNA signatures in human cancers. *Nat Rev Cancer*; **6**;857-866 (2006).
11. C. Liu, et al., The microRNA miR-34a inhibits prostate cancer stem cells and metastasis by directly repressing CD44. Nat Med; 17:211-215 (2011).
12. Liu C, Kelnar K, Vlassov AV, Brown D, Wang J, Tang DG. Distinct microRNA expression profiles in prostate cancer stem/progenitor cells and tumor suppressive functions of let-7. Cancer Res. 72:3393-404 (2012).
13. Korpal, M., E. S. Lee, G. Hu, and Y. Kang. The miR-200 family inhibits epithelial-mesenchymal transition and cancer cell migration by direct targeting of E-cadherin transcriptional repressors ZEB1 and ZEB2. J Biol Chem; 283:14910-4 (2008).
14. Burk, U., J. Schubert, U. Wellner, O. Schmalhofer, E. Vincan, S. Spaderna, and T. Brabletz. A reciprocal repression between ZEB1 and members of the miR-200 family promotes EMT and invasion in cancer cells. EMBO Rep.; 9:582-9 (2008).

15. Gregory PA, Bert AG, Paterson EL, Barry SC, Tsykin A, Farshid G, Vadas MA, Khew-Goodall Y, Goodall GJ. The miR-200 family and miR-205 regulate epithelial to mesenchymal transition by targeting ZEB1 and SIP1. Nat Cell Biol.; 10:593-601 (2008).
16. Brabletz S, Brabletz T. The ZEB/miR-200 feedbackloop – a mother of cellular plasticity in development and cancer? EMBO Rep.; 11:670-7 (2010).
17. Shimono Y, Zabala M, Cho RW, Lobo N, Dalerba P, Qian D, Diehn M, Liu H, Panula SP, Chiao E, Dirbas FM, Somlo G, Pera RA, Lao K, Clarke MF. Downregulation of miRNA-200c links breast cancer stem cells with normal stem cells. Cell. 2009 ;138:592-603.

nature medicine

The microRNA miR-34a inhibits prostate cancer stem cells and metastasis by directly repressing CD44

Can Liu[1,2], Kevin Kelnar[3], Bigang Liu[1], Xin Chen[1,2], Tammy Calhoun-Davis[1], Hangwen Li[1], Lubna Patrawala[2], Hong Yan[1], Collene Jeter[1], Sofia Honorio[1], Jason F Wiggins[3], Andreas G Bader[3], Randy Fagin[4], David Brown[3] & Dean G Tang[1,2]

Cancer stem cells (CSCs), or tumor-initiating cells, are involved in tumor progression and metastasis[1]. MicroRNAs (miRNAs) regulate both normal stem cells and CSCs[2–5], and dysregulation of miRNAs has been implicated in tumorigenesis[6]. CSCs in many tumors—including cancers of the breast[7], pancreas[8], head and neck[9], colon[10,11], small intestine[12], liver[13], stomach[14], bladder[15] and ovary[16]—have been identified using the adhesion molecule CD44, either individually or in combination with other marker(s). Prostate CSCs with enhanced clonogenic[17] and tumor-initiating and metastatic[18,19] capacities are enriched in the CD44$^+$ cell population, but whether miRNAs regulate CD44$^+$ prostate cancer cells and prostate cancer metastasis remains unclear. Here we show, through expression analysis, that miR-34a, a p53 target[20–24], was underexpressed in CD44$^+$ prostate cancer cells purified from xenograft and primary tumors. Enforced expression of miR-34a in bulk or purified CD44$^+$ prostate cancer cells inhibited clonogenic expansion, tumor regeneration, and metastasis. In contrast, expression of miR-34a antagomirs in CD44$^-$ prostate cancer cells promoted tumor development and metastasis. Systemically delivered miR-34a inhibited prostate cancer metastasis and extended survival of tumor-bearing mice. We identified and validated CD44 as a direct and functional target of miR-34a and found that CD44 knockdown phenocopied miR-34a overexpression in inhibiting prostate cancer regeneration and metastasis. Our study shows that miR-34a is a key negative regulator of CD44$^+$ prostate cancer cells and establishes a strong rationale for developing miR-34a as a novel therapeutic agent against prostate CSCs.

Many human cancers contain CSCs, which possess an enhanced tumor-initiating capacity, can self-renew, partially recreate the cellular heterogeneity of the parental tumor, and seem to be generally more resistant than other cancer cells to conventional anticancer therapeutics. Because of these properties, CSCs have been linked to tumor recurrence and distant metastasis[1]. Consequently, it is essential to elucidate the signaling and regulatory mechanisms that are unique to CSCs in order to design CSC-specific therapies. To this end, we used quantitative RT-PCR (qRT-PCR) to compare the miRNA expression[25,26] of CD44$^+$ and CD44$^-$ prostate cancer cells. The CD44$^+$ prostate cancer cell population harbors tumor-initiating and metastatic cells[18,19] and is enriched in the self-renewal gene *NANOG* (ref. 27). We purified CD44$^+$ prostate cancer cells from three xenograft models[18,19,27,28]—LAPC9, LAPC4 and Du145. For comparison, we also purified LAPC4 CD133$^+$ and LAPC9 side-population cells. CD133$^+$ prostate cancer cells are clonogenic *in vitro*[17], and the LAPC9 side population is also enriched in tumor-initiating cells[28]. We first used unsorted cells to measure the levels of 324 sequence-validated human miRNAs and found that 137 miRNAs were expressed at reliably detectable levels (**Fig. 1a**). We then compared the expression of these 137 miRNAs in marker-positive versus marker-negative prostate cancer cell populations and found that miR-34a (1p36.22) was prominently underexpressed in all CD44$^+$ populations (**Fig. 1a**), being expressed at < 3% of the level in the corresponding CD44$^-$ cells (**Fig. 1b**). The other two miR-34 family members, miR-34b and miR-34c (11q23.1), did not show consistent differences between CD44$^+$ and CD44$^-$ prostate cancer cells (not shown). Underexpression of miR-34a in CD44$^+$ prostate cancer cells was more pronounced than that of let-7b (**Fig. 1b**), a tumor-suppressive miRNA[6] and an important regulator of both normal and cancer stem cells[3,4]. We also found that miR-34a was underexpressed in LAPC4 CD133$^+$ (**Fig. 1b**) and LAPC9 side-population (not shown) cells. To validate the underexpression of miR-34a in CD44$^+$ prostate cancer cells and to determine its clinical relevance, we purified CD44$^+$ and CD44$^-$ prostate cancer cells from 18 human prostate cancer (HPCa; **Supplementary Table 1**) samples[27,29,30] and compared the expression of miR-34a. CD44$^+$ HPCa cells expressed miR-34a at levels ~25–70% of those in CD44$^-$ cells from the same tumors (**Fig. 1c**). These results suggest that miR-34a is underexpressed in the CD44$^+$ prostate cancer cells in both xenograft and primary tumors.

The expression of miR-34a is regulated by p53, and miR-34a induces apoptosis, cell-cycle arrest or senescence when introduced into cancer cells[20–24,31]. We found that the expression of miR-34a in ten normal human prostate (NHP) epithelial strains, immortalized (but non-tumorigenic) NHP cells and prostate cancer cell lines correlated with

[1]Department of Molecular Carcinogenesis, the University of Texas M.D. Anderson Cancer Center, Science Park, Smithville, Texas, USA. [2]Program in Molecular Carcinogenesis, The University of Texas Graduate School of Biomedical Sciences (GSBS), Houston, Texas, USA. [3]Mirna Therapeutics, Inc., Austin, Texas, USA. [4]The Hospital at Westlake, Austin, Texas, USA. Correspondence should be addressed to D.G.T. (dtang@mdanderson.org).

Received 14 May 2010; accepted 30 November 2010; published online 16 January 2011; doi:10.1038/nm.2284

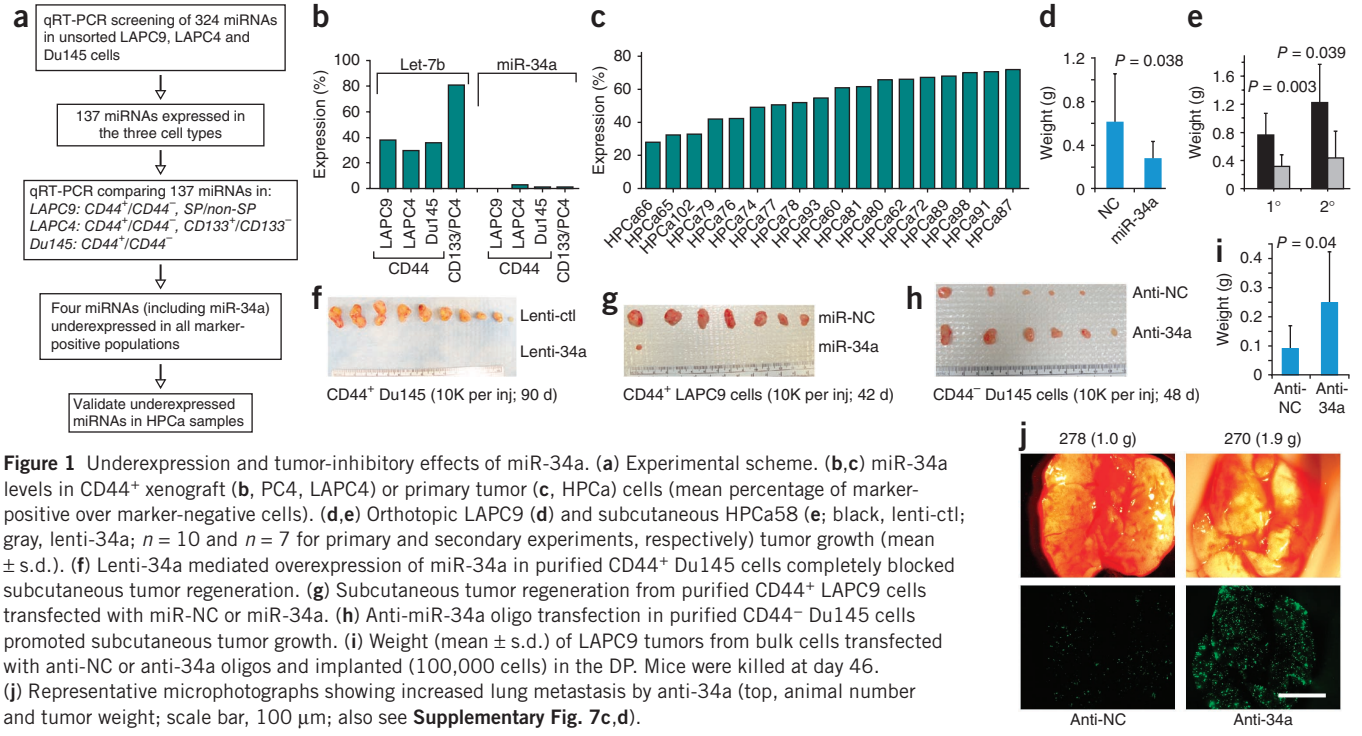

Figure 1 Underexpression and tumor-inhibitory effects of miR-34a. (**a**) Experimental scheme. (**b**,**c**) miR-34a levels in CD44+ xenograft (**b**, PC4, LAPC4) or primary tumor (**c**, HPCa) cells (mean percentage of marker-positive over marker-negative cells). (**d**,**e**) Orthotopic LAPC9 (**d**) and subcutaneous HPCa58 (**e**; black, lenti-ctl; gray, lenti-34a; $n = 10$ and $n = 7$ for primary and secondary experiments, respectively) tumor growth (mean ± s.d.). (**f**) Lenti-34a mediated overexpression of miR-34a in purified CD44+ Du145 cells completely blocked subcutaneous tumor regeneration. (**g**) Subcutaneous tumor regeneration from purified CD44+ LAPC9 cells transfected with miR-NC or miR-34a. (**h**) Anti-miR-34a oligo transfection in purified CD44− Du145 cells promoted subcutaneous tumor growth. (**i**) Weight (mean ± s.d.) of LAPC9 tumors from bulk cells transfected with anti-NC or anti-34a oligos and implanted (100,000 cells) in the DP. Mice were killed at day 46. (**j**) Representative microphotographs showing increased lung metastasis by anti-34a (top, animal number and tumor weight; scale bar, 100 μm; also see **Supplementary Fig. 7c**,**d**).

their p53 status (**Supplementary Fig. 1** and **Supplementary Results**). Transfection of synthetic miR-34a oligonucleotides (oligos), but not the negative control (NC) miRNA oligos, induced cell-cycle arrest, apoptosis or senescence in p53-mutant and p53-null prostate cancer cells (**Supplementary Figs. 2** and **3** and **Supplementary Results**).

To determine whether miR-34a can inhibit tumor development, we manipulated miR-34a levels (**Supplementary Fig. 4**) in a variety of prostate cancer cell types and then implanted the cells subcutaneously or orthotopically in the dorsal prostate in NOD-SCID mice (**Fig. 1d**,**e** and **Supplementary Fig. 5**). LAPC9 (**Fig. 1d** and **Supplementary Fig. 5a**) and HPCa58 (**Fig. 1e**) cells transfected with miR-34a produced significantly smaller tumors than the same cells transfected with miR-NC oligos. LAPC9 cells are androgen dependent, whereas HPCa58 cells were from an early-generation xenograft tumor (**Supplementary Methods**). miR-34a also inhibited the secondary transplantation of HPCa58 cells (**Fig. 1e**). miR-34a showed similar tumor-inhibitory effects on androgen-dependent LAPC4 (**Supplementary Fig. 5b**) and androgen-independent Du145 (**Supplementary Fig. 5d**) and PPC-1 (**Supplementary Fig. 5g**) cells. As expected, miR-34a–transfected prostate cancer cells showed miR-34a levels at several orders of magnitude higher than cells with miR-NC (**Supplementary Fig. 4a**). In contrast to freshly transfected cells, the residual tumors showed only a marginal or no increase in miR-34a levels (**Supplementary Fig. 4b**), suggesting that transfected mature miR-34a oligo were gradually lost *in vivo* and explaining why miR-34a–overexpressing prostate cancer cells still regenerated some tumors. To complement the oligo transfection studies, we also infected prostate cancer cells with lentiviral or retroviral vectors encoding pre-miR-34a (**Supplementary Fig. 1d**) before implantation. The viral vector–mediated overexpression of miR-34a also inhibited tumor regeneration of LAPC4 (**Supplementary Fig. 5c**), Du145 (**Supplementary Fig. 5e**,**f**), and LAPC9 (not shown) cells. Notably, LAPC9 and LAPC4 cells transfected with miR-34a oligos (**Supplementary Fig. 5a**,**b**) and Du145 cells infected with the MSCV-34a retroviral vectors (**Supplementary Fig. 5e**) all developed fewer tumors compared to the corresponding controls ($P < 0.01$ for tumor incidence). Histological and immunohistochemical examination of tumor sections (**Supplementary Fig. 6**) showed increased necrotic areas and reduced Ki-67+ cells in miR-34a transfected tumors, which also showed increased expression of HP-1γ (a protein that is associated with cell-cycle arrest and senescence). These overexpression experiments in unfractionated prostate cancer cells show that miR-34a possesses strong tumor-inhibitory effects.

To evaluate whether miR-34a–mediated inhibition of tumor development might be due to an effect on the CSC populations, we performed tumor growth experiments using purified CD44+ or CD44− prostate cancer cells that had been subjected to manipulation of miR-34a levels. When we infected purified CD44+ Du145 cells with lenti-34a, tumor regeneration was completely blocked in that tumor incidence was 10/10 for the lenti-ctl group, whereas the incidence for the lenti-34a group was 0/10 (**Fig. 1f**). When we transfected CD44+ LAPC9 cells with miR-NC or miR-34a oligos, tumor incidence was 7/7 and 1/8, respectively ($P = 0.016$), and the only tumor observed in the miR-34a group was much smaller (0.03 g versus the mean tumor weight of 0.5 g for the miR-NC group) (**Fig. 1g**). Similarly, lenti-34a infection of CD44+ LAPC9 cells also inhibited tumor regeneration (tumor incidences for the lenti-ctl and lenti-34a groups were 7/7 and 2/7, respectively; $P = 0.01$) (**Supplementary Fig. 5h**).

We also performed the opposite experiments by introducing an antisense inhibitor of miR-34a (that is, anti-34a or miR-34a antagomir) into purified CD44−Du145 or LAPC9 cells, which are less tumorigenic than the corresponding CD44+ cells[18,19]. The antagomir-transfected LAPC9 cells showed reduced endogenous miR-34a (**Supplementary Fig. 4c**) and increased mRNA levels of *CDK4* (**Supplementary Fig. 4d**), a known miR-34a target[26], validating the specificity of anti-34a. We observed that CD44− Du145 cells transfected with anti-34a developed larger tumors than those with anti-NC oligos (0.2 g versus 0.05 g; $P = 0.038$) (**Fig. 1h**), which we verified in a repeat experiment (**Supplementary Fig. 5i**). Likewise, in two independent experiments,

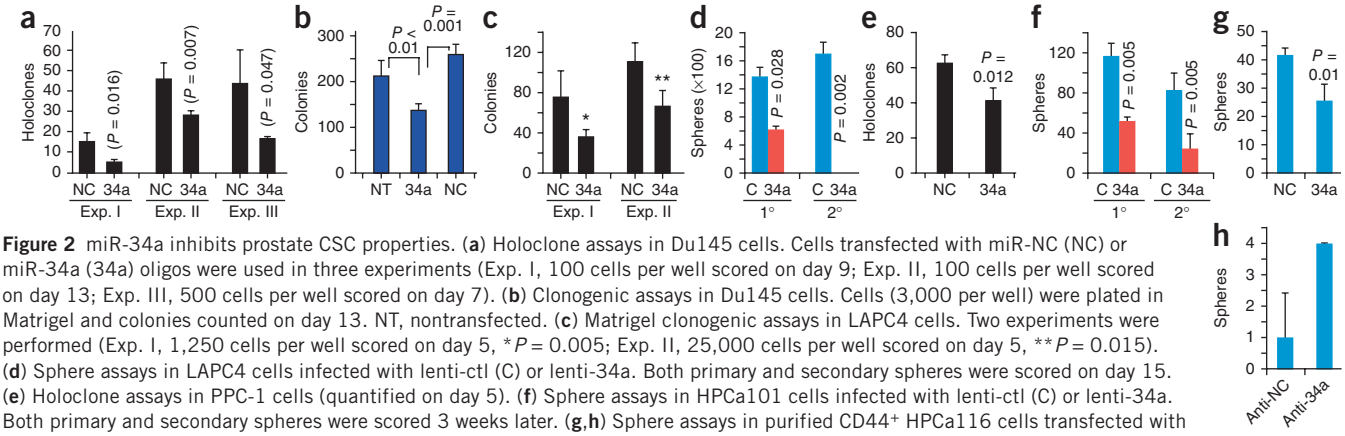

Figure 2 miR-34a inhibits prostate CSC properties. (**a**) Holoclone assays in Du145 cells. Cells transfected with miR-NC (NC) or miR-34a (34a) oligos were used in three experiments (Exp. I, 100 cells per well scored on day 9; Exp. II, 100 cells per well scored on day 13; Exp. III, 500 cells per well scored on day 7). (**b**) Clonogenic assays in Du145 cells. Cells (3,000 per well) were plated in Matrigel and colonies counted on day 13. NT, nontransfected. (**c**) Matrigel clonogenic assays in LAPC4 cells. Two experiments were performed (Exp. I, 1,250 cells per well scored on day 5, $*P = 0.005$; Exp. II, 25,000 cells per well scored on day 5, $**P = 0.015$). (**d**) Sphere assays in LAPC4 cells infected with lenti-ctl (C) or lenti-34a. Both primary and secondary spheres were scored on day 15. (**e**) Holoclone assays in PPC-1 cells (quantified on day 5). (**f**) Sphere assays in HPCa101 cells infected with lenti-ctl (C) or lenti-34a. Both primary and secondary spheres were scored 3 weeks later. (**g**,**h**) Sphere assays in purified CD44$^+$ HPCa116 cells transfected with NC or miR-34a oligos (**g**) or CD44$^-$ HPCa116 cells transfected with anti-NC or anti-34a oligos (**h**). Spheres were scored on day 15.

bulk LAPC9 cells transfected with anti-34a oligos generated larger orthotopic tumors than those with anti-NC oligos (**Fig. 1i** and **Supplementary Fig. 7a**). Anti-34a also promoted subcutaneous tumor growth in purified CD44$^-$ LAPC9 cells (**Supplementary Fig. 7b**). Notably, in the two orthotopic LAPC9 tumor experiments (**Fig. 1i** and **Supplementary Fig. 7a**), we observed lung metastasis in 5/9 (56%; for anti-NC) and 8/11 (73%; for anti-34a) tumor-bearing mice, respectively. When we quantified the GFP-bright foci (≥1 mm^3) in the five anti-NC and eight anti-34a mouse lungs, the latter showed higher levels of metastasis (**Fig. 1j** and **Supplementary Fig. 7c**,**d**). Taken together, these *in vivo* experiments in purified prostate cancer cells suggest that miR-34a negatively regulates the tumor-initiating capacity of prostate CSCs.

To further investigate the effects of miR-34a on prostate CSC properties, we performed holoclone, clonogenic and sphere formation assays[18,19,27,32,33]. Prostate cancer cell holoclones contain self-renewing cancer cells[32], and sphere-formation assays have been widely used to measure the activity of stem or progenitor cells[1,33]. We first established stringent competition assays in which clones (holoclones formed in culture dishes), colonies (formed in Matrigel or methylcellulose) and (floating) spheres were all of clonal origin (**Supplementary Fig. 8**). Under these conditions, miR-34a overexpression inhibited holoclone formation, clonogenic capacity, or sphere establishment in Du145 (**Fig. 2a**,**b** and **Supplementary Fig. 2d**,**e**), LAPC4 (**Fig. 2c**,**d**) and PPC-1 (**Fig. 2e** and **Supplementary Fig. 3h**,**i**) cells. In addition, miR-34a inhibited sphere formation by primary HPCa cells (**Fig. 2f** and **Supplementary Fig. 9a**). HPCa cells overexpressing miR-34a formed tiny or differentiated spheres (**Supplementary Fig. 9b**). Notably, miR-34a overexpression abrogated secondary sphere establishment (**Fig. 2d**,**f**) and inhibited sphere formation in purified CD44$^+$ HPCa116 cells (**Fig. 2g**). By contrast, anti-34a increased the inherently low sphere-forming capacity of CD44$^-$ HPCa116 cells several-fold (**Fig. 2h**). These observations collectively indicate that miR-34a negatively regulates prostate CSC properties.

Subsequently, we performed four sets of therapeutic experiments (**Fig. 3** and Online Methods) in NOD-SCID mice with established prostate tumors. We first observed that repeated intratumoral injections of miR-34a into subcutaneous PPC-1 tumors halted tumor growth (**Supplementary Fig. 5g**). We then established orthotopic PC3 tumors and, 3 weeks later, injected miR-34a or miR-NC oligos complexed with a lipid-based delivery agent[26] into the tail veins of mice every 2 d. Systemically delivered miR-34a reduced PC3 tumor burden by 50% (**Fig. 3a**). In two therapeutic experiments with orthotopic LAPC9 tumors, miR-34a reduced lung metastasis (**Fig. 3b**,**e**,**f** and **Supplementary Fig. 10**) without affecting tumor growth (**Fig. 3c**). miR-34a also extended the survival of tumor-bearing mice (**Fig. 3d**). These results indicate that miR-34a has therapeutic efficacy against established prostate tumors.

Cyclin D1, CDK4 and 6, E2F3, N-Myc, c-MET and BCL-2 have been reported to be direct targets of miR-34a[20–24,26,31,34,35]. A survey of some of these molecules revealed that miR-34a affected the levels of cyclin D1, CDK4, CDK6 and c-MET in our prostate cancer models (**Supplementary Figs. 4d**,**e** and **6d**,**e**). There was a consistent and strong inverse correlation between miR-34a levels and CD44 (**Fig. 4a**,**b**, **Supplementary Figs. 1a**, **4e** and **11a–c** and **Supplementary Table 2**). For example, CD44 protein and CD44$^+$ prostate cancer cells were reduced in miR-34a–treated tumors (**Fig. 4a**). Transfected miR-34a downregulated CD44 in prostate cancer cells (**Fig. 4b** and **Supplementary Fig. 11a**,**b**). By contrast, CD44 mRNA (**Supplementary Fig. 4e**) and protein

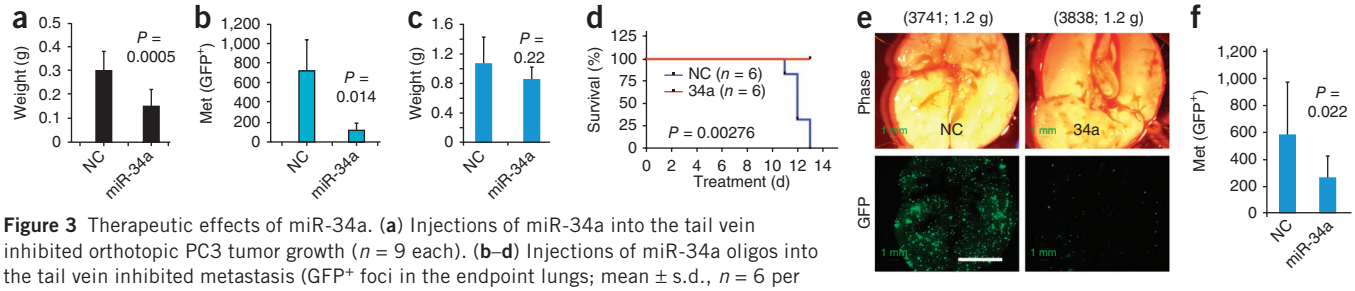

Figure 3 Therapeutic effects of miR-34a. (**a**) Injections of miR-34a into the tail vein inhibited orthotopic PC3 tumor growth ($n = 9$ each). (**b**–**d**) Injections of miR-34a oligos into the tail vein inhibited metastasis (GFP$^+$ foci in the endpoint lungs; mean ± s.d., $n = 6$ per group) of orthotopic LAPC9-GFP tumors (**b**) without significantly affecting tumor growth (**c**) and extended mouse survival (**d**; Kaplan-Meier analysis and log-rank test). (**e**,**f**) The fourth set of therapeutic experiments in LAPC9 cells. Representative lung images (**e**, animal number and tumor weight indicated on top; scale bar, 100 μm) and quantification of lung metastases (**f**; mean ± s.d., $n = 10$ per group).

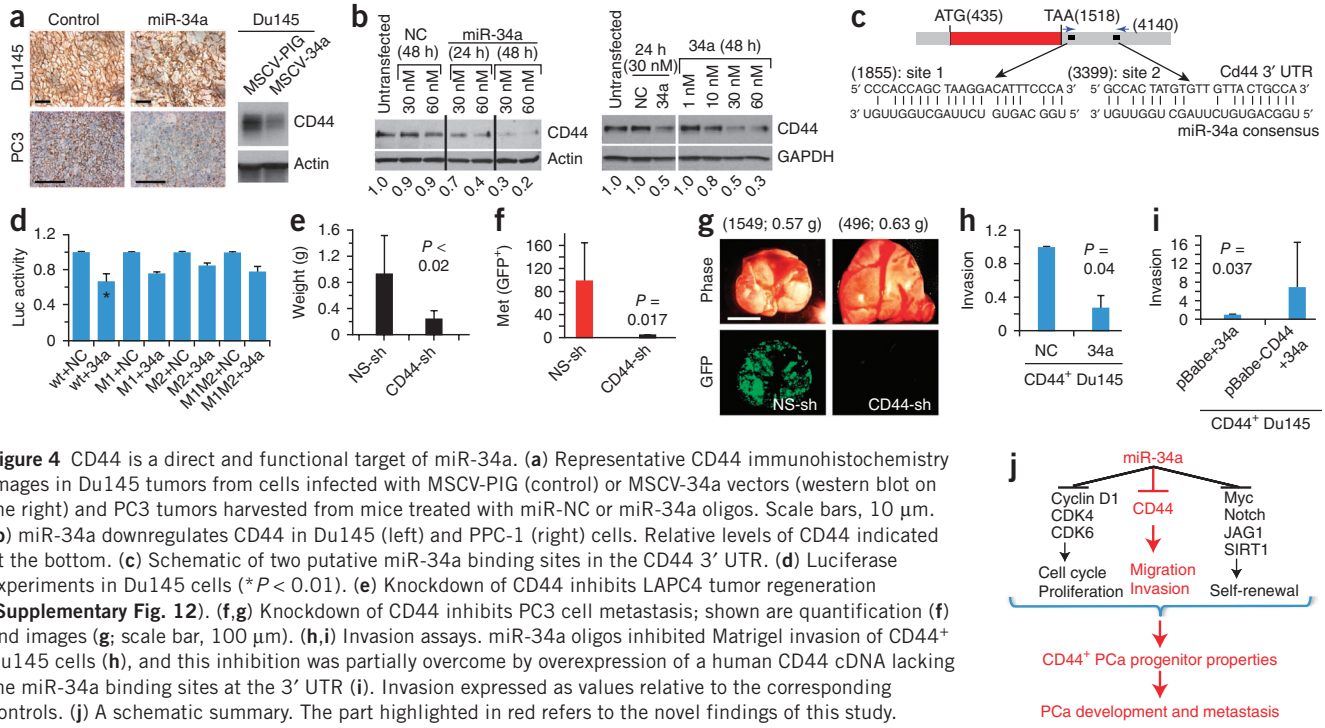

Figure 4 CD44 is a direct and functional target of miR-34a. (**a**) Representative CD44 immunohistochemistry images in Du145 tumors from cells infected with MSCV-PIG (control) or MSCV-34a vectors (western blot on the right) and PC3 tumors harvested from mice treated with miR-NC or miR-34a oligos. Scale bars, 10 μm. (**b**) miR-34a downregulates CD44 in Du145 (left) and PPC-1 (right) cells. Relative levels of CD44 indicated at the bottom. (**c**) Schematic of two putative miR-34a binding sites in the CD44 3′ UTR. (**d**) Luciferase experiments in Du145 cells (*$P < 0.01$). (**e**) Knockdown of CD44 inhibits LAPC4 tumor regeneration (**Supplementary Fig. 12**). (**f**,**g**) Knockdown of CD44 inhibits PC3 cell metastasis; shown are quantification (**f**) and images (**g**; scale bar, 100 μm). (**h**,**i**) Invasion assays. miR-34a oligos inhibited Matrigel invasion of CD44$^+$ Du145 cells (**h**), and this inhibition was partially overcome by overexpression of a human CD44 cDNA lacking the miR-34a binding sites at the 3′ UTR (**i**). Invasion expressed as values relative to the corresponding controls. (**j**) A schematic summary. The part highlighted in red refers to the novel findings of this study.

(**Supplementary Fig. 11c**) were increased in tumors transfected with anti-34a. The target-prediction program rna22 (ref. 36) revealed two putative miR-34a binding sites in the 3′ UTR of CD44 mRNA (**Fig. 4c**). When we cloned the 3′ UTR fragment containing both putative miR-34a binding sites downstream of a luciferase coding sequence (**Supplementary Fig. 11d**,**e**), co-transfection of the luciferase reporter and miR-34a oligos into three prostate cancer cell types produced lower luciferase activity than in cells co-transfected with the NC oligos. However, mutation of the seed sequence in either site, especially the distal site, partially abrogated the suppressive effect of miR-34a (**Fig. 4d** and **Supplementary Fig. 11f**,**g**). These results suggest that miR-34a regulates CD44 expression through two binding sites in the 3′ UTR of the gene that encodes CD44.

To determine whether CD44 is a functionally important target of miR-34a in the context of prostate cancer development, we reduced CD44 expression using a lentiviral vector carrying a short hairpin RNA (shRNA) against CD44 (**Supplementary Fig. 1d**) in LAPC4, PC3 and Du145 cells. Knockdown of CD44 in LAPC4 cells inhibited both orthotopic tumor formation (**Fig. 4e**) and lung metastasis (**Supplementary Fig. 12**). In PC3 cells, it markedly inhibited metastasis (**Fig. 4f**,**g** and **Supplementary Fig. 13**) without affecting tumor growth (data not shown). Knockdown of CD44 in Du145 cells inhibited tumor development in both subcutaneous and orthotopic sites (**Supplementary Fig. 14a**,**b**) as well as metastasis (not shown). These results not only show that CD44 has a key role in determining the tumorigenic and metastatic capacity of prostate cancer cells but also indicate that knockdown of CD44 phenocopies the anti–prostate cancer effects of miR-34a. Mechanistically, the CD44$^+$ prostate cancer cells showed higher migratory (**Supplementary Fig. 14c**,**d**) and invasive (**Supplementary Fig. 14e**) capacities than CD44$^-$ cells, and these capacities were partially inhibited by miR-34a (**Fig. 4h** and **Supplementary Fig. 14f**,**g**). 'Rescue' experiments wherein CD44 was overexpressed using a cDNA that lacked the 3′ UTR containing the miR-34a binding sites abrogated miR-34a–mediated inhibition of invasion of CD44$^+$ Du145 cells (**Fig. 4i**), reinforcing the idea that CD44 is a direct and functional target of miR-34a. By contrast, overexpression of CD44 did not significantly relieve the inhibition of prostate cancer cell proliferation by miR-34a (**Supplementary Fig. 15**).

We have shown that miR-34a is underexpressed in tumorigenic CD44$^+$ prostate cancer cells and that it has potent antitumor and antimetastasis effects. Our results establish miR-34a as a key negative regulator of CD44$^+$ prostate cancer cells and CD44 as an important target of miR-34a. Our findings suggest that reduced expression of miR-34a in prostate CSCs contributes to prostate cancer development and metastasis by regulating expression of CD44 and the migratory, invasive and metastatic properties of CSCs (**Fig. 4j**). It is noteworthy that p53, which directly activates miR-34a, also negatively regulates CD44 through a noncanonical p53-binding site in the promoter[37]. Considering the widespread expression of CD44 in CSCs[7–16] and the functional involvement of CD44 in mediating CSC migration and homing[38] and in metastasis of many cancers, the suppression of CD44 by miR-34a reveals a previously unknown signaling pathway that regulates prostate CSCs (**Fig. 4j**). The emerging role of miR-34a in regulating other CSC[35,39] properties, coupled with the therapeutic effects of miR-34a on lung[26] and prostate tumors (this study), establishes a strong rationale for developing miR-34a as a therapeutic agent that targets prostate CSCs.

METHODS

Methods and any associated references are available in the online version of the paper at http://www.nature.com/naturemedicine/.

Note: Supplementary information is available on the Nature Medicine website.

ACKNOWLEDGMENTS

We thank K. Claypool and P. Whitney for FACS, the Histology Core for help with immunohistochemistry, K. Lin for statistical analysis, G. Calin for critically reading the manuscript and other members of the Tang lab for support and discussions. We also thank G. Hannon (Cold Spring Harbor Laboratory, Cold Spring Harbor, New York, USA) for the MSCV-PIG vector. This work was supported in part by grants

from the US National Institutes of Health (R01-AG023374, R01-ES015888, R21-ES015893, R21-CA150009), the US Department of Defense (W81XWH-07-1-0616, W81XWH-08-1-0472) and Elsa Pardee Foundation (D.G.T.) and by two M.D. Anderson Cancer Center grants (CCSG-5 P30 CA016672-34 and ES007784). C. Liu and H. Li were supported in part by predoctoral fellowships from the US Department of Defense.

AUTHOR CONTRIBUTIONS

C.L., K.K., B.L., X.C. and L.P. designed and performed the experiments with help from C.J., T.C.-D., H.L., S.H., H.Y., J.F.W. and A.G.B., R.F. provided all HPCa samples. C.L. and D.G.T. prepared the manuscript. D.G.T., with help from D.B., designed the experiments and supervised the whole project. All authors discussed the results and commented on the manuscript.

COMPETING FINANCIAL INTERESTS

The authors declare competing financial interests: details accompany the full-text HTML version of the paper at http://www.nature.com/naturemedicine/.

Published online at http://www.nature.com/naturemedicine/.
Reprints and permissions information is available online at http://npg.nature.com/reprintsandpermissions/.

1. Visvader, J.E. & Lindeman, G.J. Cancer stem cells in solid tumours: accumulating evidence and unresolved questions. *Nat. Rev. Cancer* **8**, 755–768 (2008).
2. Croce, C.M. & Calin, G.A. miRNAs, cancer, and stem cell division. *Cell* **122**, 6–7 (2005).
3. Melton, C., Judson, R.L. & Blelloch, R. Opposing microRNA families regulate self-renewal in mouse embryonic stem cells. *Nature* **463**, 621–626 (2010).
4. Yu, F. *et al.* let-7 regulates self-renewal and tumorigenicity of breast cancer cells. *Cell* **131**, 1109–1123 (2007).
5. Shimono, Y. *et al.* Downregulation of miRNA-200c links breast cancer stem cells with normal stem cells. *Cell* **138**, 592–603 (2009).
6. Esquela-Kerscher, A. & Slack, F.J. Oncomirs—microRNAs with a role in cancer. *Nat. Rev. Cancer* **6**, 259–269 (2006).
7. Al-Hajj, M., Wicha, M.S., Benito-Hernandez, A., Morrison, S.J. & Clarke, M.F. Prospective identification of tumorigenic breast cancer cells. *Proc. Natl. Acad. Sci. USA* **100**, 3983–3988 (2003).
8. Li, C. *et al.* Identification of pancreatic cancer stem cells. *Cancer Res.* **67**, 1030–1037 (2007).
9. Prince, M.E. *et al.* Identification of a subpopulation of cells with cancer stem cell properties in head and neck squamous cell carcinoma. *Proc. Natl. Acad. Sci. USA* **104**, 973–978 (2007).
10. Dalerba, P. *et al.* Phenotypic characterization of human colorectal cancer stem cells. *Proc. Natl. Acad. Sci. USA* **104**, 10158–10163 (2007).
11. Du, L. *et al.* CD44 is of functional importance for colorectal cancer stem cells. *Clin. Cancer Res.* **14**, 6751–6760 (2008).
12. Zeilstra, J. *et al.* Deletion of the WNT target and cancer stem cell marker CD44 in Apc(Min/+) mice attenuates intestinal tumorigenesis. *Cancer Res.* **68**, 3655–3661 (2008).
13. Yang, Z.F. *et al.* Significance of CD90+ cancer stem cells in human liver cancer. *Cancer Cell* **13**, 153–166 (2008).
14. Takaishi, S. *et al.* Identification of gastric cancer stem cells using the cell surface marker CD44. *Stem Cells* **27**, 1006–1020 (2009).
15. Chan, K.S. *et al.* Identification, molecular characterization, clinical prognosis, and therapeutic targeting of human bladder tumor-initiating cells. *Proc. Natl. Acad. Sci. USA* **106**, 14016–14021 (2009).
16. Zhang, S. *et al.* Identification and characterization of ovarian cancer-initiating cells from primary human tumors. *Cancer Res.* **68**, 4311–4320 (2008).
17. Collins, A.T., Berry, P.A., Hyde, C., Stower, M.J. & Maitland, N.J. Prospective identification of tumorigenic prostate cancer stem cells. *Cancer Res.* **65**, 10946–10951 (2005).
18. Patrawala, L. *et al.* Highly purified CD44$^+$ prostate cancer cells from xenograft human tumors are enriched in tumorigenic and metastatic progenitor cells. *Oncogene* **25**, 1696–1708 (2006).
19. Patrawala, L., Calhoun-Davis, T., Schneider-Broussard, R. & Tang, D.G. Hierarchical organization of prostate cancer cells in xenograft tumors: the CD44$^+\alpha2\beta1^+$ cell population is enriched in tumor-initiating cells. *Cancer Res.* **67**, 6796–6805 (2007).
20. He, L. *et al.* A microRNA component of the p53 tumour suppressor network. *Nature* **447**, 1130–1134 (2007).
21. Raver-Shapira, N. *et al.* Transcriptional activation of miR-34a contributes to p53-mediated apoptosis. *Mol. Cell* **26**, 731–743 (2007).
22. Chang, T.C. *et al.* Transactivation of miR-34a by p53 broadly influences gene expression and promotes apoptosis. *Mol. Cell* **26**, 745–752 (2007).
23. Bommer, G.T. *et al.* p53-mediated activation of miRNA34 candidate tumor-suppressor genes. *Curr. Biol.* **17**, 1298–1307 (2007).
24. Tarasov, V. *et al.* Differential regulation of microRNAs by p53 revealed by massively parallel sequencing: miR-34a is a p53 target that induces apoptosis and G1-arrest. *Cell Cycle* **6**, 1586–1593 (2007).
25. Johnson, C.D. *et al.* The let-7 microRNA represses cell proliferation pathways in human cells. *Cancer Res.* **67**, 7713–7722 (2007).
26. Wiggins, J.F. *et al.* Development of a lung cancer therapeutic based on the tumor suppressor microRNA-34. *Cancer Res.* **70**, 5923–5930 (2010).
27. Jeter, C.R. *et al.* Functional evidence that the self-renewal gene *NANOG* regulates human tumor development. *Stem Cells* **27**, 993–1005 (2009).
28. Patrawala, L. *et al.* Side population (SP) is enriched in tumorigenic, stem-like cancer cells whereas ABCG2$^+$ and ABCG2$^-$ cancer cells are similarly tumorigenic. *Cancer Res.* **65**, 6207–6219 (2005).
29. Bhatia, B. *et al.* Critical and distinct roles of p16 and telomerase in regulating the proliferative lifespan of normal human prostate epithelial progenitor cells. *J. Biol. Chem.* **283**, 27957–27972 (2008).
30. Li, H.W. *et al.* Methodologies in assaying prostate cancer stem cells. *Methods Mol. Biol.* **568**, 85–138 (2009).
31. Hermeking, H. The miR-34 family in cancer and apoptosis. *Cell Death Differ.* **17**, 193–199 (2010).
32. Li, H., Chen, X., Calhoun-Davis, T., Claypool, K. & Tang, D.G. PC3 Human prostate carcinoma cell holoclones contain self-renewing tumor-initiating cells. *Cancer Res.* **68**, 1820–1825 (2008).
33. Dontu, G. *et al.* In vitro propagation and transcriptional profiling of human mammary stem/progenitor cells. *Genes Dev.* **17**, 1253–1270 (2003).
34. Yamakuchi, M., Ferlito, M. & Lowenstein, C.J. miR-34a repression of SIRT1 regulates apoptosis. *Proc. Natl. Acad. Sci. USA* **105**, 13421–13426 (2008).
35. Li, Y. *et al.* MicroRNA-34a inhibits glioblastoma growth by targeting multiple oncogenes. *Cancer Res.* **69**, 7569–7576 (2009).
36. Miranda, K.C. *et al.* A pattern-based method for the identification of microRNA-target sites and their corresponding RNA/RNA complexes. *Cell* **126**, 1203–1217 (2006).
37. Godar, S. *et al.* Growth-inhibitory and tumor-suppressive functions of p53 depend on its repression of CD44 expression. *Cell* **134**, 62–73 (2008).
38. Jin, L., Hope, K.J., Zhai, Q., Smadja-Joffe, F. & Dick, J.E. Targeting of CD44 eradicates human acute myeloid leukemic stem cells. *Nat. Med.* **12**, 1167–1174 (2006).
39. Ji, Q. *et al.* MicroRNA miR-34 inhibits human pancreatic cancer tumor-initiating cells. *PLoS ONE* **4**, e6816 (2009).

ONLINE METHODS

Quantification of mature miRNA levels using qRT-PCR. We quantified miRNA levels using TaqMan MicroRNA Assays (Applied Biosystems)[25,26]. Briefly, we first isolated total RNA from unsorted LAPC9, LAPC4 and Du145 xenograft-derived cells and then recovered small RNA fractions (<200 nucleotides) using the mirVANA PARIS miRNA Isolation Kit (Ambion). We measured RNA concentrations using absorbance at 260 nm. We used the small RNAs from unsorted cells to measure the levels of a library of 324 sequence-validated human miRNAs and then compared the expression of 137 miRNAs in $CD44^+$ and $CD44^-$ LAPC9, LAPC4 and Du145 cells, side-population and non–side-population LAPC9 cells, and $CD133^+$ and $CD133^-$ LAPC4 cells (**Fig. 1a**). For qRT-PCR analysis[25,26], we defined the threshold cycle (*C*t) as the fractional cycle number at which fluorescence exceeds the fixed threshold of 0.2. Quantitative miRNA expression data were analyzed using d*C*t (the *C*t value normalized to internal 'housekeeping' miRNAs such as miR-24 and miR-103) and dd*C*t (difference between the d*C*t of positive population and that of the negative population) values for each of the miRNAs. When necessary, we converted dd*C*t to percentage of expression using the formula $2^{-\mathrm{dd}Ct}$. We used total RNA (10 ng) for all other measurements of individual miRNA levels, including those in primary tumor–derived cells.

Therapeutic experiments. We performed four sets of therapeutic experiments. (i) We repeatedly injected subcutaneous PPC-1 tumors intratumorally[26] with miR-NC or miR-34a oligos mixed with siPORT amine (Ambion). (ii) We implanted 500,000 PC3-GFP cells in the dorsal prostate of male NOD-SCID mice and allowed tumors to develop for 3 weeks. Starting from day 22, we injected miR-34a or NC oligos complexed with RNALancerII *in vivo* delivery reagent (BIOO Scientific) into tail veins of randomly selected mice ($n = 9$ for each group) every 2 d at a rate of 1 mg of oligos per kg of body weight[26]. All animals were killed after the fifth injection, and DP tumors were isolated and analyzed. (iii) We implanted 500,000 LAPC9-GFP cells each in the dorsal prostate of NOD-SCID mice. On day 22, animals were randomly assigned to miR-34a and NC groups ($n = 6$ for each), injected in the same way, and killed when they became moribund. The experiment was ended 13 d after initiation of injections. We removed tumors and lungs as well as several other organs including the pancreas, lymph nodes, liver and kidney to assess metastasis. Representative lung images were captured and quantified for metastases (GFP^+ foci). (iv) We carried out the same procedure as in (iii) but with more animals ($n = 10$ for each group) and more injections (15).

miR-34a binding sites, site-specific mutagenesis and luciferase experiments. We used rna22 program (ref. 36; http://cbcsrv.watson.ibm.com/rna22.html) to compute putative target sites for miR-34a in the human CD44 mRNAs and found two potential miR-34a binding sites at 3′-UTR (Gi48255940). To characterize the identified sites, we first amplified the 3′ UTR of human CD44 from LNCaP genomic DNA using primers 5′-AGAGCTCCACCTACACCA TTATCTTG-3′ and 5′-TAAGCTTGGAAGTCTTCAGGAGACAC-3′. The 2.55-kb PCR fragment was cloned into pGEM-T vector (Promega) and its sequence confirmed. For site-specific mutagenesis, we mutated the regions in the CD44 3′ UTR complementary to the seed sequence of miR-34a (M1, CATTTCCCA to GCAATCGGT; M2, GTTACTGCCA to CCGCGACAGT) using the QuikChange II Site-Directed Mutagenesis Kit (Stratagene). For luciferase assays, we cloned wild-type or mutant CD44 3′ UTRs into the HindIII and SacI sites of the 3′-UTR/pMIR vector (Ambion). We seeded prostate cancer cells in 24-well plates (3×10^4 cells per well) and co-transfected them with 1 μg reporters with 24 pmol miR-34a or miR-NC together with *Renilla* luciferase internal normalization plasmid (phRL-CMV). We determined the ratio of firefly to *Renilla* luciferase activity with a dual luciferase assay (Promega) 48 h later.

Migration and invasion assays, CD44 knockdown and 'rescue' experiments. We performed knockdown experiments using pGIPz-CD44shRNA (CD44-sh) or pGIPz-NS (non-silencing) lentiviruses (Open Biosystems) at a multiplicity of infection (MOI) of 20 (see **Supplementary Fig. 1d** for vectors and knockdown effects). We performed invasion assays in $CD44^+$ and $CD44^-$ Du145 cells using Matrigel Invasion Chamber (8-μm pore size, BD). We carried out migration assays in a similar way but without the Matrigel. In some experiments, purified $CD44^+$ Du145 cells were first transfected with NC or miR-34a oligos. We seeded cells (5×10^4) in the upper chamber of the insert and used medium containing 20% FBS in the lower chamber as a chemoattractant. After 22 h, we removed non-invaded (or non-migrated) cells with a cotton swab, stained invaded or migrated cells with HEMA3 (Fisher Scientific), and counted them under a microscope. For the rescue experiments, we infected $CD44^+$ Du145 cells with pBabe-puro (vector) or pBabe-CD44 (Addgene) retroviruses in the presence of 8 μg ml^{-1} polybrene. After 24 h, we transfected cells with miR-34a oligos (24 h) before invasion assays. In these experiments ($n = 3$–4), the percentage of invaded cells was converted into an invasion index, which was considered as one in all control groups.

Additional methods. Detailed methodology is described in **Supplementary Methods**.

doi:10.1038/nm2284

SUPPLEMENTARY INFORMATION

The microRNA miR-34a inhibits prostate cancer stem cells and metastasis by directly repressing CD44

Can Liu[1,2], Kevin Kelnar[3], Bigang Liu[1], Xin Chen[1,2], Tammy Calhoun-Davis[1], Hangwen Li[1], Lubna Patrawala[3], Hong Yan[1], Collene Jeter[1], Sofia Honorio[1], Jason Wiggins[3], Andreas G. Bader[3], Randy Fagin[4], David Brown[3] & Dean G. Tang[1,2]

[1]*Department of Molecular Carcinogenesis, the University of Texas M.D. Anderson Cancer Center, Science Park, Smithville, TX 78957, USA*

[2]*Program in Molecular Carcinogenesis, The University of Texas Graduate School of Biomedical Sciences (GSBS), Houston, TX 77030, USA*

[3]*Mirna Therapeutics, Inc., Austin, TX 78744, USA*

[4]*The Hospital at Westlake, Austin, TX 78759, USA*

This PDF contains:

Nature Medicine: doi:10.1038/nm.2284

SUPPLEMENTARY RESULTS

The expression levels of miR-34a, but not miR-34b and miR-34c, in normal prostate and prostate cancer cells correlate with the p53 status.

To determine whether miR-34a expression in normal prostate and prostate cancer cells might be regulated by p53, we employed qRT-PCR analysis to correlate the expression levels of endogenous miR-34a (localized on chromosome 1p36.22) with the p53 status in ten prostate cells (**Supplementary Fig. 1a,b**). These cells included primary prostate epithelial cell strains NHP8 (normal human prostate epithelial strain 8) and NHP9 (normal human prostate epithelial strain 9) (4); immortalized NHP9 cells (NHP9-IM) (4); cultured prostate cancer cell lines LNCaP, LNCaP C4-2 (a LNCaP subline), PC3, PPC-1, and Du145; and prostate cancer cells LAPC4 and LAPC9 freshly purified from xenograft tumors. The NHP8, NHP9, NHP9-IM, and two LNCaP lines express wild-type (wt) p53 (1,4), as evidenced by low levels of p53 protein in these cells (**Supplementary Fig. 1b**). LAPC9 cells also expressed wt p53 as revealed by our genomic DNA sequencing of exons 5-8 (data not shown). PC3 and PPC-1 cells were p53 null whereas Du145 and LAPC4 cells harbor mutant p53 (1), as supported by Western blotting analysis (**Supplementary Fig. 1b**). qRT-PCR analysis revealed that the four prostate cancer cells harboring mutant or null p53 displayed much lower levels of miR-34a than the six cell types with wt p53 (**Supplementary Fig. 1a**; note that we utilized PPC-1 cells, which expressed the lowest level of miR-34a mRNA, as the normalization control), suggesting that p53 regulates the baseline miR-34a expression in prostate and prostate cancer cells. Interestingly, among the six p53-wt cells, LNCaP and C4-2 cells expressed higher levels of miR-34a than NHP8, NHP9, NHP9-IM, and LAPC9 cells (**Supplementary Fig. 1a**).

To determine whether p53 may also regulate the baseline expression levels of the other two miR-34 family members, miR-34b and miR-34c, which are localized on chromosome 11 q23.1 and were not differentially expressed between the $CD44^+$ and $CD44^-$ prostate cancer cells, we also employed qRT-PCR to measure their levels in the same ten prostate cells. In contrast to miR-34a, miR-34a and miR-34c showed similar expression patterns and were not strictly correlated with the p53 status (**Supplementary Fig. 1a**). For

Nature Medicine: doi:10.1038/nm.2284

example, in p53 null or mutant cells, although PPC-1, PC3, and LAPC4 cells exhibited undetectable miR-34b and miR-34c, Du145 cells showed extremely high levels of both miRNAs (**Supplementary Fig. 1a**), suggesting p53-independent regulation of miR-34b and miR-34c in certain prostate cancer cells. Similarly, miR-34b and miR-34c levels showed wide variations in the six p53-wt cells.

Finally, we measured the baseline levels of let-7b in the ten prostate cells as this miRNA was also downregulated in the $CD44^+$ prostate cancer cells (**Fig. 1b**). The let-7b expression pattern was somewhat like that of miR-34a in that it was much higher in LNCaP and C4-2 cells (**Supplementary Fig. 1a**). However, unlike miR-34a, its expression was readily detectable in p53 mutant or null prostate cancer cells (**Supplementary Fig. 1a**).

Transfection of miR-34a oligos induced cell-cycle arrest, apoptosis or senescence in p53-mutant and p53-null prostate cancer cells.

Since p53 is frequently mutated in advanced prostate cancer, we transfected p53-mutant or null Du145, PC3, and PPC-1 cells with synthetic mature miR-34a oligonucleotides (oligos) or the negative control miRNA (miR-NC or NC) that contains a scrambled sequence and does not specifically target any human gene products (**Supplementary Fig. 1c**). The miR-34a mimics the dicer cleavage product that is loaded into the RISC in the cytoplasm and therefore, no processing of the pre-miRNA is required for it to be activated (thus it represents a mature miRNA). Transfected miR-34a oligos caused inhibitory effects in all three prostate cancer cells (**Supplementary Figs. 2** and **3**). In Du145 cells, miR-34a oligo transfection reduced cell numbers and population doublings (**Supplementary Fig. 2a,b**) as a result of inhibition of cell proliferation (**Supplementary Fig. 2c**). In PC3 cells, miR-34a oligos inhibited population doublings by causing apoptosis (**Supplementary Fig. 3a–c**). In PPC-1 cells, transfected miR-34a oligos inhibited proliferation, increased senescence, and induced apoptosis resulting in reduced total cell numbers and cumulative population doublings (**Supplementary Fig. 3d–g**).

Nature Medicine: doi:10.1038/nm.2284

SUPPLEMENTARY METHODS

Cells and animals. We obtained prostate cancer cell lines, LNCaP, LNCaP C4-2, PC3, PPC-1, and Du145, from ATCC and maintained them as described[1-3]. Primary and immortalized normal human prostate (NHP) epithelial cells were detailed elsewhere[4]. We purified LAPC4 and LAPC9 (and, sometimes, Du145) cells from xenograft tumors (see below)[3,5-8]. Immune-deficient mice, NOD–SCID (non-obese diabetic severe combined immune deficient) and NOD–SCIDγ, were produced mostly from our own breeding colonies and purchased occasionally from the Jackson Laboratories (Bar Harbor) and maintained in standard conditions according to the Institutional guidelines. All animal experiments were approved by our institutional IACCUC.

Prostate cancer cell purification. We routinely maintained human xenograft prostate tumors, *i.e.*, LAPC9 (bone metastasis; AR^+ and PSA^+), LAPC4 (lymph node metastasis; AR^+ and PSA^+), and Du145 (brain metastasis; AR^- and PSA^-), in NOD–SCID mice. We first purified human prostate cancer cells out of xenografts by depleting murine cells. $CD44^+$ and $CD44^-$ cells were further purified using fluorescence-activated cell sorting (FACS) with the purities of both populations being >98% (5,6). $CD133^+$ and $CD133^-$ LAPC4 cells were purified using biotinylated monoclonal antibody to CD133 (AC133) and the magnetic beads (MACS) by following the manufacturer's instructions (Miltenyi Biotech). Post-sort analysis revealed purities of both populations being >95%. We purified the side population (SP) of LAPC9 cells by FACS as previously described[3]. We obtained primary human prostate tumors (HPCa; Supplementary Table 1) with the patients' consent from Da Vinci robotic surgery. All work with HPCa samples was approved by the M.D. Anderson Cancer Center Institutional Review Board (IRB LAB04-0498). We purified epithelial HPCa cells through a multi-step process and by depleting lineage-positive hematopoietic, stromal, and endothelial cells[4,7,8]. We then purified Lin^-CD44^+ HPCa cells using MACS or FACS (Supplementary Table 1).

Transient transfection with oligos. We plated bulk or purified $CD44^+$ prostate cancer cells 24 h before transfection with 33 nM of miR-34a or non-targeting negative control miRNA (miR-NC) oligos (Ambion) by using Lipofectamine 2000 (Invitrogen). Alternatively, we transfected bulk or purified $CD44^-$ prostate cancer cells with 33 nM of anti-miR-34a (anti-34a) or anti-miR-NC (anti-NC) oligos (Ambion). In some experiments (see below), oligos were electroporated into prostate cancer cells. We generally harvested the transfected cells for *in vitro* or *in vivo* studies after culturing for overnight to 24 h.

Retroviral and lentiviral mediated overexpression of miR-34a. Basic retroviral and lentiviral procedures were previously described[4,7] and the key vectors used in the present study were presented in Supplementary Fig. 1d. An MSCV retroviral vector directing the expression of pre-miR-34a (MSCV-34a) and the empty control vector, MSCV-PIG (Puromycin-IRES-GFP), were used in previous studies[9]. prostate cancer cells were infected with the retroviral supernatant for 48 h in the presence of 8 μg ml^{-1} polybrene. Two days after infection, puromycin was added to the media at 3 μg ml^{-1}, and cell populations were selected for 2 weeks. A lentiviral vector encoding pre-miR-34a (lenti-34a) and the control vector

Nature Medicine: doi:10.1038/nm.2284

(lenti-ctl) (Supplementary Fig. 1d) were obtained from Systems Biosciences (SBI). Lentivirus was produced in 293FT packaging cells and titers determined for GFP using HT1080 cells. prostate cancer cells were infected at an MOI of 10 - 20 and harvested 48–72 h post-infection.

Experiments correlating miR-34a levels in normal prostate and prostate cancer cells with the p53 status. We employed qRT-PCR to quantify the levels of miR-34a, and, for comparisons, of miR-34b, miR-34c, and let-7b in NHP8, NHP9, and NHP9-IM, LNCaP, LNCaP C4-2, PC3, PPC-1, Du145, LAPC4, and LAPC9 cells. For qRT-PCR analysis[10], we prepared total RNA from these cells and assayed the levels of miR-34a (assay ID 000426, TaqMan miRNA Assay, ABI), miR-34b (ABI assay ID 000427), miR-34c (ABI assay ID 000428), and hsa-let-7b (let-7b; ABI assay ID 000378).

BrdU incorporation assays, senescence β-gal (SA-βgal) staining, Western blotting, immunofluorescence, flow cytometry analysis (FACS), and immunohistochemistry (IHC). These procedures were previously described[2-8]. For Western blotting of p53 in ten prostate cells, protein lysate (50 μg) was separated on SDS-PAGE, transferred to nitrocellulose membrane, and probed with a monoclonal Ab to p53 (clone MO-1). For characterization of the knockdown effect of pGIPz-CD44shRNA, PC3 or Du145 cells were infected with this vector or the pGIPz control vector (MOI 20; 72 h) and cells were harvested for Western blotting of CD44 or β-actin (loading control) (see Supplementary Fig. 1d).

***In vitro* effects of miR-34a overexpression on bulk prostate cancer cells.** For studies in Du145 cells, we first electroporated cells (Bio-Rad GenePulserXcell, 150 mV, 25 mS) in 200 μl of serum-free OPTIMEM in triplicate with 1.6 μmol L^{-1} miR-34a or miR-NC oligos. Immediately after electroporation, we added 800 μl of serum-containing medium to each cuvette, and plated one million live cells in triplicate on d 0. At the end of 1 week, cells were dissociated, counted, re-electroporated (600,000 cells/well in triplicate), and plated. We repeated this process one week later at d 14 and terminated the whole experiment at the end of the third week (d 21). We then determined the cumulative cell numbers and population doublings (PDs). For BrdU incorporation assays, we transfected Du145 cells with miR-NC or miR-34a oligos (33 nM) using Lipofectamine and plated cells at two different densities (*i.e.*, 10,000 or 5,000 cells/well) on glass coverslips. Cells were terminated either 2 or 5 d after plating and used in BrdU staining.

For studies in PC3 cells, we also electroporated cells with miR-NC or miR-34a oligos, plated one million cells of each type in triplicate, and cultured them in RPMI-1640 plus 7% FBS. At the end of one week, cells were photographed and then dissociated, counted, re-electroporated (600,000 cells each in triplicate), and replated. The procedure was repeated at the end of the second week and at the end of the third week (*i.e.*, 21 d), cells were harvested and experiments terminated. We electroporated PPC-1 cells with miR-NC or miR-34a oligos on d 0 and carried out subsequent experiments as for PC3 cells except that we enumerated cells every 2–3 d. For BrdU assays, we transfected PPC-1 cells with miR-NC or miR-34a oligos (33 nM) for 24 h and then plated 15,000 cells each on glass coverslips. 24 h later, we terminated cells and performed BrdU staining.

Nature Medicine: doi:10.1038/nm.2284

Clonal, clonogenic, and sphere-formation assays. *For holoclone assays*[8,11], we plated prostate cancer cells at a clonal density (*i.e.*, 100 cells/well) in a 6-well dish, counted the number of holoclones several days later, and presented the percentage of cells that established a holoclone as cloning efficiency. *For clonogenic assays*[5,7,8], we plated cells generally at 1,000 cells/well in Matrigel (MG) or methylcellulose (MC) at 1:1 ratio in 100–200 μl and enumerated colonies 1–2 weeks after plating. *For sphere-formation assays*[5,7,8], we generally plated cells at 5,000–10,000 cells/well in serum-free prostate epithelial basal medium (PrEBM) supplemented with 4 μg ml^{-1} insulin, B27 (Invitrogen), and 20 ng ml^{-1} EGF and bFGF in ultra-low attachment (ULA) plates. Floating spheres that arose in 1–2 weeks were counted. For sphere-formation assays in HPCa cells, we purified HPCa cells from human primary tumors, i.e., HPCa101 (Gleason 9), HPCa107 (Gleason 7), HPCa109 (Gleason 7), and HPCa112 (Gleason 6), and infected with lenti-ctl or lenti-34a vectors (MOI 20) overnight. Next day, equal numbers of live cells (20,000/well) were plated in triplicate in ULA plates in serum-free medium containing B27, EGF, and bFGF and spheres enumerated at 11 d (for HPCa107), 33 d (for HPCa109), or 9 d (for HPCa112) after plating. For all above experiments, we run a minimum of triplicate wells for each condition and repeated experiments whenever feasible.

Tumor transplantation experiments. Basic procedures for subcutaneous (s.c) and orthotopic (DP) tumor transplantations can be found in our earlier publications[3-8]. *For tumor experiments in LAPC9 cells*, we acutely purified LAPC9 cells from the maintenance tumors and transfected with miR-34a or miR-NC oligos (33 nM). 24 h later, 100,000 cells each were implanted, in 50% Matrigel, into the DP of intact male NOD-SCID mice. *For tumor experiments in LAPC4 cells*, we freshly purified LAPC4 cells from xenograft tumors and transfected with miR-NC or miR-34a oligos (33 nM). 100,000 cells each were injected s.c in male NOD-SCID mice. Alternatively, purified LAPC4 cells were infected with either the control (lenti-ctl) or lenti-miR-34a (lenti-34a) lentiviral vectors (both at an MOI of 10). 24 h after infection, 10,000 cells each were injected s.c in male NOD-SCID mice. *For tumor experiments in Du145 cells*, in addition to oligo transfection, we also infected cultured Du145 cells with either the control retroviral vector (MSCV-PIG) or a retroviral vector encoding miR-34a (MSCV-34a)(9), followed by puromycin selection and s.c injection in Matrigel. Alternatively, Du145 cells were infected with lenti-ctl or lenti-34a vectors (MOI 10) and, 24 h after infection, 10,000 cells of each type (n = 10) were injected s.c in NOD-SCID mice. *For tumor experiments in PPC1 cells*, we electroporated cultured PPC-1 cells with miR-34a or NC oligos (1.6 μM or 5 μg) on d 0. We injected 500,000 live cells s.c in NOD-SCID mice and measured tumor volumes, using a digital caliper, starting from d 3. On d 7, 13, 20, and 25, we injected miR-NC or miR-34a oligos mixed with siPORT amine (Ambion) intra-tumorally[10].

Experiments with HPCa58 early-generation xenograft tumors. HPCa58 xenograft tumor

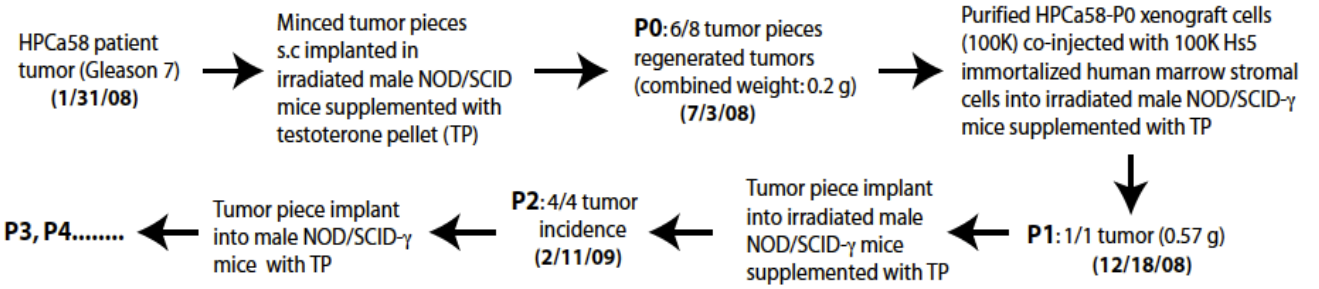

Nature Medicine: doi:10.1038/nm.2284

was established using the *Scheme* below. Briefly, the primary tumor pieces were first implanted into γ-irradiated (4 Gy; X-ray) male NOD-SCID mice. The P0 xenograft tumors were pooled and used to purify out human prostate cancer cells as described above, which were then co-injected with the Hs5 immortalized human marrow stromal cells in male NOD-SCIDγ mice. Subsequent passaging of the first-generation (P1) xenografts was performed by implanting tumor pieces or by injecting purified HPCa58 cells alone without Hs5 cells. We have utilized similar strategies to establish about 8 early-generation human prostate cancer xenografts (including HPCa87 and HPCa91 xenografts; see Supplementary Table 1). These xenograft tumors were of the human origin and morphologically epithelial with detectable cytokeratin 8 and 18. RT-PCR analysis detected *AR* whereas Western blotting detected racemase expression in most xenografts (Chen et al., manuscript in preparation). For the present study, HPCa58 cells were purified from a P3 xenograft tumor (see *Scheme*) and infected with lenti-ctl or lenti-34a vectors (MOI 20). 24 h later, 100,000 cells of each were s.c injected into the NOD-SCIDγ mice. The 1° tumors were harvested 21 d later and 10,000 purified GFP^+ (*i.e.*, infected) tumor cells from respective 1° tumors were injected and the 2° tumors were harvested 26 d later.

Monitoring metastasis. For metastasis analysis[5,8], we first observed tumor-bearing animals for symptoms such as hunched posture, irregular breathing and gait, and paraplegia. When systemic symptoms or primary tumor burden became obvious or when the animals became moribund, we sacrificed them by CO2 euthanization and cervical dislocation. We then performed comprehensive necropsy to isolate individual organs, which were examined for gross metastases. Finally, GFP^+ metastatic foci in each organ (primarily, the lung) were examined and quantified under a Nikon SMZ1500 whole-mount epifluorescence dissecting microscope.

Measuring cell migration by time-lapse videomicrocopy

We seeded bulk Du145 or purified $CD44^+$ and $CD44^-$ cells onto the glass-bottom dish (CELLview^{tm}, 4 compartments, Greiner Bio-One GmbH) and cultured them overnight to create a monolayer. We introduced a homogeneous ‘wound’ track using the tip of a fine forceps. Cells were washed with PBS to remove the debris and smoothen the wound edges. We then placed cells in the culture chamber connected to the time-lapse microscope (Nikon, BioStation IM). We acquired phase-contrast images of at least 20 selected fields of each group at the interval of 30 min for a total of 24 h. We analyzed images using the NIS Elements software (Nikon, NIS elements- 2.35) and quantified cell migration by measuring the time required to close the induced wounds.

Statistical analyses. In general, we used unpaired two-tailed Student’s *t*-test to compare differences in cell numbers, cumulative PDs, percentages of $CD44^+$, % $BrdU^+$ or SA-βgal^+ cells, cloning efficiency, tumor weights, migration, invasion, and other related parameters. We employed Fisher’s Exact Test and χ^2 test to compare incidence and latency. We used the Log-Rank test to analyze the survival curves and ANOVA (F-test) to compare differences in multiple groups. In all these analyses, a $P < 0.05$ was considered statistically significant.

Nature Medicine: doi:10.1038/nm.2284

SUPPLEMENTARY REFERENCES

1. Pienta, K.J. *et al*. The current state of preclinical prostate cancer animal models. *Prostate* **68**, 629-639 (2008).
2. Bhatia, B. *et al*. Evidence that senescent human prostate epithelial cells enhance tumorigenicity: Cell fusion as a potential mechanism and inhibition by p16INK4a and hTERT. *Int. J. Cancer* **122**, 1483-1495 (2008).
3. Patrawala, L. *et al*. Side population (SP) is enriched in tumorigenic, stem-like cancer cells whereas ABCG2$^+$ and ABCG2$^-$ cancer cells are similarly tumorigenic. *Cancer Res*. **65**, 6207-6219 (2005).
4. Bhatia, B. *et al*. Critical and distinct roles of p16 and telomerase in regulating the proliferative lifespan of normal human prostate epithelial progenitor cells. *J. Biol. Chem.* **283**, 27957-27972 (2008).
5. Patrawala, L. *et al*. Highly purified CD44$^+$ prostate cancer cells from xenograft human tumors are enriched in tumorigenic and metastatic progenitor cells. *Oncogene* **25**, 1696-1708 (2006).
6. Patrawala, L., Calhoun-Davis, T., Schneider-Broussard, R. & Tang, D.G. Hierarchical organization of prostate cancer cells in xenograft tumors: the CD44$^+\alpha 2\beta 1^+$ cell population is enriched in tumor-initiating cells. *Cancer Res.* **67**, 6796-6805 (2007).
7. Jeter, C. *et al*. Functional evidence that the self-renewal gene NANOG regulates human tumor development. *Stem Cells* **27**, 993-1005, 2009.
8. Li, H.W. *et al*. Methodologies in assaying prostate cancer stem cells. *Methods Mol. Biol.* **569**, 85-138 (2009).
9. He, L. *et al*. A microRNA component of the p53 tumour suppressor network. *Nature* **447**, 1130-1134 (2007).
10. Wiggins, J.F. *et al*. Development of a lung cancer therapeutic based on the tumor suppressor microRNA-34. *Cancer Res*. 70, 5923-5930 (2010).
11. Li, H.W., Chen, X., Calhoun-Davis, T., Claypool, K. & Tang, D.G. PC3 Human prostate carcinoma cell holoclones contain self-renewing tumor-initiating cells. *Cancer Res*. 68, 1820-1825 (2008).

Nature Medicine: doi:10.1038/nm.2284

Supplementary Figure 1. miR-34a levels in prostate cells correlate with p53 status.

(a) qRT-PCR quantification of miR-34a, miR-34b, miR-34c, and let-7b in 10 prostate cell lines. The relative expression levels (mean ± S.D) are presented by setting the miRNA levels in PPC-1 cells as one. Shown below the bar graphs are the p53 statuses (N, null; M, mutant; W, wild-type) and the % of $CD44^+$ cells in each cell type as determined by flow cytometry or immunofluorescence staining (U.D, undetectable).

(b) Western blotting of p53 in prostate (cancer) cells.

(c) The four oligonucleotides (oligos) used in the current study. All oligos were obtained from Ambion and at least 3 studies (references indicated) have utilized and characterized miR-34a and miR-NC oligos. Use of anti-miR-NC oligos has been published in at least one study (i.e., reference 25) and anti-miR-34a was characterized in the present study.

(d) Retroviral and lentiviral vectors utilized in the present study. Shown at the bottom was the characterization of the knockdown effect of pGIPz-CD44shRNA by Western blotting.

Nature Medicine: doi:10.1038/nm.2284

Supplementary Figure 1

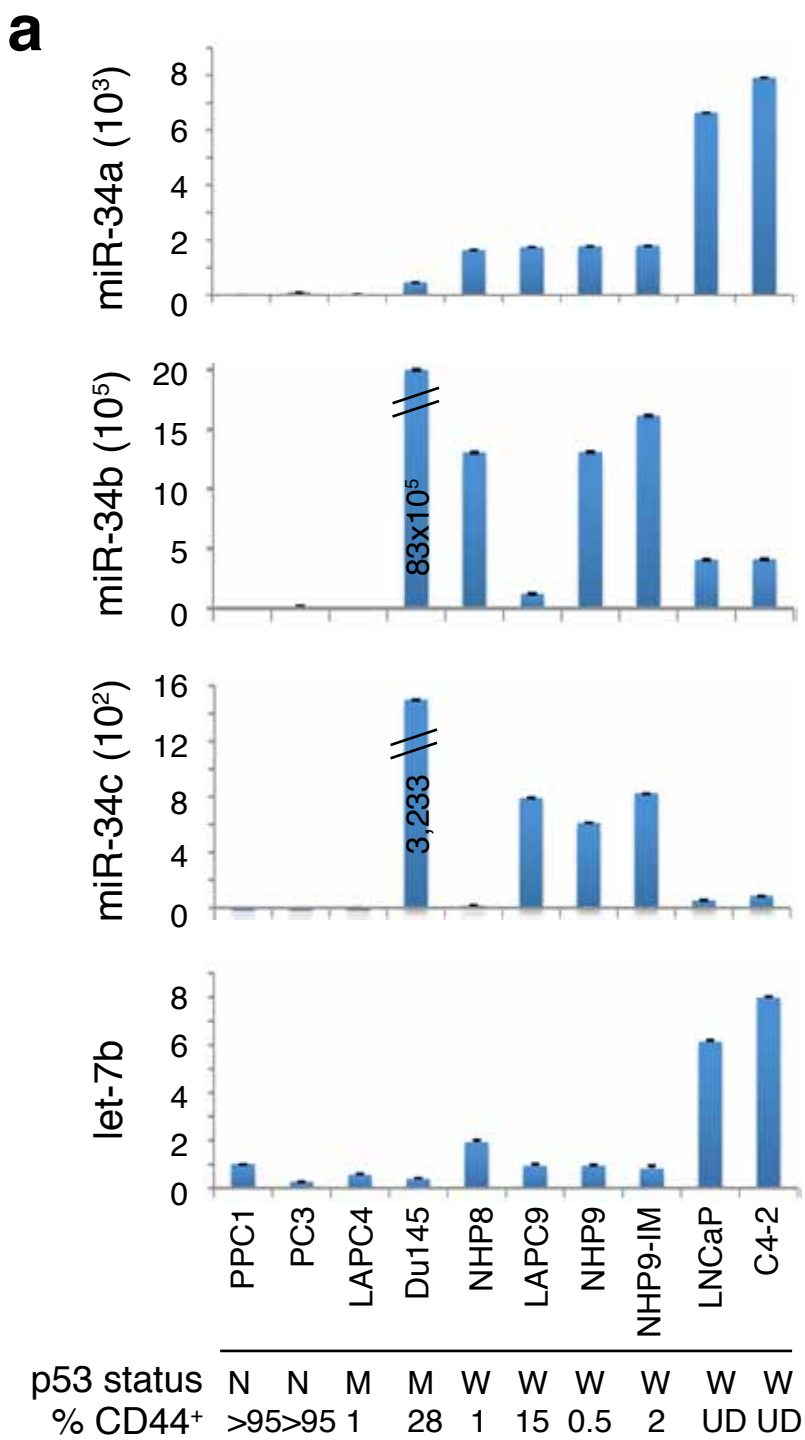

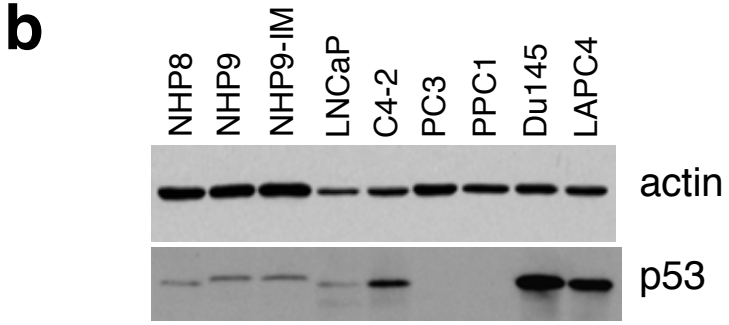

c

Name	Source	Ref.
miR-34a (mature) oligos	Ambion	26,31,32
miR-NC (neg. control) oligos	Ambion	26,31,32
anti-miR-34a oligos	Ambion	this study
anti-miR-NC oligos	Ambion	25

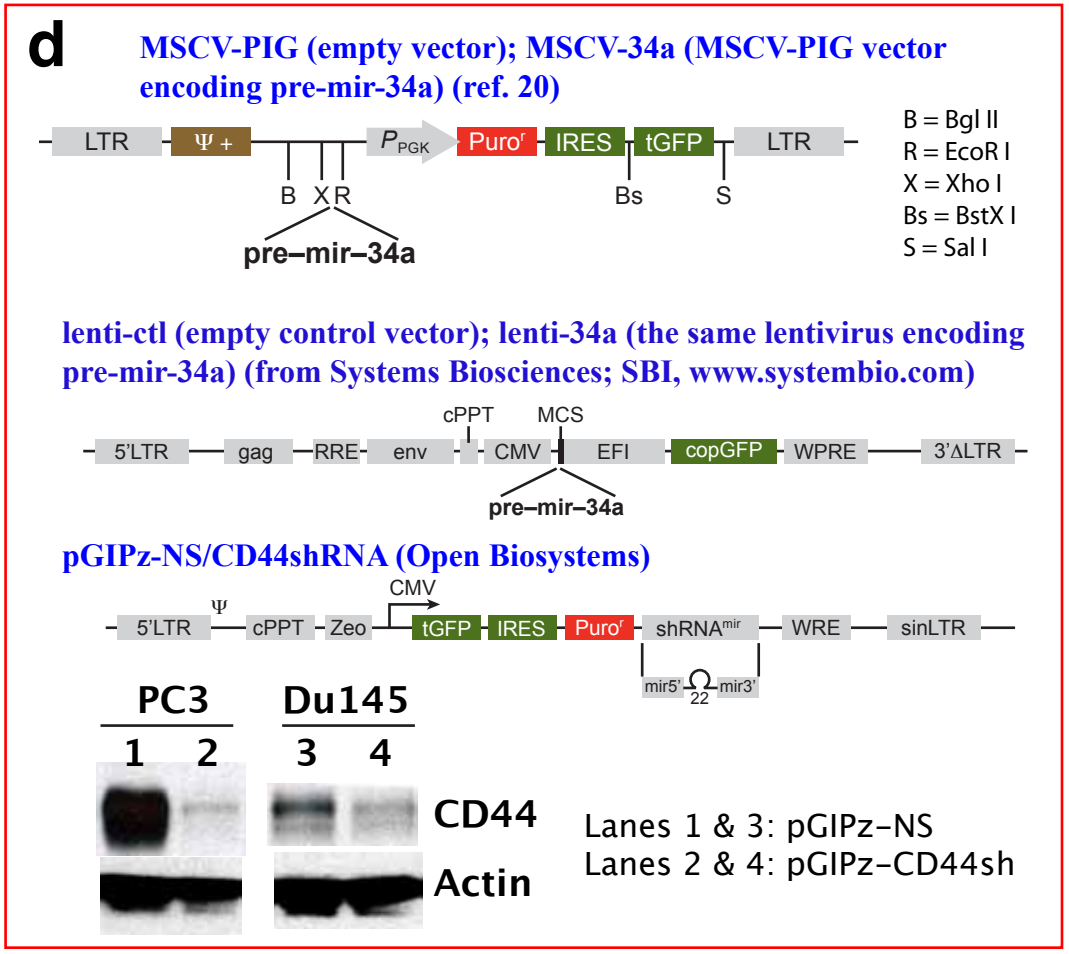

Nature Medicine: doi:10.1038/nm.2284

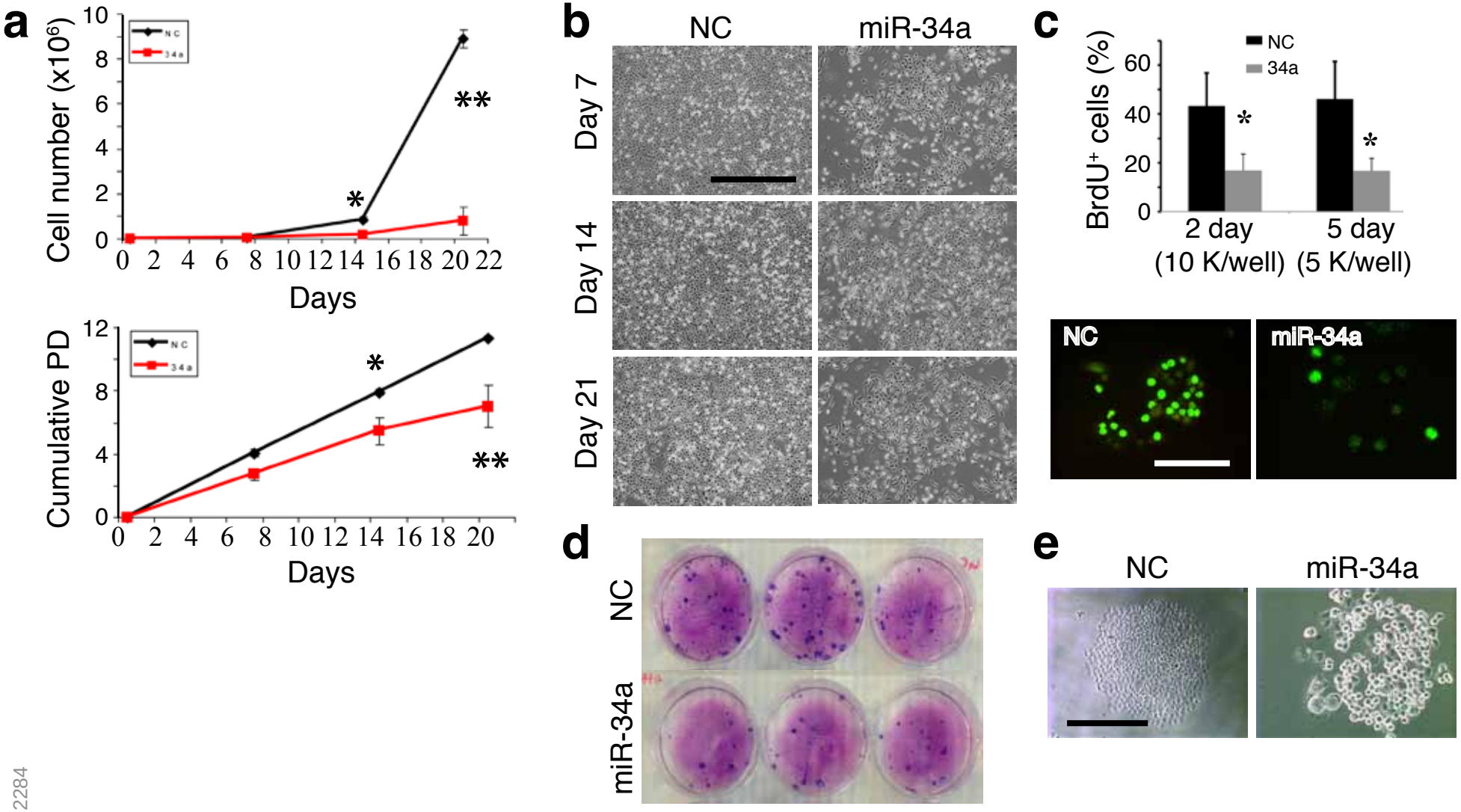

Supplementary Figure 2. miR-34a inhibits Du145 cell proliferation and clonal expansion.

(**a**,**b**) Exogenous miR-34a reduces Du145 cell number. Plotted is the cumulative cell numbers or population doublings (PDs) as a function of time and bars represent the mean ± S.D (*$P < 0.05$; **$P < 0.001$). Shown in b are representative microphotographs (scale bar, 10 μm). (**c**) miR-34a inhibits Du145 cell proliferation. Presented is the mean % of BrdU-positive cells counted from a total of 800–1,000 cells performed under two conditions (*$P < 0.001$). Below are representative images (scale bar, 10 μm) of BrdU staining in the 2-d samples. (**d,e**) miR-34a inhibits Du145 clonal expansion. Cells transfected with miR-NC or miR-34a oligos (33 nM) were plated in triplicate at 100 cells/well. The experiment was terminated at 9 d and wells were Giemsa-stained (d). Shown in e are clonal images (scale bar, 10 μm). Results shown in d and e were representative of two independent experiments.

Nature Medicine: doi:10.1038/nm.2284

Supplementary Figure 3. Effects of miR-34a overexpression on PC3 and PPC-1 cells.

(**a**,**b**) Exogenous miR-34a reduces PC3 cell number. Cumulative cell numbers and PDs were presented and bars represent the mean ± S.D (*$P < 0.05$; **$P < 0.001$). Shown in b are representative microphotographs of treated PC3 cells at 7, 14, and 21 d post treatment (scale bar, 10 μm).

(**c**) miR-34a induces apoptosis in PC3 cells. Samples harvested at the end of 21 d (above) were used in DEVDase assays, which measure caspase-3 or 7 (C3/7) activities.

(**d**,**e**) miR-34a transfection reduces PPC-1 cell number. PPC-1 cells were electroporated with miR-NC or miR-34a oligos on d 0 and subsequent experiments were carried out as for PC3 cells except that cells were enumerated every 2-3 d using triplicate samples and re-electroporation was done on d 4 and 11, respectively (arrows). Cumulative cell numbers and PDs were presented (d). Shown in e are representative microphotographs (scale bar, 10 μm) of treated PPC-1 cells at d 7.

(**f**–**i**) miR-34a inhibits PPC-1 cell proliferation and induces senescence. Presented in f is the % of $BrdU^+$ cells (mean ± S.D; $n = 3$). g, 100,000 PPC-1 cells transfected with NC or miR-34a oligos were plated for SA-βgal staining. Shown are total number of SA-βgal^+ cells in each well ($n = 3$) and representative microphotographs (below; scale bar, 10 μm). h, Holoclone assays in PPC-1 cells. 500 cells/well were plated in triplicate and holoclones imaged on d 5 (scale bar, 25 μm). i, Sphere-formation assays. 1,000 PPC-1 cells transfected with miR-NC or miR-34a oligos were plated in triplicate in 6-well ULA plates. Spheres were counted on d 10. Bars are mean ± SD ($n = 3$).

Nature Medicine: doi:10.1038/nm.2284

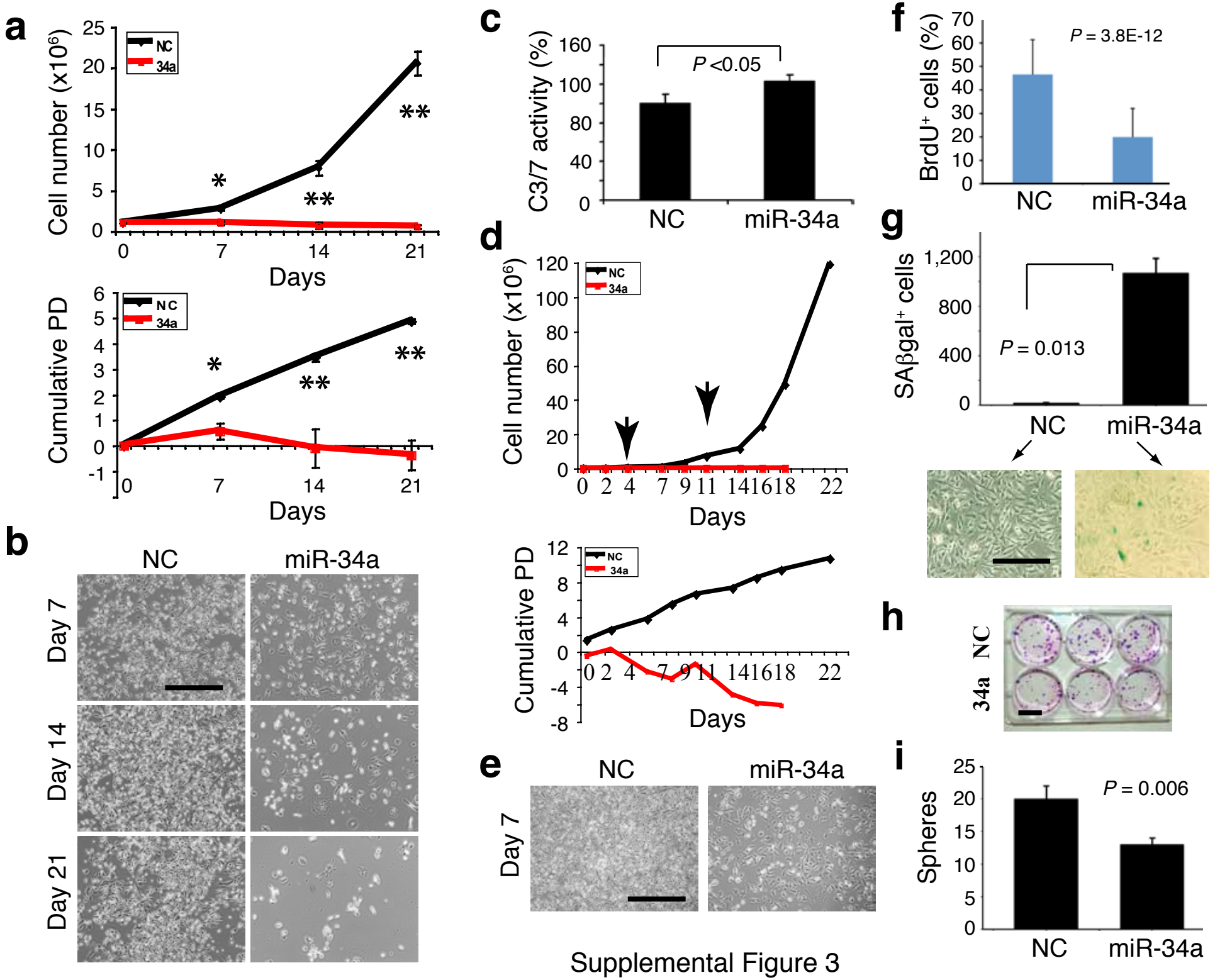

Supplemental Figure 3

Nature Medicine: doi:10.1038/nm.2284

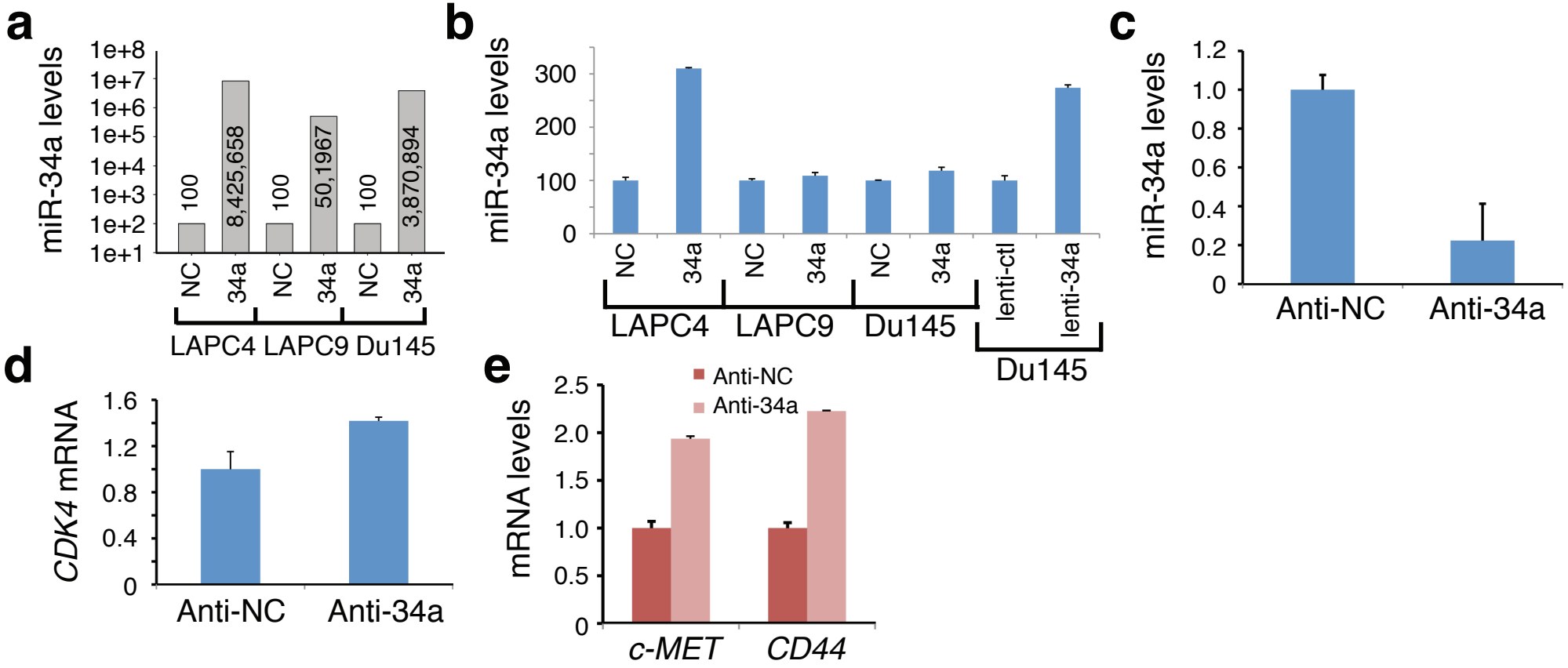

Supplementary Figure 4. Validations of miR-34a and anti-miR-34a.

(**a**) PCa cells freshly transfected with miR-34a oligos showed miR-34a levels several orders of magnitude higher than those transfected with miR-NC oligos. The indicated PCa cells purified from xenograft tumors were transfected with miR-34a or miR-NC oligos and, 24 h later, were harvested and used in tumor experiments whereas a small number of cells were set aside and used in qRT-PCR measurement of miR-34a. Shown are the mean miR-34a levels (in log scale; $n = 3$) in miR-34a transfected cells relative to those in the miR-NC transfected cells (actual mean values indicated in the bars).

(**b**) Loss of miR-34a in residual tumors. Residual tumors (see Supplementary Fig. 5) derived from cells transfected with miR-34a oligos or from Du145 cells infected with lenti-34a were used in qRT-PCR analysis of miR-34a. Shown are the miR-34a levels (in linear scale; mean ± S.D) relative to the respective control tumors.

(**c**) Anti-miR-34a reduces endogenous miR-34a levels. LAPC9 cells were transfected with anti-NC or anti-34a oligos (33 nM) and harvested 24 h later to prepare total RNA for qRT-PCR analysis of miR-34a. Presented are the relative levels normalized to the control miR-191 and miR-24 with the miR-34a in anti-NC-transfected cells set at one.

(**d**) Anti-miR-34a increases the *CDK4* mRNA levels. LAPC9 cells prepared as above were used in qRT-PCR measurement of *CDK4* mRNA (see Supplementary ref. 10). The abundance of *CDK4* mRNA was expressed as the levels relative to the anti-NC transfected cells.

(**e**) Anti-miR-34a increases the mRNA levels of c-MET and CD44. Du145 tumors from $CD44^-$ cells transfected with anti-34a or anti-NC were used in qRT-PCR of *c-MET* and *CD44* mRNAs (mean ± S.D; $n = 3$).

Nature Medicine: doi:10.1038/nm.2284

Supplementary Figure 5. Effects of miR-34a on tumor growth

Indicated are tumor incidence (tumors developed/numbers of injections; %), harvest time (including actual injection and termination dates), mean tumor weight (in grams), and the *P* values for tumor weights. Gross tumor images are not to the same scale.

(**a**) miR-34a oligo transfection inhibits orthotopic LAPC9 tumor regeneration.

(**b**) miR-34a oligo transfection inhibits LAPC4 tumor growth.

(**c**) miR-34a overexpression by lentiviral infection inhibits LAPC4 tumor growth. Note that all lenti-ctl tumors were green whereas most lenti-34a tumors were white and had little GFP-positive cells, suggesting that the small lenti-34a tumors were derived from the uninfected cells or from the infected cells that had lost miR-34a expression.

(**d**) miR-34a oligo transfection inhibits Du145 tumor growth.

(**e**) miR-34a overexpression by retroviral infection inhibits Du145 tumor regeneration. The MSCV-34a tumors were ~3 times smaller than the control tumors but the difference was at the statistical borderline due to small numbers of animals in each group that developed tumors.

(**f**) miR-34a overexpression by lentiviral infection inhibits Du145 tumor growth. Tumors were harvested at 49 d.

(**g**) miR-34a inhibits PPC-1 tumor development. Animals were terminated on d 46. Arrowheads indicate repeated intra-tumoral oligo injections. Shown are the tumor volumes (mean ± S.D; $n = 7$ for each group) measured on the indicated time points (d).

(**h**) miR-34a re-expression in purified $CD44^+$ LAPC9 inhibits tumor regeneration.

(**i**) Anti-miR-34a promotes tumor growth of purified $CD44^-$ Du145 cells. This represents an independent repeat experiment to Fig. 1h.

Nature Medicine: doi:10.1038/nm.2284

a

LAPC9 (100,000 cells/DP inj.)	Incidence	Harvest	Weight (g)	P value
miR-NC	8/8 (100%)	38 d (2/21/08 - 3/31/08)	0.62 ± 0.44	
miR-34a	5/7 (71%)	38 d	0.28 ± 0.15	0.038

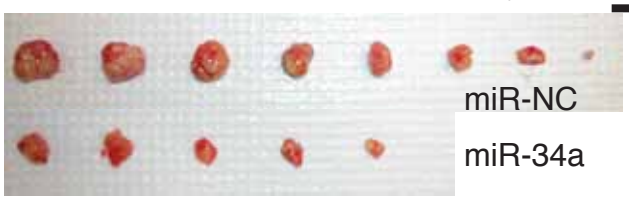

b

LAPC4 (100,000 cells/s.c inj.)	Incidence	Harvest	Weight (g)	P value
miR-NC	8/8 (100%)	10 d (2/03/08 - 2/13/08)	0.56 ± 0.27	
miR-34a	6/8 (75%)	10 d	0.29 ± 0.16	0.02

c

LAPC4 (10,000 cells/s.c inj.)	Incidence	Harvest	Weight (g)	P value
lenti-ctl	6/6 (100%)	69 d (2/11/09 - 4/21/09)	0.54 ± 0.32	
lenti-34a	6/6 (100%)	69 d	0.15 ± 0.09	0.015

d

Du145 (100,000 cells/s.c inj.)	Incidence	Harvest	Weight (g)	P value
miR-NC	8/8 (100%)	62 d (1/31/09 - 4/03/09)	0.82 ± 0.39	
miR-34a	8/8 (100%)	62 d	0.5 ± 0.18	0.03

e

Du145 (100,000 cells/s.c inj.)	Incidence	Harvest	Weight (g)	P value
MSCV -PIG	5/10 (50%)	37 d (1/29/09 - 3/07/09)	0.71 ± 0.47	
MSCV -34a	2/10 (20%)	37 d	0.28 ± 0.15	0.05

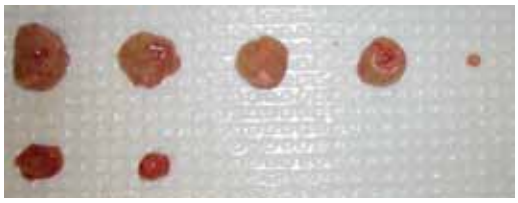

f

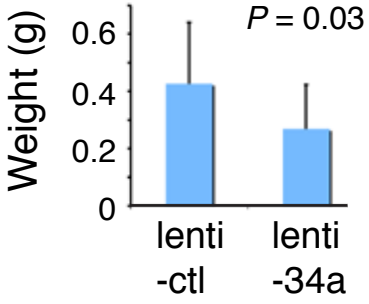

g

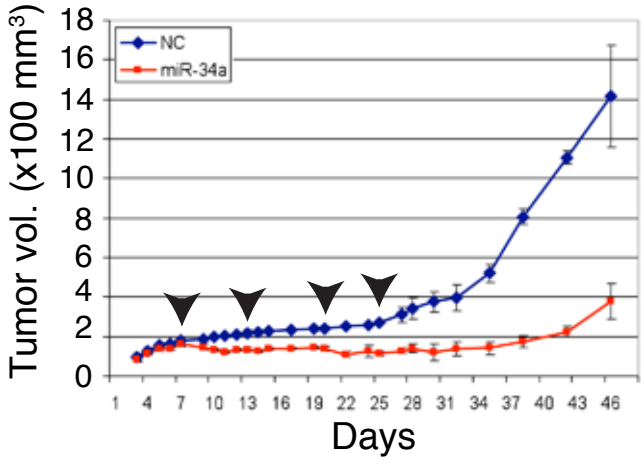

h

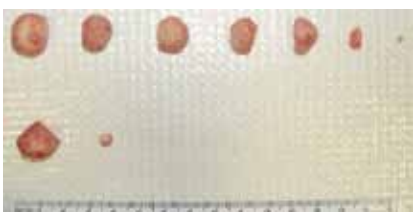

CD44+ LAPC9 cells (10K/inj; 43 d)

i

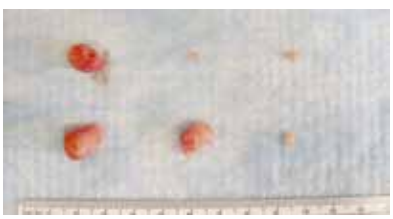

CD44- Du145 cells (10K/inj; 82 d)

Supplementary Figure 5

Nature Medicine: doi:10.1038/nm.2284

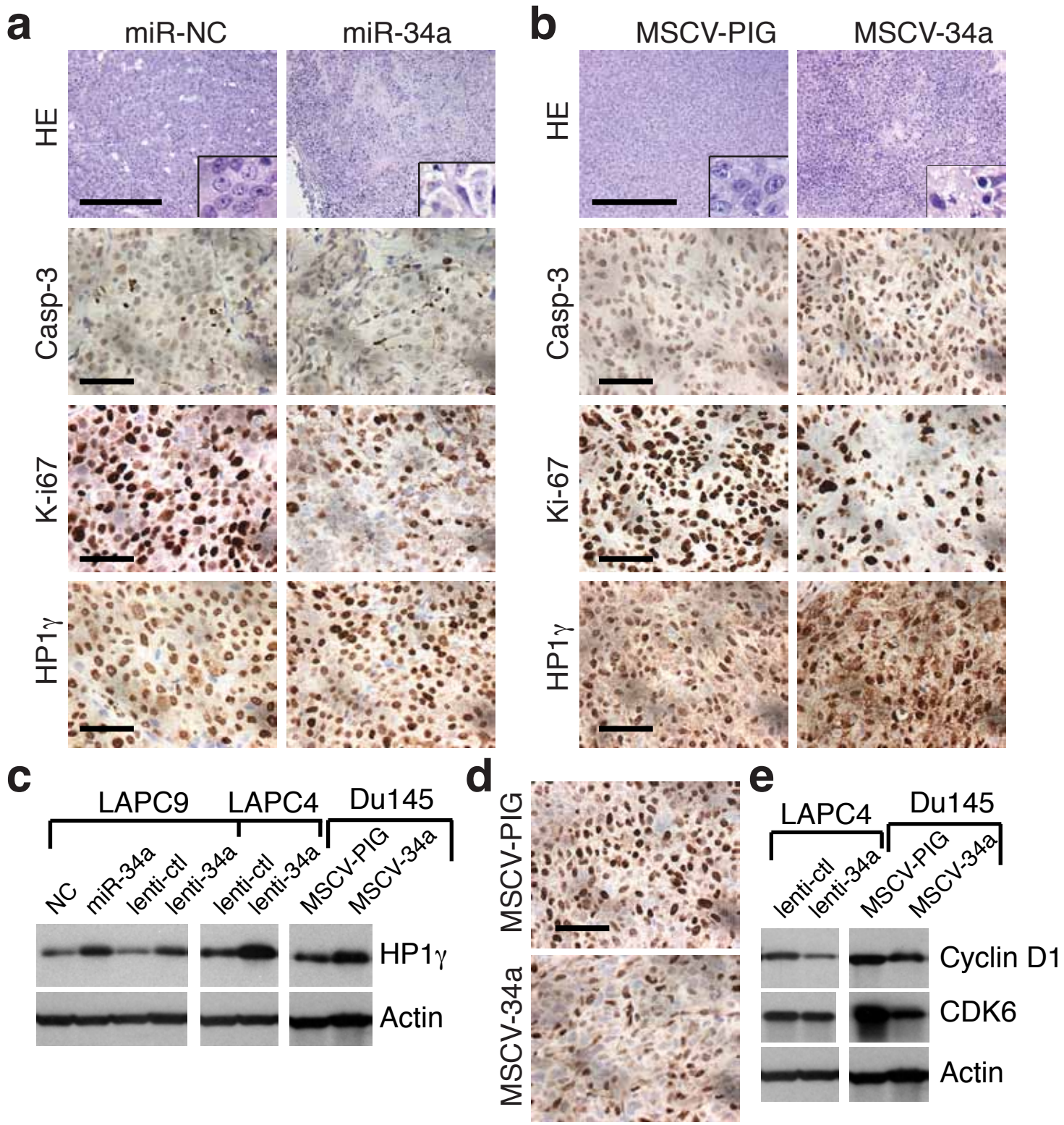

Supplementary Figure 6. Characterizations of miR-34a-overexpressing tumors.

(**a**,**b**) Paraffin-embedded sections of LAPC9 tumors (a) derived from cells transfected with miR-NC or miR-34a oligos (Supplementary Fig. 5a) or Du145 tumors (b) derived from cells infected with MSCV-PIG or MSCV-34a (Supplementary Fig. 5e) were used in HE or IHC staining for the molecules indicated. Depicted in the insets in the top rows is a more differentiated morphology of the cells in miR-34a overexpressing tumors. Shown below are representative images displaying reduced Ki-67 and increased HP1γ but no changes in active caspase-3 in the miR-34a overexpressing tumors. Scale bars, 20 μm.

(**c**) Increased HP-1γ in tumors derived from PCa cells overexpressing miR-34a by Western analysis.

(**d**,**e**) IHC (d) and Western blotting (e) showing reduced cyclin D1 and CDK6 in Du145 tumors from cells infected with MSCV-34a and LAPC4 tumors from cells infected with lenti-34a vectors.

Nature Medicine: doi:10.1038/nm.2284

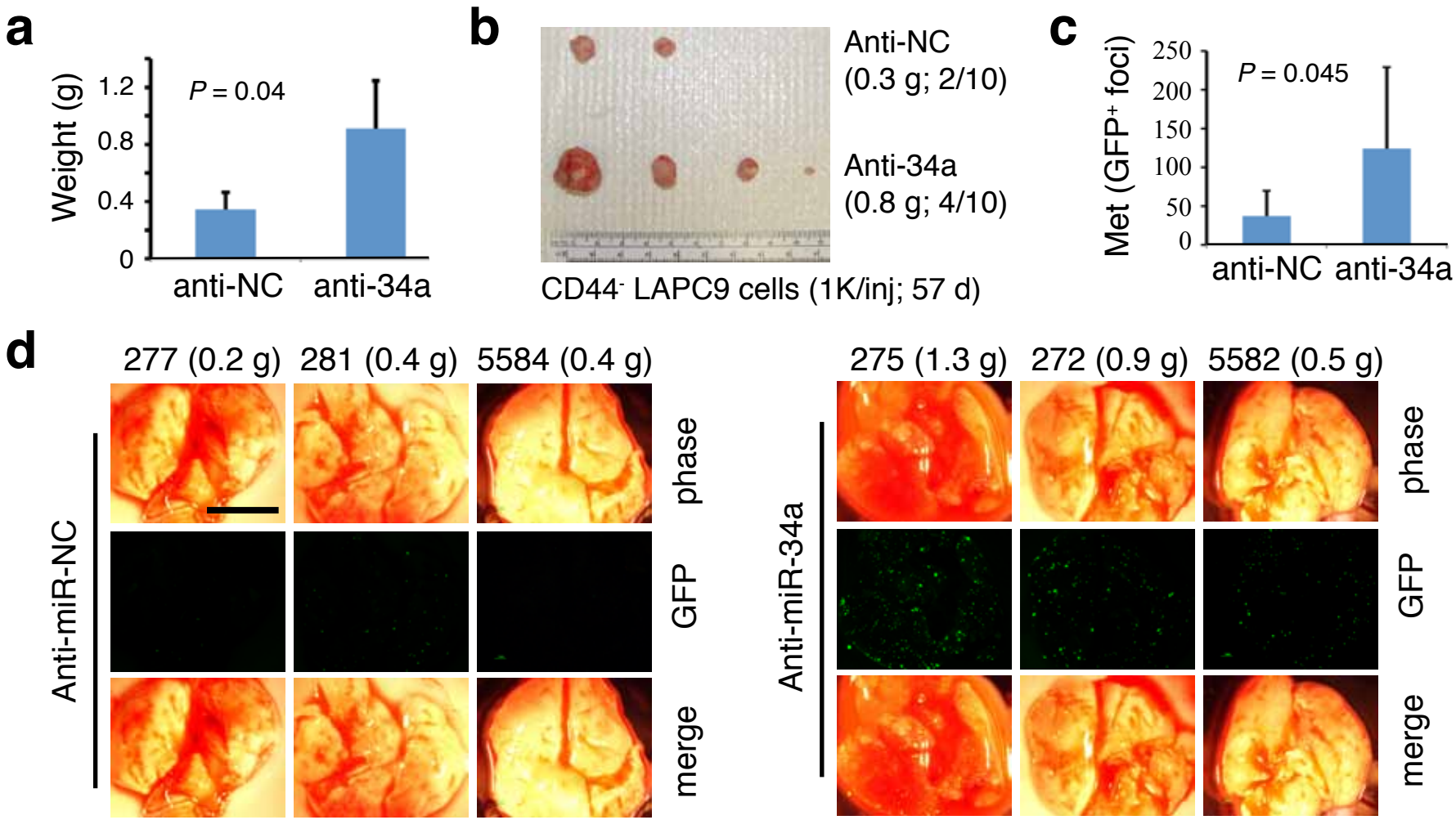

Supplementary Figure 7. Anti-miR-34a enhances LAPC9 tumor growth and lung metastasis.

(**a**) Anti-miR-34a promotes orthotopic LAPC9 tumor growth. This represents a repeat experiment to Fig. 1i. Shown are the mean weights of tumors derived from LAPC9-GFP cells transfected with anti-NC or anti-34a oligos and implanted in the DP of intact male NOD-SCID mice (sacrificed at 50 d). Tumor incidences for both groups were 4/7.

(**b**) Anti-34a promotes tumor growth of purified CD44$^-$ LAPC9 cells. Shown are the end-point tumors derived from CD44$^-$ LAPC9 cells transfected with anti-NC or anti-34a and s.c implanted in male NOD-SCID mice (euthanized at 60 d).

(**c**,**d**) Anti-miR-34a promotes orthotopic LAPC9 lung metastasis with data pooled from the two orthotopic tumor experiments (Fig. 1i and Supplementary Fig. 7a). Shown in d (and in Fig. 1j) are representative phase and GFP images of 4 lungs from each group (scale bar, 100 μm) and in c is the quantification of GFP$^+$ foci/lung.

Nature Medicine: doi:10.1038/nm.2284

Supplementary Figure 8. Competition experiments demonstrating clonality of PCa cell colonies and spheres.

(**a**) Clonal assays. Du145 cells were mixed with Du145-GFP cells at 1:1 ratio (50 cells each) and plated in 6-well plate. Images were taken on d 10 and shown are 3 representative fields.

(**b**,**c**) Clonogenic assays in methylcellulose (MC) or in Matrigel (MG). Du145 cells were mixed with DU145-GFP cells at 1:1 ratio and a total of 6,000 cells were plated for clonogenic assays in MC (b) or in MG (c). Photos were taken on d 5 after plating and shown are representative fields.

(**d**) Clonogenic assays in MC. Du145-RFP cells were mixed with Du145-GFP cells at 1:1 ratio and a total of 2,000 cells were plated in MC. Images were taken on d 4 and shown are two representative fields.

(**e**) Sphere-formation assays. Du145 cells were mixed with Du145-GFP cells at 1:1 ratio and a total of 2,000 cells were plated in ULA plates. Photos were taken on d 5 after plating and shown are a representative GFP^+ (left) and GFP^- (right) sphere.

Scale bars, 20 μm.

Nature Medicine: doi:10.1038/nm.2284

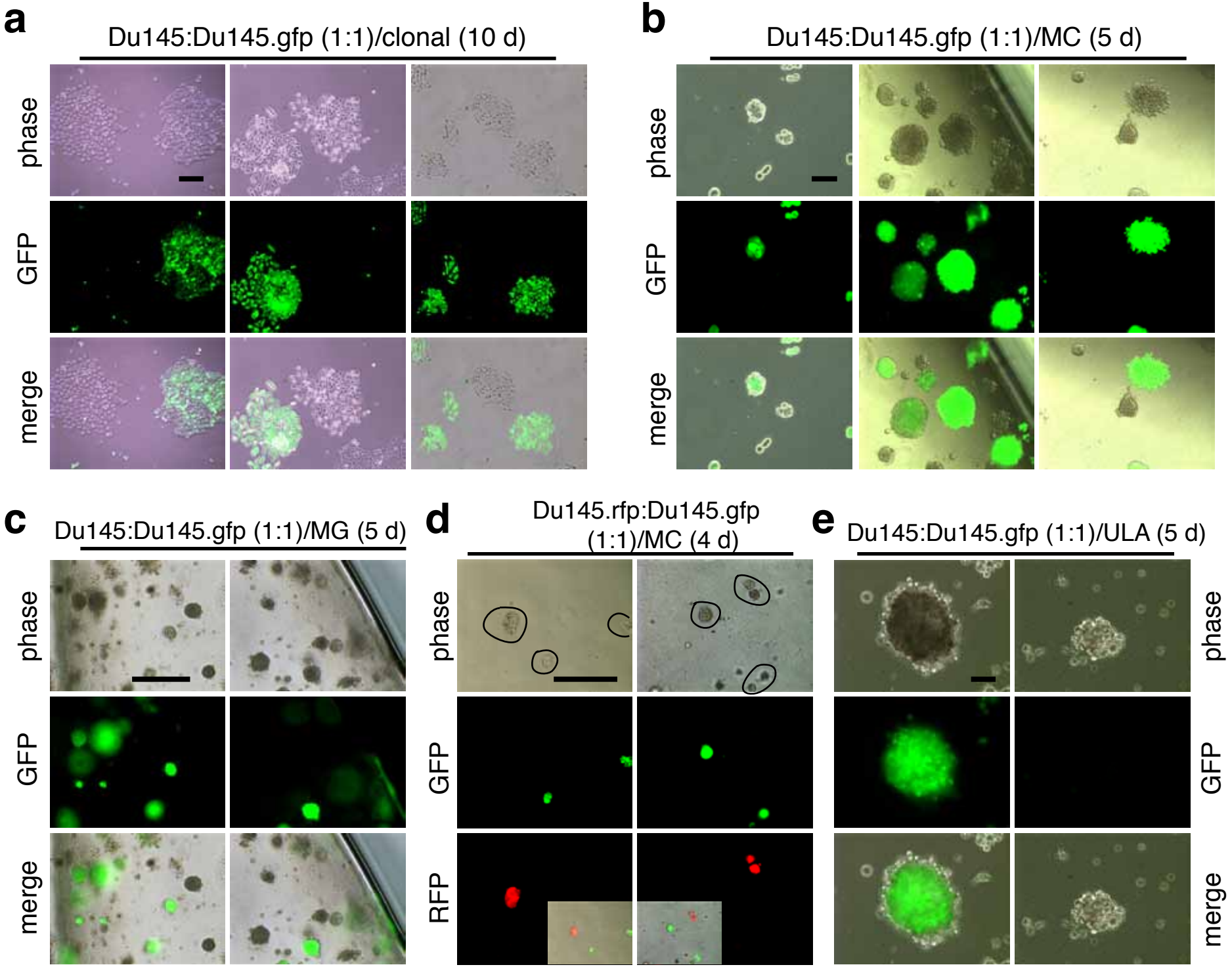

Nature Medicine: doi:10.1038/nm.2284

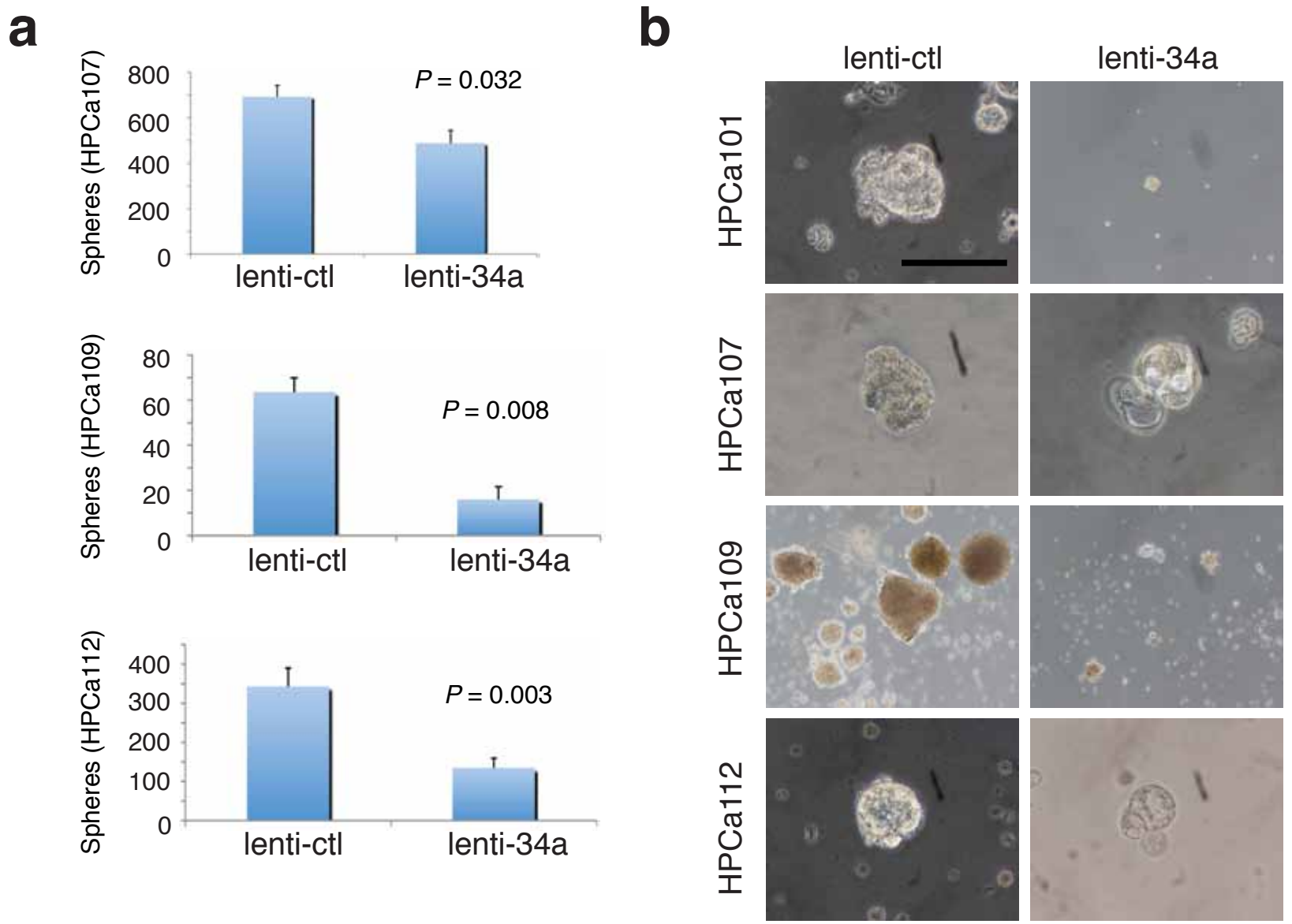

Supplementary Figure 9. miR-34a inhibits prostasphere formation in HPCa cells.
Presented in **a** are the numbers of spheres formed by HPCa cells freshly purified from the indicated patient primary tumors and infected with either lenti-ctl or lenti-34a vectors. Bars represent the mean ± s.d (n = 3–6). Shown in **b** are representative images of spheres formed by primary HPCa cells. Scale bar, 20 μm.

Nature Medicine: doi:10.1038/nm.2284

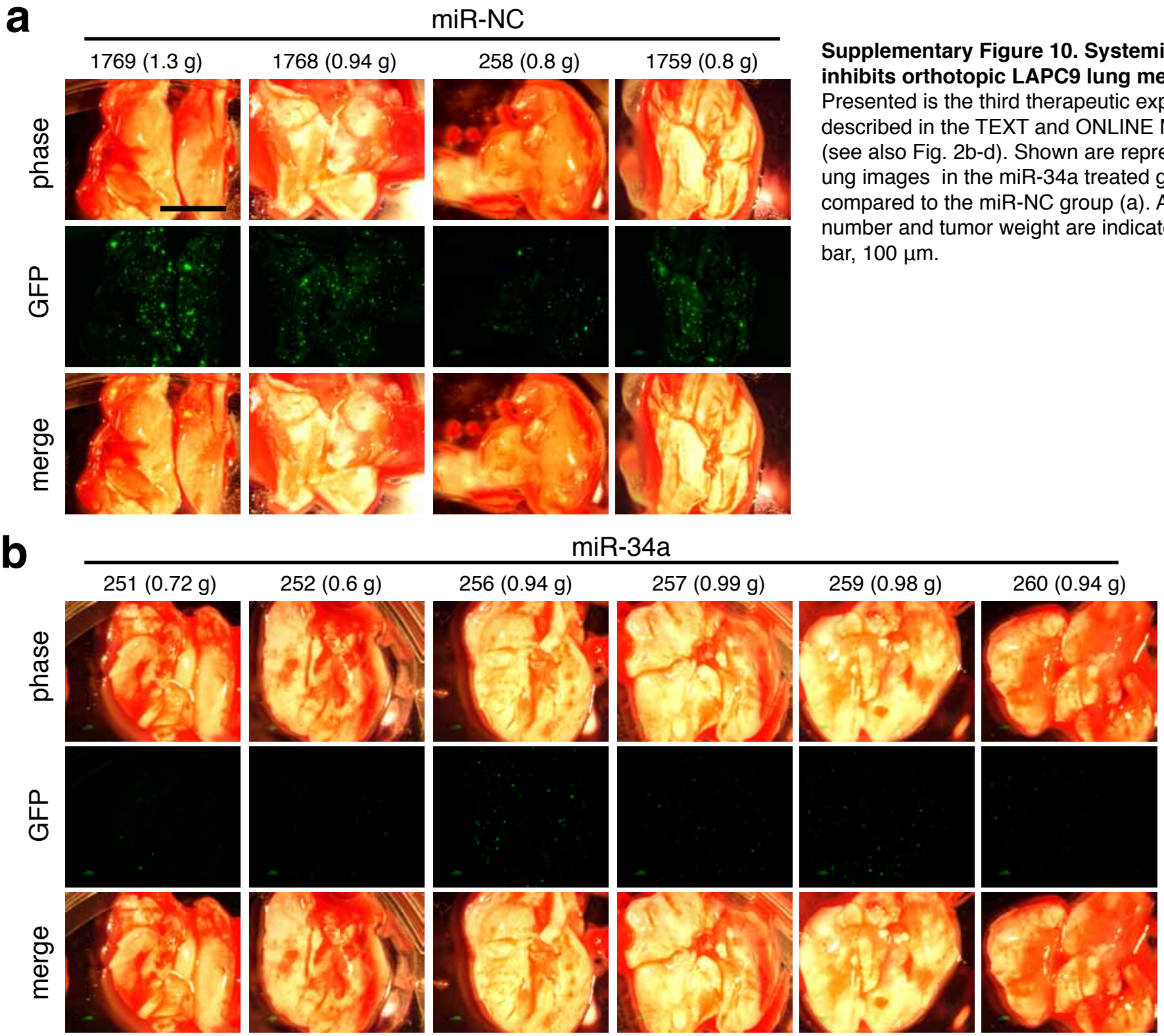

Supplementary Figure 10. Systemic miR-34a inhibits orthotopic LAPC9 lung metastasis. Presented is the third therapeutic experiment described in the TEXT and ONLINE METHODS (see also Fig. 2b-d). Shown are representative l ung images in the miR-34a treated group (b) compared to the miR-NC group (a). Animal tag number and tumor weight are indicated. Scale bar, 100 μm.

Nature Medicine: doi:10.1038/nm.2284

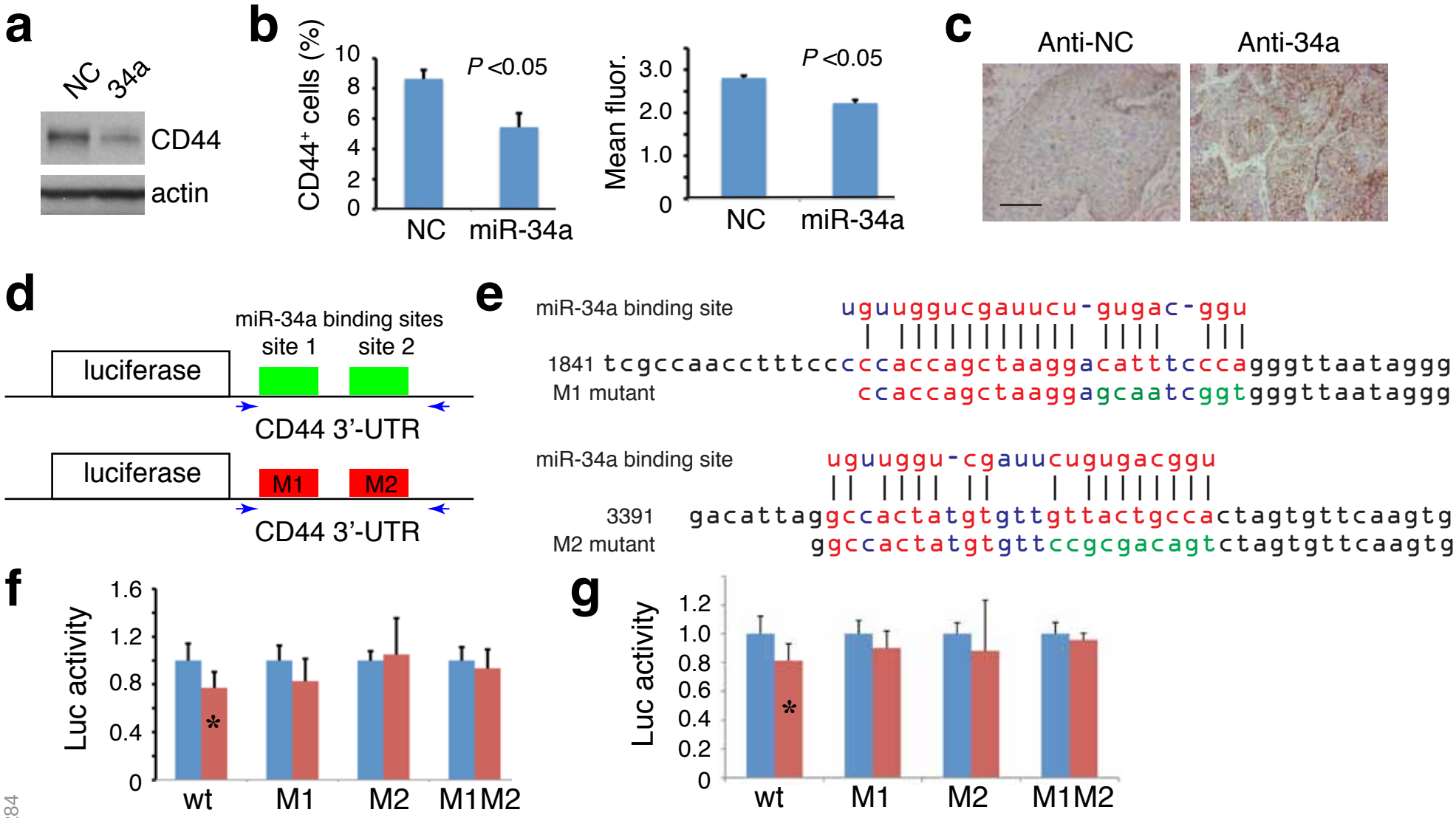

Supplementary Figure 11. miR-34a directly targets CD44.

(**a**) PC3 cells transfected with miR-NC or miR-34a oligos (33 nM, 48 h) were harvested and used in Western blotting of CD44 or β-actin.

(**b**) Purified LAPC9 cells were transfected with miR-NC or miR-34a oligos (33 nM; 72 h) and then used in flow cytometric analysis of CD44. Shown are CD44⁺ cells (%; $n = 3$) and the mean fluorescence intensity of CD44 expression.

(**c**) Two representative IHC images of CD44 staining in LAPC9 tumors derived from cells transfected with anti-34a or anti-NC. Scale bar, 10 μm.

(**d,e**) Schematic of the 2.55-kb wt CD44 3'-UTR containing the two miR-34a binding sites and the two mutants (i.e., M1 and M2) that were cloned downstream the luciferase cDNA in the 3'UTR/pMIR plasmid (d). Shown in e are the actual mutated sequences (in green).

(**f,g**) LNCaP (d) or LNCaP C4-2 (e) cells were co-transfected with wt or mutant luciferase construct together with NC (blue bars) or miR-34a (red bars) oligos. Each condition was run in 6 replicates and the experiment was repeated 2-3 times. The results were expressed as luciferase activity relative to the wt group after normalizing to the Renilla luciferase (internal control). Bars represent the mean ± SEM (*$P < 0.01$).

Nature Medicine: doi:10.1038/nm.2284

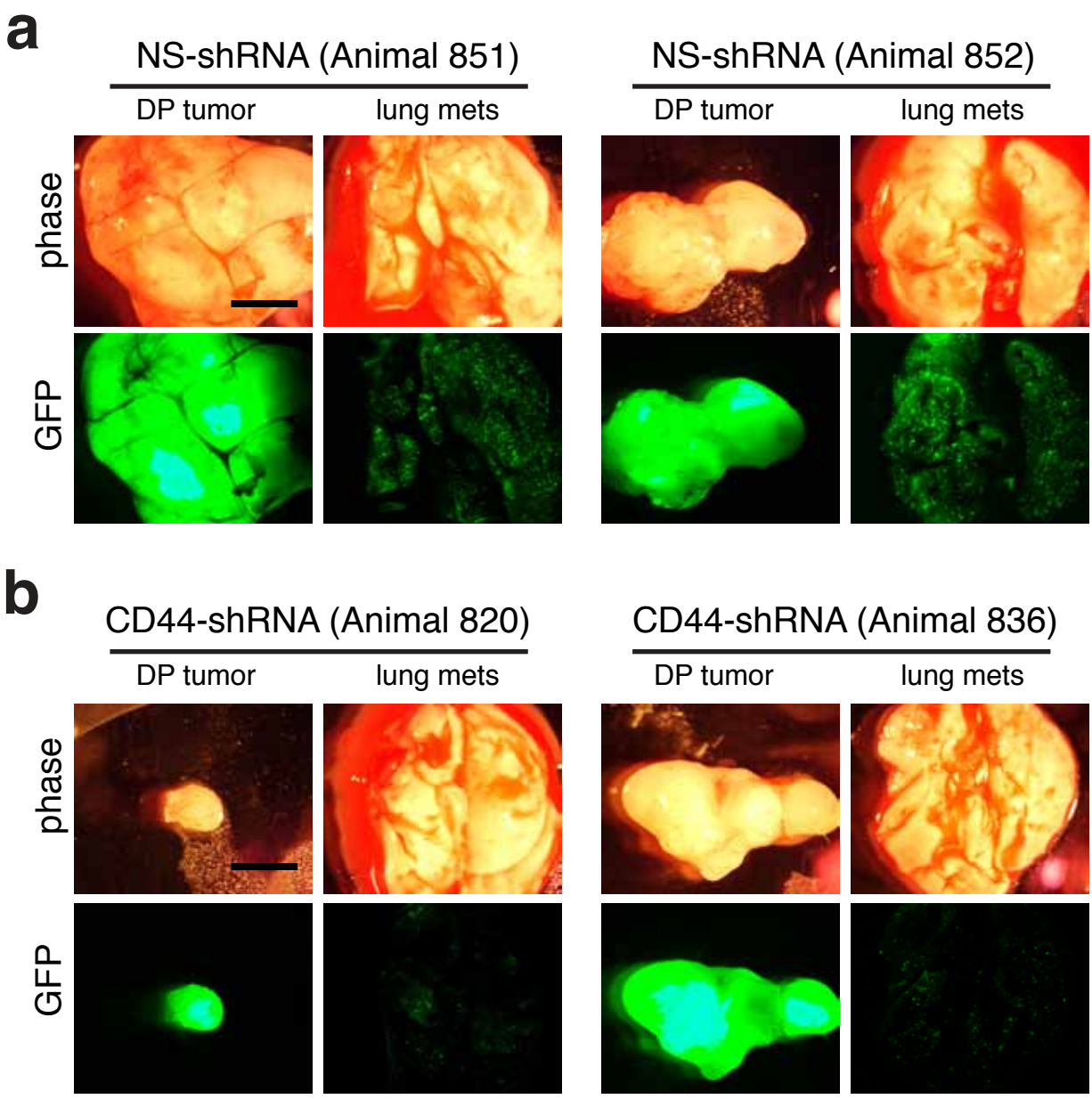

Supplementary Figure 12. CD44 knockdown inhibits LAPC4 lung metastasis. Purified LAPC4 cells infected with either non-silencing (NS) pGIPz control lentiviral vector or pGIPz-CD44shRNA (see Supplementary Fig. 1d) were implanted in the DP of male NOD-SCID mice (euthanized at 76 d). Shown are the images of DP tumors and the lungs from two representative animals in each group ($n = 7$). The CD44-shRNA animals (b) had both smaller DP tumors and less lung metastasis (GFP^+ foci) than in NS-shRNA animals. Scale bar, 100 μm.

Nature Medicine: doi:10.1038/nm.2284

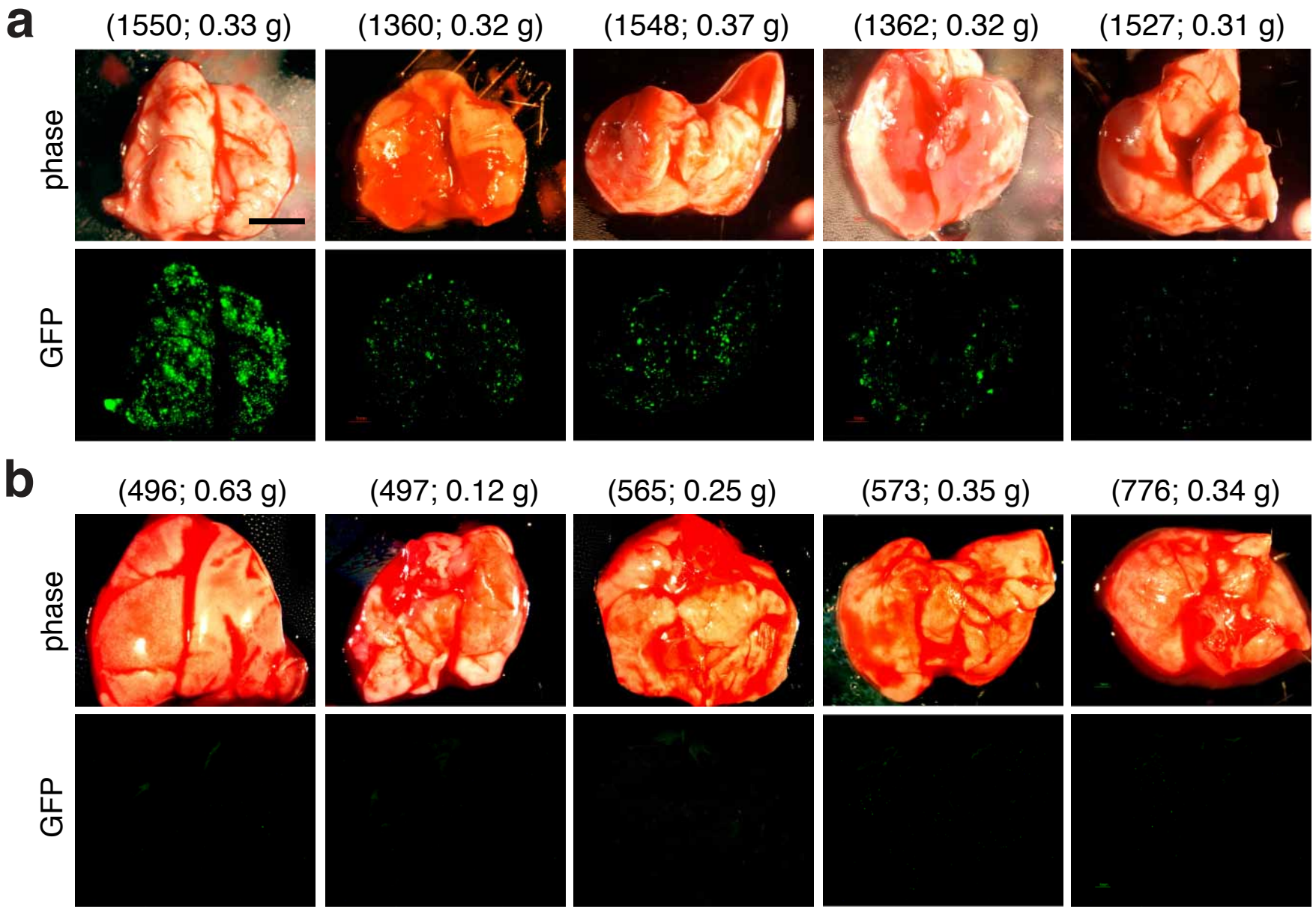

Supplementary Figure 13. CD44 knockdown inhibits PC3 cell lung metastasis.
Shown are phase and GFP images of five representative lungs in the animals bearing orthotopic PC3 tumors derived from cells infected with pGIPz control (**a**) or pGIPz-CD44shRNA (**b**) lentiviral vectors ($n = 8$ for each group; animals sacrificed at 40 d). Scale bar, 100 μm.

Nature Medicine: doi:10.1038/nm.2284

Supplementary Figure 14. Effects of CD44 knockdown or miR-34a overexpression on Du145 cells.

(**a**) Shown are the weights (above; mean ± s.d, $*P < 0.05$) and images (below; incidence, 5/5 for both groups) of subcutaneous tumors derived from Du145 cells infected with NS-shRNA or CD44-shRNA (MOI 20, 72 h; harvested at 56 d).

(**b**) Shown are the weights (above; mean ± s.d) and images (below) of orthotopic tumors derived from Du145 cells infected with NS-shRNA or CD44-shRNA (harvested at 41 d). Tumor incidence for the NS-shRNA and CD44-shRNA group was 7/7 and 5/8, respectively.

(**c**) Shown are the relative migratory abilities of purified $CD44^+$ and $CD44^-$ Du145 cells plated on the top of the Boyden chamber without Matrigel.

(**d**) Shown are two representative static images of $CD44^+$ (out of a total of 17 movies) and $CD44^-$ (out of a total of 14 movies) Du145 cells at the beginning of recording and at 7 h post wounding. In the movie images (scale bar, 20 μm) shown, the $CD44^+$ but not $CD44^-$ Du145 cells had closed the wound by 7 h.

(**e**) Shown are the relative invasive capacities of purified $CD44^+$ and $CD44^-$ Du145 cells plated on the top of the Boyden chamber with Matrigel.

(**f**) Shown are two representative static images of $CD44^+$ Du145 cells transfected with miR-NC (out of a total of 25 movies) or miR-34a oligos (out of a total of 29 movies) at the beginning of recording and at 5 h post wounding. Scale bar, 20 μm.

(**g**) Quantitative presentation of results in f.

Nature Medicine: doi:10.1038/nm.2284

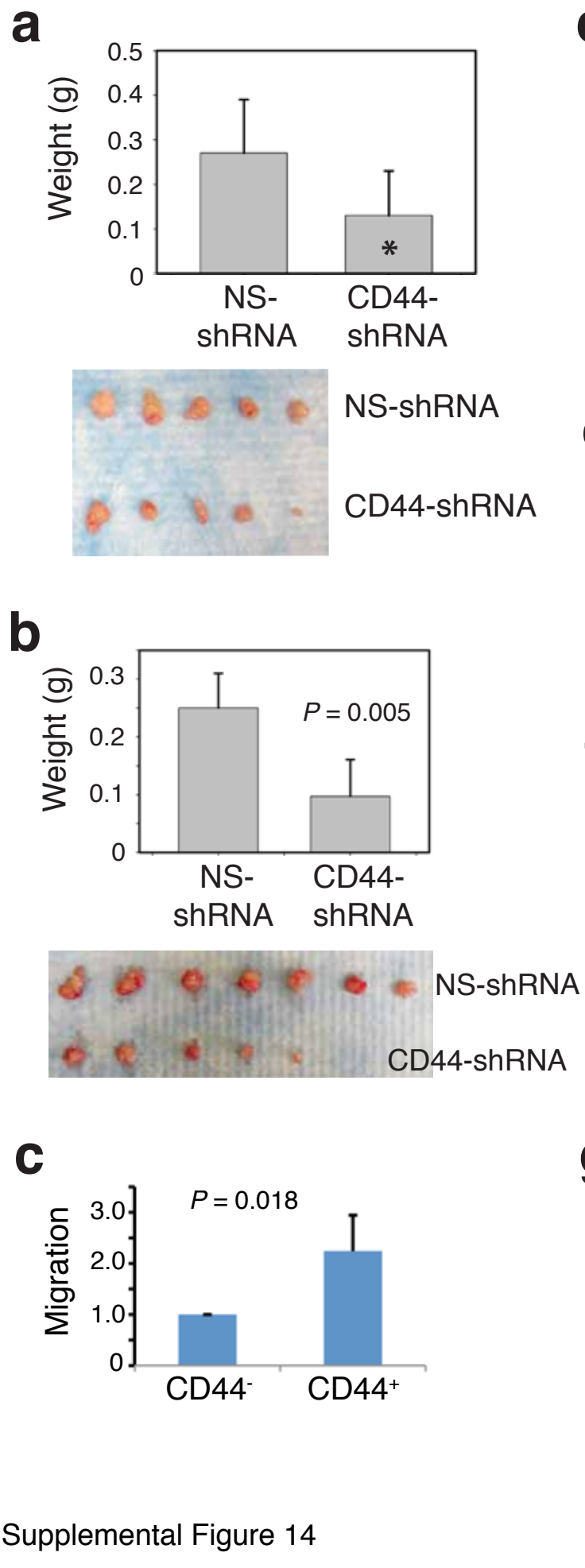

Supplemental Figure 14

Nature Medicine: doi:10.1038/nm.2284

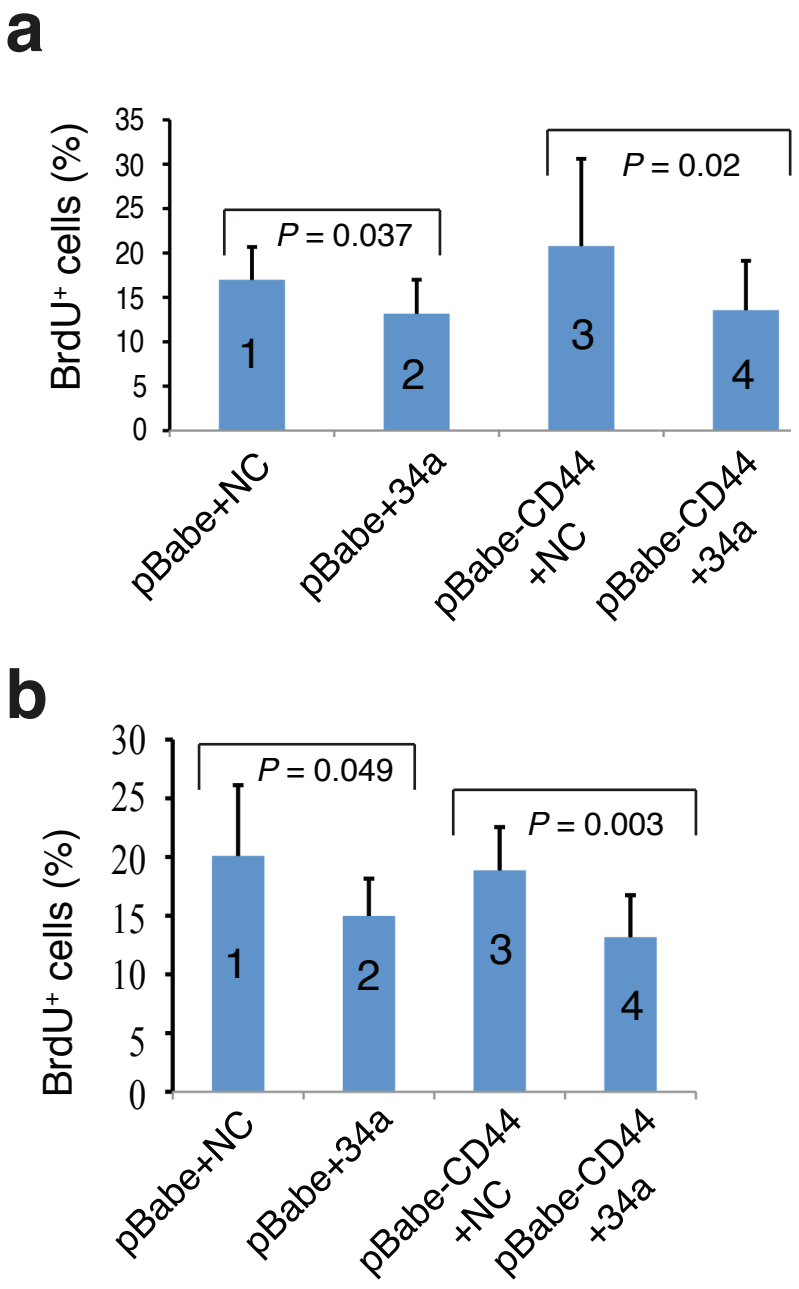

Supplementary Figure 15. CD44 overexpression does not relieve miR-34a-mediated inhibition of proliferation.

BrdU immunostaining in PPC-1 (**a**) or LNCaP (**b**) cells first infected with pBabe-CD44 (which encodes human CD44 cDNA that lacks the two miR-34a binding sites at the 3'-UTR) or its empty control vector (pBabe) and then (48 h later) transfected with miR-NC or miR-34a oligos oligos. Presented are the % BrdU$^+$ cells from counting a total of 400–500 cells in 2-3 experiments. In both cell types, miR-34a oligos reduced BrdU$^+$ percentages in cells infected with pBabe (conditions 1 and 2) or pBabe-CD44 (conditions 3 and 4). There were no differences between conditions 4 and 2 or between conditions 3 and 1 ($P > 0.1$).

Nature Medicine: doi:10.1038/nm.2284

Supplementary Table 1. Primary human prostate tumors (HPCa) used to purify CD44$^+$ and CD44$^-$ cells for qRT-PCR analysis

HPCa sample[a]	Age	Gleason	%CD44$^+$[b]	Purification[c]	Purity (%)[d]
HPCa60	54	8	8.7	MACS	CD44$^+$: ~50 CD44$^-$: N.A
HPCa62	59	7	2.4	MACS	CD44$^+$: ~50 CD44$^-$: 100
HPCa65	59	7	19.9	MACS	CD44$^+$: 67 CD44$^-$: 100
HPCa 66	58	6	15.0	FACS	CD44$^+$: N.A CD44$^-$: 94
HPCa72	58	7	10.2	MACS	CD44$^+$: 33 CD44$^-$: 100
HPCa74	59	7	16.2	MACS	CD44$^+$: 70 CD44$^-$: 100
HPCa76	64	7	0.02	MACS	CD44$^+$: ~10 CD44$^-$: 100
HPCa77	46	6	14.2	MACS	CD44$^+$: 45 CD44$^-$: 100
HPCa78	64	7	19.2	MACS	CD44$^+$: 45 CD44$^-$: 100
HPCa79	67	7	8.2	MACS	CD44$^+$: 15 CD44$^-$: 100
HPCa80	65	9	4.4	MACS	CD44$^+$: 13 CD44$^-$: 85
HPCa81	54	7	20.9	MACS	CD44$^+$: 64 CD44$^-$: 90
HPCa87*	57	9	N.D	MACS	CD44$^+$: 93 CD44$^-$: 100
HPCa89	55	9	24	MACS	CD44$^+$: 87 CD44$^-$: 90
HPCa91*	60	8	N.D	MACS	CD44$^+$: 95 CD44$^-$: 90
HPCa93	58	7	0.99	FACS	CD44$^+$: 87 CD44$^-$: 100
HPCa98	64	8	5.74	FACS	CD44$^+$: 79 CD44$^-$: 100
HPCa102	55	7	24.8	FACS	CD44$^+$: 99 CD44$^-$: 85

[a]Human primary tumors were obtained from the robotic (Da Vinci) surgery. The age and Gleason score of each tumor are indicated. *For HPCa87 and HPCa91, the first-generation xenograft tumors established in our lab were used in purifying CD44$^+$ and CD44$^-$ cells.

[b]The % of CD44$^+$ HPCa cells was determined by flow analysis prior to sorting. N.D, not determined.

[c]CD44$^+$ and CD44$^-$ cells were purified out using MACS (magnetic cell sorting) or FACS (fluorescence activated cell sorting). Four of the eighteen samples (shaded) were sorted using FACS as the MACS approach was more gentle on primary tumor cells.

[d]The purity of MACS-purified cells, determined by counting CD44$^+$ cells under a fluorescence microscope, was variable for both CD44$^+$ and CD44$^-$ cell populations. The purity of FACS-purified cells, determined by post-sort flow analysis, was ~80-99% for CD44$^+$ HPCa cells and 85-100% for CD44$^-$ cells. N.A, not available.

Nature Medicine: doi:10.1038/nm.2284

Supplementary Table 2. Correlation of CD44 levels with miR-34 manipulations in PCa cells

Tumor systems	Comments
LAPC9	– LAPC9 cells transfected with miR-34a oligos exhibit reduced CD44 protein expression levels and $CD44^+$ cells (**Supplementary Fig. 11b**). – LAPC9 tumors derived from cells transfected with anti-34a expressed higher levels of CD44 than tumors derived from the cells transfected with anti-NC (**Supplementary Fig. 11c**).
Du145	– Residual Du145 tumors from cells infected with MSCV-34a show reduced CD44 protein (**Fig. 4a**). – Du145 cells transfected with miR-34a oligos show time- and dose-dependent reduction in CD44 protein (**Fig. 4b**). – Du145 tumors derived from $CD44^-$ Du145 cells transfected with anti-34a expressed higher levels of CD44 mRNA than tumors derived from the same cells transfected with anti-NC (**Supplementary Fig. 4e**).
PC3	– Residual orthotopic PC3 tumors in animals treated with miR-34a display reduced CD44 protein (**Fig. 4a**). – PC3 cells transfected with miR-34a oligos show reduced CD44 protein (**Supplementary Fig. 11a**).
PPC-1	– PPC-1 cells transfected with miR-34a oligos show reduced CD44 protein (**Fig. 4b**).

Nature Medicine: doi:10.1038/nm.2284

Published OnlineFirst June 19, 2012; DOI:10.1158/0008-5472.CAN-11-3864

Cancer Research

Distinct microRNA Expression Profiles in Prostate Cancer Stem/Progenitor Cells and Tumor-Suppressive Functions of let-7

Can Liu, Kevin Kelnar, Alexander V. Vlassov, et al.

Cancer Res 2012;72:3393-3404. Published OnlineFirst June 19, 2012.

Published OnlineFirst June 19, 2012; DOI:10.1158/0008-5472.CAN-11-3864

Distinct microRNA Expression Profiles in Prostate Cancer Stem/Progenitor Cells and Tumor-Suppressive Functions of let-7

Can Liu[1,2], Kevin Kelnar[4], Alexander V. Vlassov[5], David Brown[4], Junchen Wang[6], and Dean G. Tang[1,2,3,6]

Abstract

MiRNAs regulate cancer cells, but their potential effects on cancer stem/progenitor cells are still being explored. In this study, we used quantitative real-time-PCR to define miRNA expression patterns in various stem/progenitor cell populations in prostate cancer, including $CD44^+$, $CD133^+$, integrin $\alpha2\beta1^+$, and side population cells. We identified distinct and common patterns in these different tumorigenic cell subsets. Multiple tumor-suppressive miRNAs were downregulated coordinately in several prostate cancer stem/progenitor cell populations, namely, miR-34a, let-7b, miR-106a, and miR-141, whereas miR-301 and miR-452 were commonly overexpressed. The let-7 overexpression inhibited prostate cancer cell proliferation and clonal expansion *in vitro* and tumor regeneration *in vivo*. In addition, let-7 and miR-34a exerted differential inhibitory effects in prostate cancer cells, with miR-34a inducing G_1 phase cell-cycle arrest accompanied by cell senescence and let-7 inducing G_2–M phase cell-cycle arrest without senescence. Taken together, our findings define distinct miRNA expression patterns that coordinately regulate the tumorigenicity of prostate cancer cells. *Cancer Res; 72(13); 3393–404. ©2012 AACR.*

Introduction

Most tumors contain a dynamic population of less differentiated and highly tumorigenic cells operationally defined as cancer stem cells (CSC) or tumor-initiating cells (1–10). CSCs may be phenotypically purified using surface markers. CD44 is one such marker widely used to enrich tumor-initiating cells, for example, in cancers of the breast (2), pancreas (5), head and neck (8), colon (9), and the prostate (6, 7). Our previous work has shown that $CD44^+$ cells from prostate cancer cell cultures or prostate cancer xenografts exhibit high proliferative and clonogenic potential *in vitro*. Moreover, using limiting dilution assays in NOD/SCID (nonobese diabetic/severe combined immunodeficient) mice, we find that $CD44^+$ prostate cancer cells possess 6 to 30 times higher tumor-regenerating capacity than $CD44^-$ cells (6, 7). CD133 has similarly been used to enrich CSCs in brain (3), colon (10), and other cancers. Several surface marker–independent strategies have also been used to enrich tumor-initiating cells (1). Side population assay is a flow cytometry–based method initially developed to enrich hematopoietic stem cells owing to their expression of high levels of drug-detoxifying surface transporter proteins such as ABCG2 and MDR1 that efficiently efflux the Hoechst dye 33342 (11). Using the side population technique, we have shown that the side population cells in LAPC9 xenografts, although representing only approximately 0.01% of the total tumor cell population, are more than 500-fold more tumorigenic than the isogenic non–side population cells (12).

With the preponderant evidence for CSCs and our increasing knowledge of CSC heterogeneity (1), it becomes apparent that we need to understand how tumorigenic cancer cells are regulated at the molecular level so that we can design CSC-specific therapeutics. MiRNAs are small noncoding RNAs that regulate many biologic processes by inhibiting the target mRNA translation or stability (13). Deregulation of miRNAs has been observed in a variety of human tumors (14, 15). In prostate cancer, several groups have conducted miRNA expression profiling studies using either miRNA microarray (16–20) or whole-genome deep sequencing (21) in prostate cancer cell lines, xenografts, or patient samples. These studies, although reporting prostate cancer–related miRNA alterations and shedding light on differential miRNA expression in prostate cancer (relative to benign tissues), have all been conducted in bulk tumor cells and thus fail to address alterations of miRNA expression and functions specifically in tumorigenic prostate cancer cell subsets. We recently conducted, for the first time,

Authors' Affiliations: [1]Department of Molecular Carcinogenesis, The University of Texas MD Anderson Cancer Center, Science Park, Smithville; [2]Program in Molecular Carcinogenesis, The University of Texas Graduate School of Biomedical Sciences at Houston; [3]Centers for Cancer Epigenetics, Stem Cell and Developmental Biology, RNA Interference and Noncoding RNAs, and Molecular Carcinogenesis, The University of Texas MD Anderson Cancer Center, Houston; [4]Mirna Therapeutics, Inc., Austin; [5]Life Technologies, Austin, Texas; and [6]Cancer Stem Cell Institute, Research Center for Translational Medicine, East Hospital, Tongji University, Shanghai, China

Note: Supplementary data for this article are available at Cancer Research Online (http://cancerres.aacrjournals.org/).

Corresponding Author: Dean G. Tang, Department of Molecular Carcinogenesis, The University of Texas MD Anderson Cancer Center, 1808 Park Rd. 1C, Smithville, TX 78957. Phone: 512-237-9575; Fax: 512-237-2475; E-mail: dtang@mdanderson.org

doi: 10.1158/0008-5472.CAN-11-3864

Published OnlineFirst June 19, 2012; DOI:10.1158/0008-5472.CAN-11-3864

an miRNA expression profiling in 6 highly purified prostate cancer stem/progenitor cell populations and reported that miR-34a, a p53 target, was underexpressed in all these populations (22). We further showed that miR-34a negatively regulated prostate CSC (PCSC) activity and inhibited prostate cancer metastasis by directly repressing CD44 (22). Herein, we present detailed miRNA expression profiling procedures and results and report the miRNAs that are commonly and differentially expressed in prostate cancer stem/progenitor cell populations. We further investigate the biologic functions of 2 commonly altered miRNAs, that is, let-7, and miR-301, in the context of regulating CSCs and prostate cancer regeneration. Finally, using miR-34a as an example, we explore potential mechanisms that may be responsible for the differential miRNA expression in prostate cancer stem/progenitor cells. Our results converge with the emerging theme that distinct miRNAs coordinately and distinctively regulate CSC properties (23).

Materials and Methods

Many basic experimental procedures have been described in our earlier publications (6, 7, 12, 22, 24–26). Some experimental procedures are described in Supplementary Methods. Primary human prostate tumors (HPCa) used in this study are presented in Supplementary Table S1.

Cells, xenografts, and animals

PPC-1, PC3, LNCaP, and Du145 cells were obtained from American Type Cell Culture and cultured in RPMI-1640 plus 7% heat-inactivated FBS. Human xenograft prostate tumors, LAPC9 [bone metastasis; androgen receptor $(AR)^+$ and prostate-specific antigen $(PSA)^+$], LAPC4 (lymph node metastasis; AR^+ and PSA^+), and Du145 (brain metastasis; AR^- and PSA^-) were maintained in NOD/SCID mice. NOD/SCID mice were produced mostly from our own breeding colonies and purchased occasionally from the Jackson Laboratories and maintained in standard conditions according to the Institutional Guidelines. All animal experiments were approved by our Institutional Animal Care and Use Committee. All these 6 prostate cancer cell types were routinely checked to be free of mycoplasma contamination using the Agilent MycoSensor QPCR Assay Kit (cat. #302107). Cell authentification by DNA fingerprinting is under way.

Transient transfection with oligonucleotides

Prostate cancer cells were transfected with 30 nmol/L of miR-34a, let-7a, let-7b, or miR-301 mirVana mimics, or nontargeting negative control miRNA (miR-NC) oligos (Ambion) using Lipofectamine RNAiMAX (Invitrogen) according to the manufacturer's instructions (22). MirVana mimics are synthetic double-stranded oligonucleotides (oligos) that mimic mature miRNAs. In some experiments, mirVana miRNA inhibitors, chemically modified antisense oligos against let-7b, miR-301, or miR-NC (Ambion) were introduced into prostate cancer cells using the same conditions. After culturing overnight for 48 hours, transfected cells were harvested for *in vitro* and *in vivo* studies.

Lentiviral-mediated overexpression of let-7a

pLL3.7-let-7a and pLL3.7 control vector were kindly provided by Dr. J. Lieberman (Harvard University, Cambridge, MA; ref. 27). Lentiviruses were produced in 293FT packaging cells and titers determined for GFP using HT1080 cells (22). Prostate cancer cells were infected with the lentiviral supernatant [multiplicity of infection (MOI), 5–10] in the presence of 8 μg/mL polybrene and harvested 48 to 72 hours after infection for experiments.

Statistical analyses

In general, the unpaired 2-tailed Student t test was used to compare differences in cell numbers, cumulative population doublings, percentages of $CD44^+$ cells, percentage of bromodeoxyuridine $(BrdUrd)^+$ cells, percentage of cell-cycle phases, cloning and sphere-formation efficiency, and tumor weights. The Fisher exact test and χ^2 test were used to compare incidence and latency. In all these analyses, a $P < 0.05$ was considered statistically significant.

Results

miRNA expression profiling in purified prostate cancer stem/progenitor cell populations

We first used the quantitative real-time-PCR (qRT-PCR; ref. 22) to determine the expression levels of 310 mature human miRNAs (Supplementary Table S2) in bulk prostate cancer cells purified from 3 xenografts, that is, LAPC9 (bone metastasis, AR^+/PSA^+), LAPC4 (lymph node metastasis, AR^+/PSA^+), and Du145 (brain metastasis, AR^-/PSA^-; Supplementary Fig. S1, step I). We then chose 136 miRNAs (Supplementary Table S3) including the top 120 abundantly expressed miRNAs and 16 less abundant miRNAs of interest (including 2 miRNAs, i.e., miR-24 and miR-103 that were used as internal controls). We measured the levels of these 136 miRNAs in $CD44^+$ (i.e., cells expressing high levels of CD44) and $CD44^-$ cells purified from LAPC9, LAPC4, and Du145 tumors; $CD133^+$ and $CD133^-$ cells from LAPC4 tumor, and integrin $\alpha2\beta1^+$ and $\alpha2\beta1^-$ cells from Du145 tumor (Supplementary Fig. S1, step II). The LAPC9, LAPC4, and Du145 tumors contain approximately 20%, 0.1%, and 30% $CD44^{hi}$ cells, respectively (6), whereas the LAPC4 tumors contain approximately 1% $CD133^+$ cells. The $CD44^+$ prostate cancer cells are enriched in tumor- and metastasis-initiating cells (6, 7), whereas $CD133^+(CD44^+\alpha2\beta1^{hi})$ cells purified from primary prostate cancer samples are highly clonogenic (28). In addition to these 5 (i.e., 3 $CD44^+$, 1 $CD133^+$, and 1 $\alpha2\beta1^+$) prostate cancer cell populations, we also purified, from the LAPC9 tumor, the side population, which harbors great tumor-regenerative activity (12). Because the side population represents less than 0.1% of the total population in LAPC9 tumor (12), we manually curated 57 miRNAs (Supplementary Table S4) that could be reliably detected and compared with their expression levels in the side population versus non–side population cells (Supplementary Fig. S1, step III). Comparisons of 6 marker-positive and -negative prostate cancer cell populations revealed interesting and informative differences in miRNA expression patterns.

Published OnlineFirst June 19, 2012; DOI:10.1158/0008-5472.CAN-11-3864

Common underexpression of multiple tumor-suppressive miRNAs in CD44$^+$ prostate cancer cells

We first compared the expression levels of 134 miRNAs between the CD44$^+$ and CD44$^-$ populations and observed cell type–related differential miRNA expression patterns (Supplementary Fig. S2A–S2C and Supplementary Table S3). The CD44$^+$ LAPC4 and LAPC9 cells had significantly more underexpressed than overexpressed miRNAs compared with the corresponding CD44$^-$ cells, whereas CD44$^+$ and CD44$^-$ Du145 cells had roughly similar numbers of overexpressed and underexpressed miRNAs (Supplementary Fig. S2). When we analyzed the miRNA expression patterns common to all 3 populations of CD44$^+$ prostate cancer cells, we found that 3 miRNAs, that is, miR-452, miR-19a, and miR-301, were commonly overexpressed and 37 miRNAs were commonly underexpressed (Table 1; Supplementary Table S3). Among the 37 underexpressed miRNAs, miR-34a was most dramatically downregulated, representing 2% of the level in CD44$^-$ cells. We have recently shown that miR-34a acts as a critical negative regulator of PCSC properties by directly targeting CD44 (22). In addition to miR-34a, 4 let-7 members (let-7a, let-7b, let-7e, and let-7f) were underexpressed in the 3 CD44$^+$ populations (Table 1). Moreover, miR-141, a miR-200 family member, was also expressed at lower levels in CD44$^+$ than in CD44$^-$ prostate cancer cells (Table 1). miR-34, let-7, and miR-200 families of miRNAs are well-established tumor-suppressive miRNAs (22, 23, 27, 29, 30).

miR-199a*, which is downregulated in many cancers (in particular, hepatocellular carcinoma) and possesses tumor-suppressive functions by targeting oncogenic molecules such as c-MET, versican, PAK4, Brm, mTOR, and AKT (31–33), was expressed in CD44$^+$ prostate cancer cells at only approximately 4% levels of the CD44$^-$ cells (Table 1). Strikingly, in other cancer cells, miR-199a* has been shown to target CD44, leading to its deficiency in CD44$^+$ cancer cells (32, 33). Of interest, miR-214 is in a cluster with miR-199a* (~6 kb apart) within human dynamin-3 gene intron (DNM3os) and was co-downregulated with miR-199a* in CD44$^+$ cells (Table 1). Similarly, miR-10a and miR-196a are embedded in the HoxB gene cluster and both were underexpressed in CD44$^+$ prostate cancer cells (Table 1). Several other clusters of miRNAs, including let-7e/miR-99b (19q13.33), miR-183/182 (7q31-34), miR106a/19b/92a (in the Chr-X *mir-106a-363* cluster), and miR-193b/365 (16p13.12), were also coordinately downregulated in the CD44$^+$ prostate cancer cells (Table 1). miR-193b targets multiple oncogenic molecules including uPA, cyclin D1, 14-3-3ζ, c-Kit, and Mcl-1 and is important for cellular differentiation (34). Many other miRNAs commonly underexpressed in CD44$^+$ prostate cancer cells (Table 1), including miR-218 (35), miR-148a (36), miR-181b (37), miR-203 (38), miR-183 (39), miR-24 (40), and miR-335 (41), all possess tumor/metastasis-inhibitory functions.

Together, our profiling results indicate that multiple tumor-suppressive miRNAs are coordinately downregulated in CD44$^+$

Table 1. miRNAs commonly over- or underexpressed in CD44$^+$ prostate cancer cells

Overexpressed		Underexpressed			
miRNA	**Fold change**	**miRNA**	**Fold change**	**miRNA**	**Fold change**
miR-452	832.77	miR-34a	0.02	miR-183	0.59
miR-19a	2.99	miR-199a*	0.04	miR-132	0.60
miR-301	1.84	miR-218	0.06	let-7e	0.62
		miR-422b	0.24	miR-340	0.62
		miR-422a	0.27	miR-30a-3p	0.64
		miR-378	0.27	miR-30a-5p	0.64
		miR-196a	0.28	miR-324-5p	0.64
		miR-10a	0.33	miR-365	0.66
		let-7b	0.35	miR-193b	0.67
		miR-214	0.39	miR-24	0.67
		miR-148a	0.41	miR-335	0.67
		miR-203	0.43	miR-191	0.68
		miR-181b	0.43	miR-92	0.70
		let-7a	0.44	miR-182	0.76
		miR-141	0.47	miR-99b	0.80
		miR-222	0.48	miR-30c	0.80
		miR-342	0.52	miR-106a	0.83
		let-7f	0.53	miR-19b	0.85
		miR-151	0.57		

NOTE: Presented are the miRNAs that are commonly over- or underexpressed in the purified CD44$^+$ Du145, LAPC9, and LAPC4 cells compared with the corresponding CD44$^-$ cells using miR-103 as the internal control. The fold changes represent the mean value of the miRNA in 3 xenograft models.

Published OnlineFirst June 19, 2012; DOI:10.1158/0008-5472.CAN-11-3864

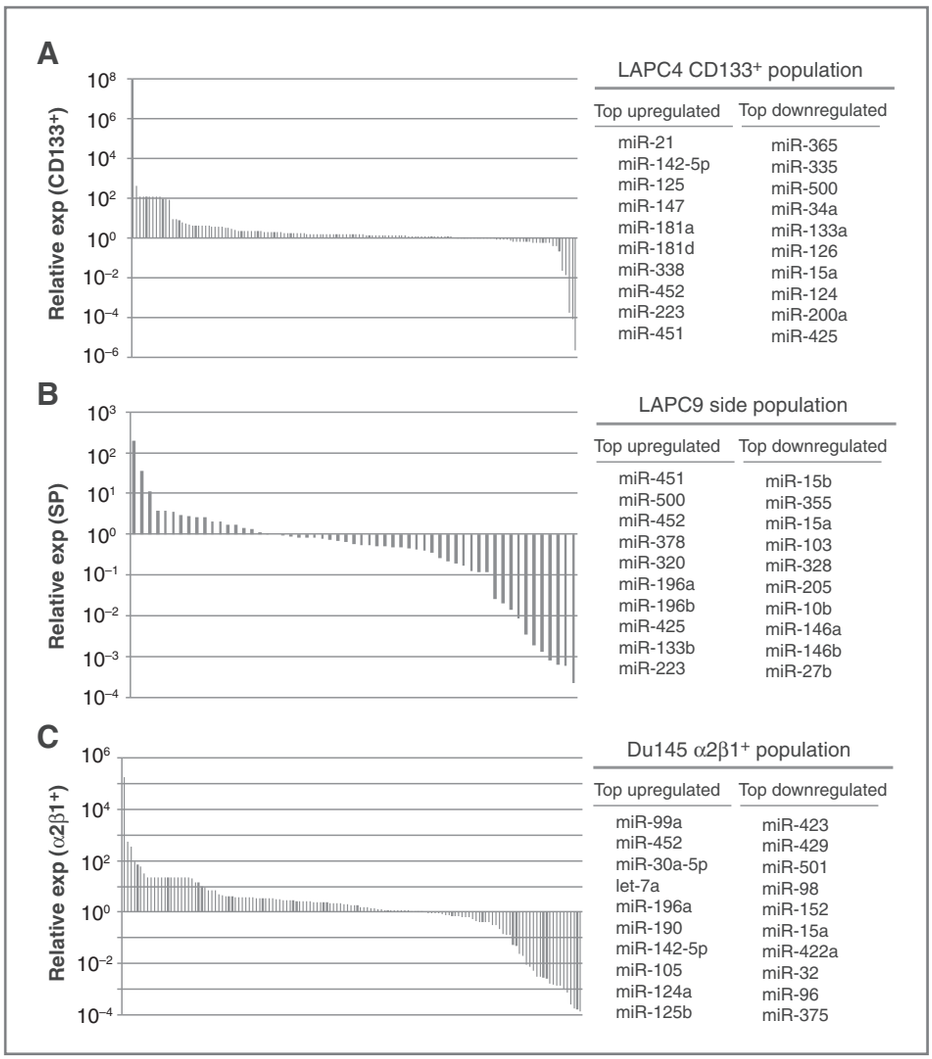

Figure 1. miRNA expression profiles in CD133$^+$, $\alpha2\beta1^+$, and side population (SP) prostate cancer cells. A–C, the miRNA expression (exp) levels in the marker-positive populations including CD133$^+$ from LAPC4 (A), side population from LAPC9 (B), and $\alpha2\beta1^+$ from Du145 (C), relative to the corresponding marker-negative populations. The top 10 over- and underexpressed miRNAs are listed on the right.

prostate cancer cells. We then used the online database Diana mir-Path (42) to probe the potential signaling pathways that might be engaged by differentially expressed miRNAs. The software conducts an enrichment analysis of multiple miRNA target genes against all known Kyoto Encyclopedia of Genes and Genomes (KEGG) pathways. When we input the set of miRNAs commonly underexpressed in CD44$^+$ cells, the top hits were TGFβ, Wnt, and mitogen-activated protein kinase (MAPK) signaling pathways (not shown).

The CD44$^+$ prostate cancer cells are generally less differentiated (e.g., expressing less AR; ref. 6). Consistent with this notion, many of the miRNAs identified here to be underexpressed in the CD44$^+$ LAPC9, LAPC4, and Du145 cells, including miR-34a, miR-141, let-7 members, miR-10a, miR-214, miR-203, miR-183, miR-365, miR-193b, miR-24, and miR-30c (Table 1) are generally depleted in (cancer) stem cells and preferentially expressed in differentiated progeny. In further support, several miRNAs underexpressed in CD44$^+$ prostate cancer cells, such as miR-148a (43) and miR-141 (44), have been shown to be androgen-responsive.

Distinctive and common miRNA expression profiles in prostate cancer stem/progenitor cell populations

We then analyzed the expression levels of 134 miRNAs in LAPC4 CD133$^+$ and Du145 $\alpha2\beta1^+$ cells and 57 miRNAs in LAPC9 side population cells in comparison to their corresponding marker-negative populations and we observed miRNA expression patterns unique to each tumor cell population (Fig. 1; Supplementary Tables S3 and S4). Interesting, the top overexpressed miRNA in CD133$^+$ LAPC4 cells was miR-21, one of the best-characterized oncomiRs widely overexpressed in human cancers (45). Among the top 10 downregulated miRNAs were many miRNAs that were also underexpressed in CD44$^+$ prostate cancer cells and several tumor-suppressive miRNAs including miR-133a, miR-126, miR-15a, and miR-200a (Fig. 1A). In general, the magnitude of downregulation (i.e., to $\sim10^{-6}$) was much more pronounced than that of upregulation (up to $\sim10^2$ for most), although surprisingly, there were more miRNAs overexpressed than underexpressed in CD133$^+$ LAPC4 cells (Fig. 1A). When we compared the 134 miRNA expression in CD133$^+$ versus CD44$^+$ LAPC4 cells, we observed

Published OnlineFirst June 19, 2012; DOI:10.1158/0008-5472.CAN-11-3864

Table 2. Commonly over- and underexpressed miRNAs in tumorigenic prostate cancer cell populations

Four populations[a]		Four populations[b]		Five populations[c]		Six populations[d]	
Overexpressed	**Underexpressed**	**Overexpressed**	**Underexpressed**	**Overexpressed**	**Underexpressed**	**Overexpressed**	**Underexpressed**
miR-19a	miR-34a	miR-301	miR-34a	miR-301	miR-34a	miR-452	miR-34a
miR-301	let-7b	miR-452	let-7b	miR-452	let-7b		
miR-452	miR-106a		miR-106a		miR-106a		
	miR-141		miR-141		miR-141		
	let-7f		let-7e				
	miR-335		miR-183				
	miR-340		miR-203				
	miR-365		miR-218				
	miR-92		miR-342				
			miR-378				
			miR-422a				
			miR-422b				

[a]These 4 populations refer to the 3 CD44$^+$ populations from LAPC9, LAPC4, and Du145, respectively, plus the CD133$^+$ population from LAPC4.

[b]These 4 populations refer to the 3 CD44$^+$ populations plus the $\alpha2\beta1^+$ population from Du145.

[c]These 5 populations refer to 3 CD44$^+$ populations from LAPC9, LAPC4, and Du145 plus the CD133$^+$ population from LAPC4 and the $\alpha2\beta1^+$ population from Du145.

[d]The 6 populations include the 5 populations in c plus the LAPC9 side population (SP).

25 commonly overexpressed and 29 commonly underexpressed miRNAs (Supplementary Fig. S3A).

In contrast to CD133$^+$ prostate cancer cells, there were significantly more miRNAs underexpressed than overexpressed in LAPC9 side population cells when compared with the isogenic non–side population cells and, again, the levels of downregulation were higher than those of upregulation (Fig. 1B). The top overexpressed miRNA was miR-451, which was recently shown to regulate the self-renewal and tumorigenicity of colorectal CSCs (46). Among the top 10 underexpressed miRNAs in side population were miR-15a/15b and several oncosuppressive miRNAs downregulated in CD44$^+$ prostate cancer cells. We observed 6 commonly overexpressed and 31 commonly underexpressed miRNAs in side population versus CD44$^+$ LAPC9 cells (Supplementary Fig. S3B). Finally, roughly similar numbers of up- and downregulated miRNAs were observed in $\alpha2\beta1^+$ and $\alpha2\beta1^-$ Du145 cells (Fig. 1C). We observed 44 commonly overexpressed and 22 commonly underexpressed miRNAs in $\alpha2\beta1^+$ versus CD44$^+$ Du145 cells (Supplementary Fig. S3C). Surprisingly, among the top 10 upregulated miRNAs were miR-30a-5p, let-7a, and miR-196a (Fig. 1C), which were commonly underexpressed in CD44$^+$ prostate cancer cells (Table 1). These observations are consistent with our earlier conclusions that the $\alpha2\beta1^+$ prostate cancer cell population overlaps with but is also distinct from the CD44$^+$ population (7).

Subsequently, we tried to identify commonly changed miRNAs. We first compared the common CD44 profiles (Table 1) with the profiles generated from CD133$^+$ or $\alpha2\beta1^+$ populations (Supplementary Tables S2 and S3) and uncovered the miRNAs that were commonly over- or underexpressed in the 4 (i.e., 3 CD44$^+$ together with CD133$^+$ or $\alpha2\beta1^+$) cell populations (Table 2). When we combined 5 populations (i.e., 3 CD44$^+$ together with CD133$^+$ and $\alpha2\beta1^+$), only 4 miRNAs, that is, let-7b, miR-106a, miR-141, and miR-34a, were commonly underexpressed and 2 miRNAs, that is, miR-301 and miR-452, were commonly overexpressed (Fig. 2A; Table 2). When we further included the expression profile from the LAPC9 side population, only one miRNA, that is, miR-34a, was commonly underexpressed and one miRNA, miR-452, was commonly overexpressed in all 6 prostate cancer cell populations (Table 2; Supplementary Fig. S4A).

Validation of commonly changed miRNAs in patient tumor (HPCa)-derived CD44$^+$ cells

The preceding miRNA library expression profiling was conducted in cells purified from 3 xenograft models. To validate the miRNA expression data, we purified CD44$^+$ and CD44$^-$ prostate cancer cells from 21 primary HPCa samples (Supplementary Table S1) and measured the levels of 4 commonly underexpressed (miR-34a, let-7b, miR-141, and miR-106a) and 2 commonly overexpressed (miR-301 and miR-452) miRNAs. This strategy has an additional advantage of establishing the potential clinical relevance. We previously verified miR-34a underexpression in all HPCa-purified CD44$^+$ prostate cancer cells (22). let-7b also showed underexpression in the majority (18 of 21) of samples in the CD44$^+$ HPCa cells (Fig. 2B). Likewise, miR-141 was detected at much lower levels in CD44$^+$ than in CD44$^-$ cells derived from most HPCa samples (data not shown). In contrast, miR-106a was underexpressed in 3 of the 5 xenograft-derived populations (Supplementary Fig. S4B) and in only approximately 50% of 21 HPCa-derived CD44$^+$ prostate cancer cells (Supplementary Fig. S4C). With the 2 commonly overexpressed miRNAs, we detected an overrepresentation of miR-301 in the CD44$^+$ cells in 18 of 21 HPCa samples (Fig. 2C). Unexpectedly, although miR-452 was dramatically upregulated

Published OnlineFirst June 19, 2012; DOI:10.1158/0008-5472.CAN-11-3864

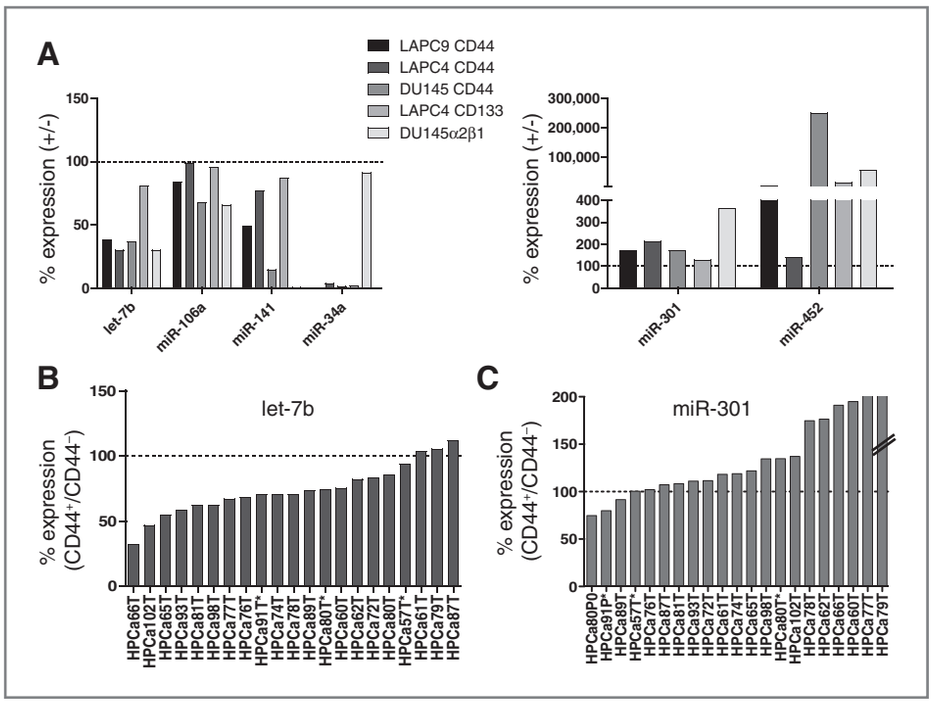

Figure 2. Commonly under- and overexpressed miRNAs in tumorigenic populations of prostate cancer cells and validation in CD44$^+$ HPCa cells. A, four commonly underexpressed miRNAs (left) and 2 commonly overexpressed miRNAs (right) in 5 marker-positive prostate cancer cell populations (see bar legend). Shown are the miRNA expression levels (%) in the marker-positive populations relative to those in the corresponding marker-negative populations. B and C, validation of let-7b (B) and miR-301 (C) expression in purified CD44$^+$ HPCa cells. Shown are the mean values of the relative expression in CD44$^+$ over CD44$^-$ HPCa cells. Note that the actual miR-301 expression level in CD44$^+$ HPCa79T (the last bar in C) was 96,848.63% relative to the corresponding CD44$^-$ HPCa79T cells.

in 4 of the 5 xenograft populations (Supplementary Fig. S4D), it was downregulated in most CD44$^+$ HPCa cells (Supplementary Fig. S4E). Altogether, of the 6 miRNAs commonly changed in the 5 prostate cancer cell populations, we could corroborate the underexpression of miR-34a, let-7b, and miR-141 and overexpression of miR-301 (i.e., 4 of 6 or 67%) using primary tumor–derived CD44$^+$ HPCa cells.

let-7 inhibits clonal and sphere formation in prostate cancer cells: differential effects from miR-34a

To investigate the biologic functions of commonly and differentially expressed miRNAs, we first focused on 2 underexpressed miRNAs, that is, miR-34a and let-7, mainly because both had been shown to possess strong tumor-suppressive functions in other systems (27, 29, 30). Our earlier studies showed that miR-34a functioned as a negative regulator of PCSCs and prostate cancer metastasis (22). Herein, we focused on let-7 as 4 let-7 miRNA family members were underexpressed in CD44$^+$ cells (Table 1) and let-7b was commonly underexpressed in 5 prostate cancer cell populations (Fig. 2A) as well as in CD44$^+$ HPCa cells (Fig. 2B). Overexpression of let-7b in Du145 cells by transfection of a let-7b mimicking oligonucleotide reduced cell number (Fig. 3A) due to inhibition of proliferation as assessed by BrdUrd incorporation assays (Fig. 3B). In addition, let-7b oligos, when compared with the negative control (NC) oligos that contain a scrambled sequence, inhibited the establishment of Du145 holoclones (Fig. 3C–E) and spheres (Fig. 3F). Prostate cancer cell holoclones contain self-renewing tumor-initiating cells (24) and prostate cancer cell spheres formed under anchorage-independent conditions harbor tumor-initiating cells (6, 12, 25). Finally, when we infected Du145 cells with a lentivirus (i.e., pLL3.7-let-7a; ref. 27) that encodes let-7a (which recognizes the same seed sequence as let-7b), both clonal development (Supplementary Fig. S5A) and sphere formation (Supplementary Fig. S5B and S5C) were inhibited. We observed similar inhibitory effects of let-7b oligos in another prostate cancer cell type, PPC-1 (Fig. 3G; Supplementary Fig. S6A–S6C). It should be noted that all miRNA mimicking oligos used in our previous (22) and present studies are mature miRNAs, which mimic the dicer cleavage product loaded into the RNA-induced silencing complex (RISC) in the cytoplasm (22).

Overall, let-7b mimicking oligos showed similar inhibitory effects to miR-34a overexpression on prostate cancer cell holoclones and spheres (Fig. 3C–G; Supplementary Fig. S6B and S6C). However, when we analyzed cell-cycle profiles in PPC-1 cells treated with miR-34a or let-7b oligos, we observed that miR-34a caused G_1 cell-cycle arrest, whereas let-7b led to prominent G_2–M phase arrest (Fig. 3H and I). Fully consistent with the differential effects between miR-34a and let-7b on cell cycle, miR-34a overexpression induced significantly increased cell senescence assessed by staining of prostate cancer cells for senescence-associated β-gal (SA-βgal) activity (Fig. 3J; Supplementary Fig. S6D). It is well documented that G_1 cell-cycle arrest generally precedes cell senescence. In contrast, let-7b oligos, which did not cause G_1 arrest, did not induce PPC-1 cell senescence (Fig. 3J; Supplementary Fig. S6D). These results altogether suggest that let-7b and miR-34a exert differential mechanisms in prostate cancer cells with respect to their effects on cell cycle and senescence.

let-7 inhibits prostate tumor regeneration: evidence for fast turnover of let-7 in prostate cancer cells

Next, we investigated the let-7 effects on tumor regeneration. We first conducted the "positive" control experiments by s.c. implanting A549 lung cancer cells that had been

Published OnlineFirst June 19, 2012; DOI:10.1158/0008-5472.CAN-11-3864

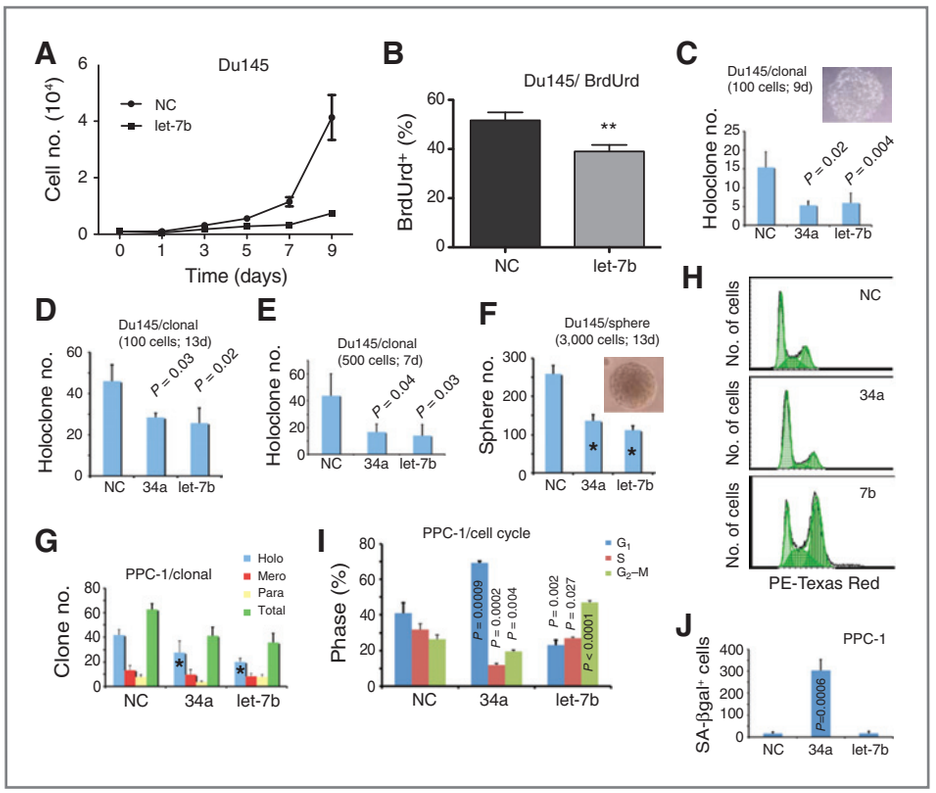

Figure 3. Biologic effects of let-7b on prostate cancer cells *in vitro*. A and B, let-7b inhibits Du145 cell proliferation. A, one thousand cells transfected with NC or let-7b oligos (30 nmol/L) were plated in 6-well plate on day 0, and cells were trypsinized and counted on days indicated. Average cell numbers were plotted. B, the mean percentage of BrdUrd-positive cells counted from a total of 800 to 1,000 cells. C–E, clonal assays in Du145 cells. Cells transfected with the indicated oligos (30 nmol/L; 24 hours) were plated in 6-well plate at clonal density. The plating cell numbers and the days when holoclones (a representative picture shown in the inset, C) were enumerated are indicated. F, sphere formation assays in Du145 cells. Cells were transfected as above and 3,000 cells mixed with Matrigel were plated in 6-well plate for sphere formation assay. Spheres were counted in approximately 2 weeks. A representative sphere is shown in the inset. G, overexpression of let-7b inhibits PPC-1 clonal growth. Cells (100) transfected with the indicated oligos (30 nmol/L; 48 hours) were plated in triplicate in 6-well culture plates. The 3 types of clones were enumerated 10 days after plating. *, $P < 0.05$ when compared with the NC group. Let-7b (and miR-34a) also reduced the total number of clones ($P < 0.05$). H and I, miR-34a induces PPC-1 cell G_1 arrest, whereas let-7b causes G_2–M phase arrest. Cells were transfected with the oligos (30 nmol/L; 48 hours) followed by cell-cycle analysis by flow. Shown are representative histograms (H) and quantification (I; $n = 4$). J, senescence-associated β-gal staining. Shown are the SA-βgal$^+$ cells. All assays were done in triplicate.

transfected with the let-7b or NC oligos in NOD/SCID mice. As reported earlier by others (30), let-7b overexpression suppressed A549 tumor development (Supplementary Fig. S7A). Surprisingly, in multiple similar tumor experiments carried out in Du145 (Supplementary Fig. S7B and S7C) or LAPC9 (Fig. 4A; Supplementary Fig. S7D) cells, let-7b oligos did not manifest obvious tumor-suppressive effects whether cells were implanted s.c. or in the dorsal prostate (DP; Supplementary Fig. S7B and S7C). Similar to let-7b oligos, let-7a oligos also did not inhibit LAPC9 tumor regeneration, although miR-34a oligos significantly retarded tumor growth (Fig. 4A). These surprising results suggested that (i) let-7 miRNAs might exert differential effects on lung (A549) versus prostate (Du145 and LAPC9) cancer cells; (ii) transfected let-7 oligos might be turned over faster in prostate cancer cells compared with lung cancer cells; (iii) let-7 and miR-34a might exert divergent regulatory roles in prostate cancer cells; and/or (iv) let-7 oligos might become degraded or turned over faster than miR-34a oligos in prostate cancer cells.

To start addressing these possibilities, we first measured let-7a/b and miR-34a levels in both freshly transfected cells and endpoint tumors (Fig. 4B–D). Du145 (Fig. 4B) and LAPC9 (Fig. 4C) cells transfected with let-7 oligos had several 100-fold higher levels of let-7 than the same cells transfected with NC oligos at 48 hours. Unexpectedly, however, A549 cells transfected with the same amount (i.e., 30 nmol/L) of let-7b possessed much higher levels of intracellular let-7b than either Du145 or LAPC9 cells (Fig. 4B and C). More surprisingly, at 48 hours after transfection of the same amount of miR-34a or let-7b (30 nmol/L for each), LAPC9 cells retained significantly higher levels of miR-34a than let-7b (Fig. 4C). As expected, the endpoint tumors all expressed similarly low levels of let-7a/b or miR-34a (Fig. 4D). These results suggest that transfected let-7 oligos, in contrast to miR-34a oligos, were rapidly degraded in prostate cancer cells, in contrast to A549 cells. Consistent with this suggestion, when we infected LAPC9 cells with pLL3.7-let-7a, the continuously delivered let-7a significantly slowed tumor

Published OnlineFirst June 19, 2012; DOI:10.1158/0008-5472.CAN-11-3864

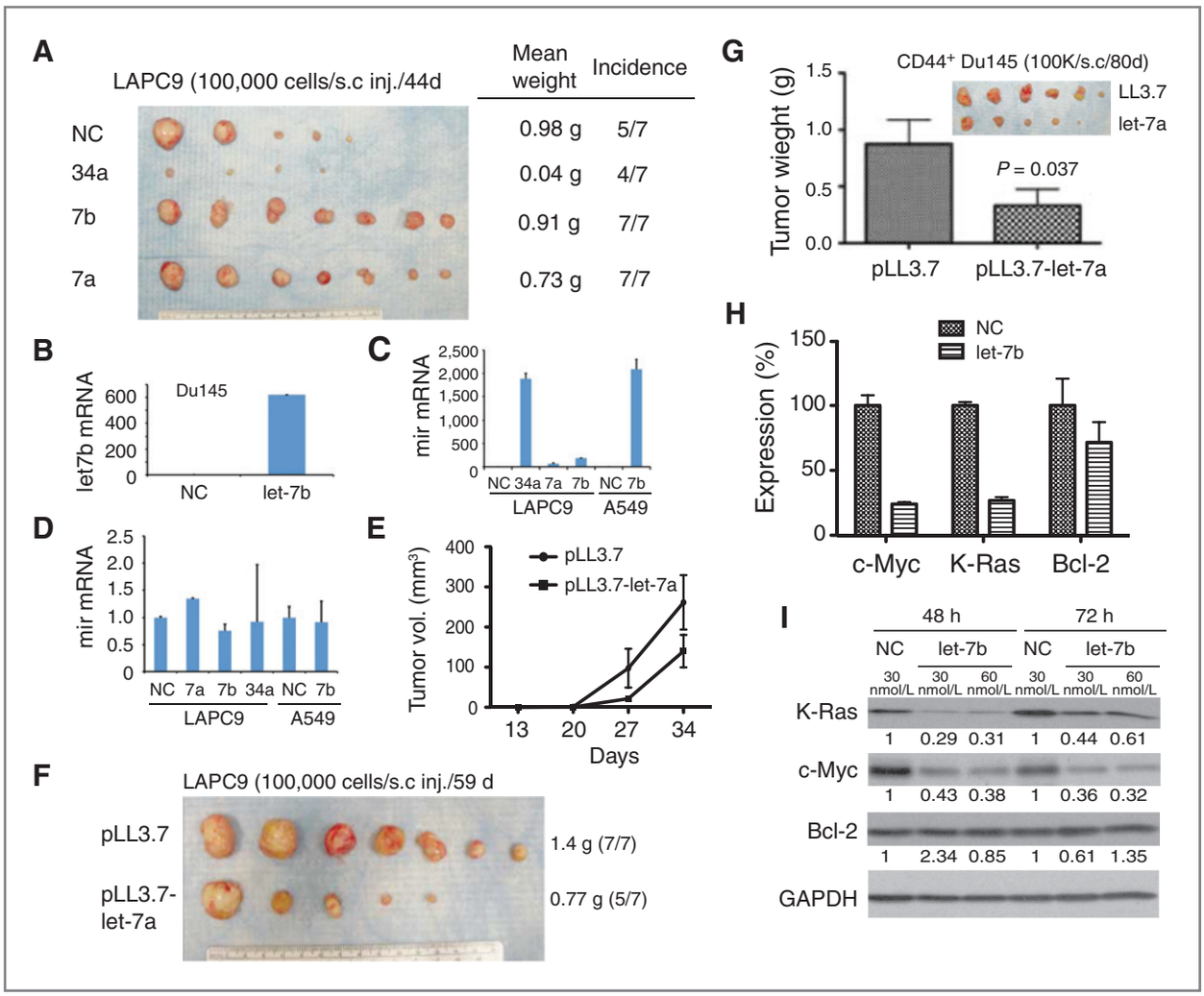

Figure 4. Effects of let-7 on prostate tumor development *in vivo*. A, overexpression of let-7b or let-7a in LAPC9 cells by oligo transfection did not inhibit tumor regeneration. Shown are tumor images harvested at 44 days after implantation. The mean tumor weight and incidence are indicated on the right. B and C, RNA levels of let-7a/b or miR-34a in freshly transfected (30 nmol/L; 48 hours) Du145 (B) or LAPC9 and A549 (C) cells measured by qRT-PCR. Shown are the expression levels (fold) relative to the corresponding NC control. C, the differences between miR-34 and let-7a or let-7b mRNA levels in LAPC9 cells were statistically significant ($P < 0.05$ for both; based on comparisons of the actual $\Delta\Delta C_t$ values). Also, the let-7b mRNA levels in A549 cells were significantly higher than those in LAPC9 ($P = 0.019$; $\Delta\Delta C_t$) or in Du145 ($P = 0.049$; $\Delta\Delta C_t$) cells. D, RNA levels of let-7a/b or miR-34a in endpoint LAPC9 or A549 tumors measured by qRT-PCR. Shown are the expression levels (fold) relative to the corresponding NC control. These endpoint tumors were derived from the corresponding transfected cells shown in A or C. E and F, overexpression of let-7a by lentiviral-mediated transduction significantly inhibited LAPC9 tumor development. Tumor sizes were measured by a caliber on the days indicated (E) and tumor images, average tumor weight, and incidence (parentheses) are presented (F). G, overexpression of let-7a inhibited tumor development from $CD44^+$ Du145 cells. H and I, validation of let-7 downstream targets by qPCR (H) and Western blotting (I) analysis. In H, Du145 cells were transfected with let-7b or NC oligos (30 nmol/L; 48 hours), and cells were harvested for qPCR analysis of *K-Ras*, *c-Myc* and *Bcl-2* mRNAs. In I, Du145 cells were transfected with the oligos (conc. and time indicated). Cells were lysed and 50 μg of whole-cell lysate was loaded in each lane for the molecules indicated. Relative densitometric values were given below. GAPDH, glyceraldehyde-3-phosphate dehydrogenase.

growth (Fig. 4E) and inhibited tumor regeneration (Fig. 4F). Impressively, pLL3.7-let-7a also inhibited tumor development of the purified $CD44^+$ Du145 cells (Fig. 4G).

The let-7 family miRNAs repress many oncogenic molecules including Ras, c-Myc, HMG, and Bcl-2 (27, 29, 30). We observed that prostate cancer cells freshly transfected with the let-7b oligos exhibited significantly reduced c-Myc and K-Ras, both at the mRNA (Fig. 4H) and protein (Fig. 4I) levels. Luciferase reporter assays confirmed K-Ras as a direct let-7 downstream target (Supplementary Fig. S8). In contrast, the Bcl-2 mRNA and protein levels were not affected by let-7b (Fig. 4H and I).

miR-301 exerted differential biologic effects on different prostate cancer cells

We also probed for the biologic functions of one commonly overexpressed miRNA, that is, miR-301 (Supplementary Figs. S9 and S10). Unexpectedly, enforced miR-301 expression via oligo-transfection in purified $CD44^-$ Du145

Published OnlineFirst June 19, 2012; DOI:10.1158/0008-5472.CAN-11-3864

cells (Supplementary Fig. S9A) or knocking down endogenous miR-301 in CD44$^+$ Du145 cells (Supplementary Fig. S9B) did not significantly affect sphere formation. Similar negative results were obtained in holoclone assays (Supplementary Fig. S9C and S9D). miR-301 overexpression and knockdown were verified by quantitative PCR (qPCR; Supplementary Fig. S9E). Manipulation of miR-301 levels also did not affect the tumor regeneration of CD44$^+$/CD44$^-$ Du145 cells (Supplementary Fig. S9F–S9I). Similarly, anti-miR-301 oligos did not alter the clonal and tumorigenic properties of PC3 cells (Supplementary Fig. S10A–S10C). In contrast, enforced miR-301 expression promoted, whereas anti-miR-301 reduced the clonal and sphere-forming capacities of xenograft-derived LAPC9 cells (Supplementary Fig. S10D and S10E).

How miRNAs might be underexpressed in prostate cancer stem/progenitor cells?

How tumor-suppressive miRNAs such as miR-34a and let-7 might be underexpressed in tumorigenic subpopulations is an interesting question. We attempted to address this question by focusing on miR-34a, whose expression is regulated in both p53-dependent and -independent mechanisms (47). The miR-34a levels in the 4 prostate cancer cell types with null or mutant p53 were significantly lower than those in the 6 prostate (cancer) cell types with wild-type (wt) p53 (22). To explore whether the lower levels of miR-34a in tumorigenic prostate cancer cells might be related to lower p53 expression/activity, we treated p53-wt LNCaP cells with paclitaxel and 3 DNA-damaging agents, that is, doxorubicin, etoposide, and γ-irradiation (X-ray). p53 was activated by etoposide and X-ray, as evidenced by both p53 protein accumulation (Fig. 5A) and increased protein and mRNA levels of p21 (Fig. 5A and B), a p53 transcriptional target. When miR-34a (1p36.22) and miR-34b/c (11q23.1) levels were measured in treated LNCaP cells, we observed that miR-34a levels did not significantly change except a slight increase at 48 hours (Fig. 5C). In contrast, both etoposide and X-ray increased miR-34b and miR-34c levels by several fold (Fig. 5C). These observations suggest that underexpression of miR-34a in CD44$^+$ prostate cancer cells might not be related to p53 expression or activity. In support, the miR-34a mRNA levels in the CD44$^+$ cells freshly purified from 14 primary HPCa cells did not correlate with *p53* (Supplementary Fig. S11A and S11B) or *p21* (not shown) mRNA levels. Previous studies suggest that c-Myc may positively regulate miR-34a (48). However, the miR-34a mRNA levels in CD44$^+$ HPCa cells also did not correlate with *c-Myc* mRNA (Supplementary Fig. S11C).

Discussion

For the first time, we have profiled the miRNA expression patterns in purified subpopulations of prostate cancer cells that possess stem/progenitor cell properties. Among the CD44$^+$, side population, CD133$^+$, and α2β1$^+$ cells studied, the CD44$^+$ prostate cancer cells are best characterized and have been consistently shown to enrich for tumor-initiating and prometastatic cells (6, 7, 22, 25). The side population is also enriched in tumorigenic cells, although it is more rare (<0.1%) and detectable only in LAPC9 cells (12, 25). The CD133$^+$ prostate cancer cells are clonogenic and may also harbor CSCs (28). In contrast, the α2β1$^+$ prostate cancer cells are proliferative progenitors that do not enrich for CSCs (7). Our current miRNA profiling substantiates the heterogeneous nature of prostate cancer stem/progenitor cells as CD44$^+$, side population, CD133$^+$, and α2β1$^+$ cell populations exhibit overall distinct miRNA expression profiles. This is perhaps best illustrated by comparing CD44$^+$ and CD133$^+$ populations—the

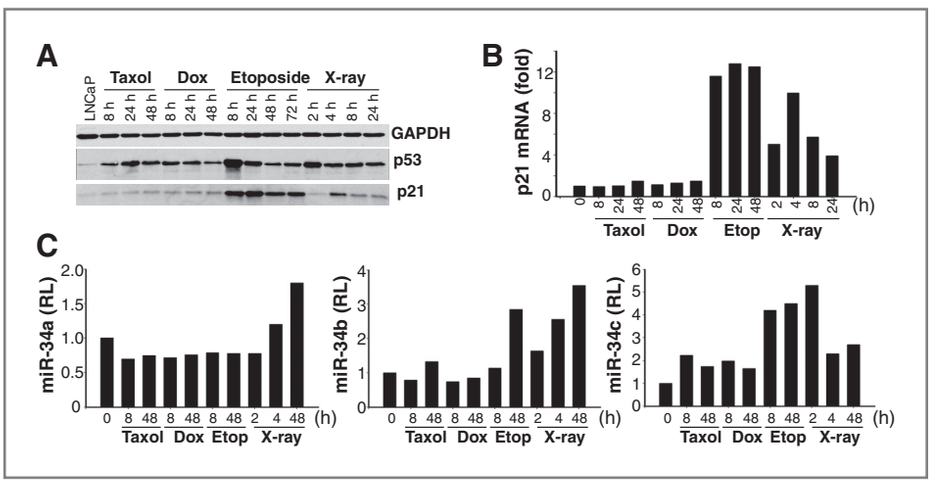

Figure 5. p53 activation in LNCaP cells differentially affects miR-34 family members. A, LNCaP cells were treated with paclitaxel (Taxol, 25 nmol/L), doxorubicin (Dox, 10 ng/mL), etoposide (Etop, 50 nmol/L), or γ-irradiation (X-ray, 10 Gy) for the time intervals indicated. Whole-cell lysate (50 μg per lane) was used in Western blotting for p53, p21, or glyceraldehyde-3-phosphate dehydrogenase (GAPDH; loading control). B, verification by qRT-PCR of upregulation of *p21* mRNA in treated LNCaP cells. C, p53 activation in LNCaP cells preferentially induces miR-34b and miR-34c over miR-34a. Among the 4 treatments, only γ-irradiation slightly increased miR-34a levels (left). In contrast, both etoposide and X-ray upregulated miR-34b expression (middle), whereas all 4 treatments increased miR-34c expression (right).

Published OnlineFirst June 19, 2012; DOI:10.1158/0008-5472.CAN-11-3864

$CD44^+$ prostate cancer cells predominantly downregulate, whereas the $CD133^+$ LAPC4 cells significantly upregulate multiple miRNAs. Some of the underexpressed miRNAs such as miR-34a and let-7 are also downregulated in prostate tumors in comparison with benign tissues (16–20).

On the other hand, different prostate cancer stem/progenitor cells also commonly over- and underexpress certain miRNAs. One of the most striking observations is that the 3 populations of $CD44^+$ prostate cancer cells commonly and coordinately downregulate 37 miRNAs, many of which exist in genomic clusters and most of which possess tumor-suppressive functions. This observation is remarkably similar to the findings that multiple tumor-suppressive miRNAs are coordinately "depleted" in other CSCs, for example, the underexpression of let-7 family, miR-200 family, and miR-30 in breast CSCs and of miR-34a, miR-128, miR-451, and others in glioblastoma stem cells (reviewed in ref. 23). More remarkably, Shimono and colleagues also reported that 37 miRNAs were differentially expressed in the $CD44^+CD24^{-/lo}$ breast CSCs including the downregulation of 3 clusters, miR-200c/141, miR-200b/200a/429, and miR-183/96/182 (39), which are also downregulated in $CD44^+/\alpha2\beta1^+$ prostate cancer cells. Because these CSC-depleted miRNAs generally target potent oncogenic molecules involved in regulating cell cycle and proliferation [e.g., E2F, HMGA2, Ras, cyclins, cyclin-dependent kinases (CDK)], cell survival (e.g., Bcl-2, Mcl-1, Bcl-XL), self-renewal (e.g., Bmi, Notch, Myc), and cell migration/invasion (e.g., CD44, c-MET, ZEB; ref. 23), it is conceivable that lack of these miRNAs would confer many stem cell properties. Many of these tumor-suppressive miRNAs are also deficient in embryonic and adult stem cells and preferentially expressed in differentiated progeny (23). Consequently, their lower expression in $CD44^+$ prostate cancer cells further supports the stem-like features of these cells and is consistent with earlier observations that the $CD44^+$ prostate cancer cells are less differentiated expressing little AR (6). In this regard, it is interesting that at least 2 androgen-responsive miRNAs, that is, miR-148a (43) and miR-141 (44), are underexpressed in the $CD44^+$ prostate cancer cells. In contrast, another androgen-regulated miRNA, miR-21 (49), is the most highly expressed miRNA in $CD133^+$ LAPC4 cells, emphasizing the difference between these 2 populations of prostate cancer cells.

More miRNAs are downregulated than upregulated in the 3 $CD44^+$ prostate cancer cell populations in common with either $CD133^+$ or $\alpha2\beta1^+$ cells (Table 2). When these 5 populations are combined for analysis, 4 miRNAs (i.e., miR-34a, let-7b, miR-106a, and miR-141) are commonly downregulated and 2 miRNAs (i.e., miR-301 and miR-452) are commonly upregulated. Using the $CD44^+$ HPCa cells freshly purified from patient tumors, we have confirmed the differential expression of 4 of the 6 (i.e., miR-34a, let-7b, miR-141, and miR-301) miRNAs in marker-positive versus -negative cells. It is presently unclear why the underexpression of miR-106a and overexpression of miR-452 observed in 3 xenograft prostate cancer cells are not borne out in $CD44^+$ HPCa cells.

To establish whether the miRNAs identified in our miRNA library screening are functionally relevant, we have by far thoroughly studied 2 commonly underexpressed (i.e., miR-34a and let-7b) and 1 commonly overexpressed (i.e., miR-301) miRNAs. Our earlier studies have uncovered a powerful role of miR-34a in restricting PCSC activity and prostate cancer regeneration/metastasis via repressing CD44 itself (22). In the present study, we report similar prostate cancer–suppressive functions of let-7b/a. Our observations are in line with the widely recognized tumor-inhibitory effects of let-7a/b (27, 29, 30) and suggest that like miR-34a, the underexpressed let-7 normally functions to inhibit certain PCSC properties. An intriguing finding is that in prostate cancer cells, the transfected mature let-7a/b oligos seem to be degraded much more rapidly than miR-34a oligos, explaining why the former do not manifest obvious tumor-inhibitory effects. In fact, even prostate cancer cells infected with the pLL3.7-let-7a lentiviral vectors, which do manifest prostate cancer–inhibitory effects, keep low steady-state levels of let-7a (Liu and colleagues, unpublished observations). Coupled with the observations in A549 lung cancer cells, our work suggests that in prostate cancer, let-7 miRNAs have a faster turnover rate than other miRNAs such as miR-34a. Future work will further explore this potentially interesting phenomenon. Another interesting finding is that let-7 and miR-34a possess mechanistic differences in suppressing prostate cancer stem/progenitor cells: miR-34a induces G_1 cell-cycle arrest followed by cell senescence, whereas let-7 causes a prominent G_2–M phase arrest without inducing senescence. Furthermore, miR-34a, but not let-7, induces apoptosis in some prostate cancer cells (22). In support, let-7 overexpression does not affect the prosurvival molecule Bcl-2 (Fig. 4I).

In contrast to consistent prostate cancer–inhibitory effects of miR-34a and let-7, miR-301, which is commonly overexpressed in prostate cancer stem/progenitor cells and recently shown to promote breast cancer cell proliferation and invasion (50), seems to exhibit cell type–dependent effects. Although manipulation of miR-301 levels does not affect Du145 and PC3 cells, its overexpression promotes, whereas its knockdown inhibits the clonogenic properties of LAPC9 cells.

It will be of general interest to understand how certain miRNAs are differentially expressed in CSCs versus non-CSCs. Because the 2 populations are isogenic, it stands to reason that the differential expression results from epigenetic events rather than genetic mutations. Indeed, many tumor-suppressive miRNAs (e.g., miR-34a) are downregulated in cancer because of promoter hypermethylation or aberrant histone modifications. When we treated $CD44^+$ prostate cancer cells with 5-aza-deoxycytidine and/or trichostatin A (an inhibitor of histone deacetylase), we did not observe any significant increase in miR-34 (Liu and colleagues, unpublished observations). The miR-34a levels also do not correlate with the 2 known upstream transcriptional regulators, that is, p53 and c-Myc. In fact, even in p53-wt bulk LNCaP cells, p53 activation does not consistently result in significant upregulation of miR-34a. Altogether, these observations argue that some other mechanisms might be operating to dampen miR-34a expression in PCSC-enriched cells.

In summary, we have successfully conducted an miRNA expression profiling study in several prostate cancer stem/progenitor cell populations, which has revealed both

Published OnlineFirst June 19, 2012; DOI:10.1158/0008-5472.CAN-11-3864

distinctively and commonly expressed miRNAs in tumorigenic prostate cancer cells. While shedding important light on how PCSCs may be regulated by miRNAs, our results converge with the emerging theme that distinct miRNAs both distinctively and coordinately regulate CSC properties (23). Finally, our study establishes that tumor-suppressive miRNAs identified herein, such as miR-34a and let-7b/a, may represent novel therapeutics to specifically target CSCs and can be used in replacement therapy regimens.

Disclosure of Potential Conflicts of Interest

K. Kelnar is the fulltime employee of Mirna Therapeutics and A. Vlassov is a fulltime employee of Life Technologies. D. Brown has ownership interest (including patents) and is employed as the Director of Research in Mirna Therapeutics. No potential conflicts of interest were disclosed by the other authors.

Authors' Contributions

Conception and design: C. Liu, D. Brown, J. Wang, D.G. Tang
Development of methodology: C. Liu, D.G. Tang
Acquisition of data (provided animals, acquired and managed patients, provided facilities, etc.): C. Liu, D.G. Tang
Analysis and interpretation of data (e.g., statistical analysis, biostatistics, computational analysis): C. Liu, K. Kelnar, D. Brown, D.G. Tang
Writing, review, and/or revision of the manuscript: C. Liu, D. Brown, D.G. Tang
Administrative, technical, or material support (i.e., reporting or organizing data, constructing databases): K. Kelnar, A.V. Vlassov, D.G. Tang
Study supervision: D.G. Tang
Coordinating several collaborating groups: D.G. Tang

Acknowledgments

The authors thank P. Whitney, B. Liu, and X. Liu for their technical assistance, Dr. J. Lieberman for providing pLL3.7-let-7 lentivector, and other Tang laboratory members for helpful discussions.

Grant Support

This work was supported, in part, by grants from the NIH (R01-ES015888, R21-CA150009), Department of Defense (W81XWH-08-1-0472, W81XWH-11-1-0331), CPRIT funding (RP120380), and the MD Anderson Cancer Center Bridge fund and Center for Cancer Epigenetics and Laura and John Arnold Foundation RNA Center pilot grant (to D.G. Tang), and by two Center Grants (CCSG-5 P30 CA016672 and ES007784). C. Liu was supported in part by a predoctoral fellowship from the Department of Defense (W81XWH-10-1-0194).

The costs of publication of this article were defrayed in part by the payment of page charges. This article must therefore be hereby marked *advertisement* in accordance with 18 U.S.C. Section 1734 solely to indicate this fact.

Received November 25, 2011; revised April 3, 2012; accepted April 20, 2012; published OnlineFirst June 19, 2012.

References

1. Tang DG. Understanding cancer stem cell heterogeneity and plasticity. Cell Res 2012;22:457–72.
2. Al-Hajj M, Wicha MS, Benito-Hernandez A, Morrison SJ, Clarke MF. Prospective identification of tumorigenic breast cancer cells. Proc Natl Acad Sci U S A 2003;100:3983–8.
3. Singh SK, Hawkins C, Clarke ID, Squire JA, Bayani J, Hide T, et al. Identification of human brain tumour initiating cells. Nature 2004;432:396–401.
4. Hermann PC, Huber SL, Herrler T, Aicher A, Ellwart JW, Guba M, et al. Distinct populations of cancer stem cells determine tumor growth and metastatic activity in human pancreatic cancer. Cell Stem Cell 2007;1:313–23.
5. Li C, Heidt DG, Dalerba P, Burant CF, Zhang L, Adsay V, et al. Identification of pancreatic cancer stem cells. Cancer Res 2007;67:1030–7.
6. Patrawala L, Calhoun T, Schneider-Broussard R, Li H, Bhatia B, Tang S, et al. Highly purified CD44$^+$ prostate cancer cells from xenograft human tumors are enriched in tumorigenic and metastatic progenitor cells. Oncogene 2006;25:1696–708.
7. Patrawala L, Calhoun-Davis T, Schneider-Broussard R, Tang DG. Hierarchical organization of prostate cancer cells in xenograft tumors: the CD44$^+\alpha2\beta1^+$ cell population is enriched in tumor-initiating cells. Cancer Res 2007;67:6796–805.
8. Prince ME, Sivanandan R, Kaczorowski A, Wolf GT, Kaplan MJ, Dalerba P, et al. Identification of a subpopulation of cells with cancer stem cell properties in head and neck squamous cell carcinoma. Proc Natl Acad Sci U S A 2007;104:973–8.
9. Dalerba P, Dylla SJ, Park IK, Liu R, Wang X, Cho RW, et al. Phenotypic characterization of human colorectal cancer stem cells. Proc Natl Acad Sci U S A 2007;104:10158–63.
10. O'Brien CA, Pollett A, Gallinger S, Dick JE. A human colon cancer cell capable of initiating tumour growth in immunodeficient mice. Nature 2007;445:106–10.
11. Goodell MA, Brose K, Paradis G, Conner AS, Mulligan RC. Isolation and functional properties of murine hematopoietic stem cells that are replicating *in vivo*. J Exp Med 1996;183:1797–806.
12. Patrawala L, Calhoun T, Schneider-Broussard R, Zhou J, Claypool K, Tang DG. Side population is enriched in tumorigenic, stem-like cancer cells, whereas ABCG2$^+$ and ABCG2$^-$ cancer cells are similarly tumorigenic. Cancer Res 2005;65:6207–19.
13. Bartel DP. MicroRNAs: genomics, biogenesis, mechanism, and function. Cell 2004;116:281–97.
14. Calin GA, Croce CM. MicroRNA signatures in human cancers. Nat Rev Cancer 2006;6:857–66.
15. van Kouwenhove M, Kedde M, Agami R. MicroRNA regulation by RNA-binding proteins and its implications for cancer. Nat Rev Cancer 2011;11:644–56.
16. Porkka KP, Pfeiffer MJ, Waltering KK, Vessella RL, Tammela TL, Visakorpi T. MicroRNA expression profiling in prostate cancer. Cancer Res 2007;67:6130–5.
17. Ozen M, Creighton CJ, Ozdemir M, Ittmann M. Widespread deregulation of microRNA expression in human prostate cancer. Oncogene 2008;27:1788–93.
18. Ambs S, Prueitt RL, Yi M, Hudson RS, Howe TM, Petrocca F, et al. Genomic profiling of microRNA and messenger RNA reveals deregulated microRNA expression in prostate cancer. Cancer Res 2008;68:6162–70.
19. Tong AW, Fulgham P, Jay C, Chen P, Khalil I, Liu S, et al. microRNA profile analysis of human prostate cancer. Cancer Gene Ther 2009;16:206–16.
20. Schaefer A, Jung M, Mollenkopf HJ, Wagner I, Stephan C, Jentzmik F, et al. Diagnostic and prognostic implications of microRNA profiling in prostate carcinoma. Int J Cancer 2010;126:1166–76.
21. Szczyrba J, Loprich E, Wach S, Jung V, Unteregger G, Barth S, et al. The microRNA profile of prostate carcinoma obtained by deep sequencing. Mol Cancer Res 2010;8:529–38.
22. Liu C, Kelnar K, Liu B, Chen X, Calhoun-Davis T, Li H, et al. The microRNA miR-34a inhibits prostate cancer stem cells and metastasis by directly repressing CD44. Nat Med 2011;17:211–5.
23. Liu C, Tang DG. MicroRNA regulation of cancer stem cells. Cancer Res 2011;71:5950–4.
24. Li H, Chen X, Calhoun-Davis T, Claypool K, Tang DG. PC3 human prostate carcinoma cell holoclones contain self-renewing tumor-initiating cells. Cancer Res 2008;68:1820–5.
25. Li H, Jiang M, Honorio S, Patrawala L, Jeter CR, Calhoun-Davis T, et al. Methodologies in assaying prostate cancer stem cells. Methods Mol Biol 2009;568:85–138.
26. Jeter CR, Badeaux M, Choy G, Chandra D, Patrawala L, Liu C , et al. Functional evidence that the self-renewal gene NANOG

Published OnlineFirst June 19, 2012; DOI:10.1158/0008-5472.CAN-11-3864

regulates human tumor development. Stem Cells 2009;27:993–1005.
27. Yu F, Yao H, Zhu P, Zhang X, Pan Q, Gong C, et al. let-7 regulates self renewal and tumorigenicity of breast cancer cells. Cell 2007;131:1109–23.
28. Collins AT, Berry PA, Hyde C, Stower MJ, Maitland NJ. Prospective identification of tumorigenic prostate cancer stem cells. Cancer Res 2005;65:10946–51.
29. Peter ME. let-7 and miR-200 microRNAs: guardians against pluripotency and cancer progression. Cell Cycle 2009;8:843–52.
30. Esquela-Kerscher A, Trang P, Wiggins JF, Patrawala L, Cheng A, Ford L, et al. The let-7 microRNA reduces tumor growth in mouse models of lung cancer. Cell Cycle 2008;7:759–64.
31. Fornari F, Milazzo M, Chieco P, Negrini M, Calin GA, Grazi GL, et al. MiR-199a* -3p regulates mTOR and c-Met to influence the doxorubicin sensitivity of human hepatocarcinoma cells. Cancer Res 2010;70:5184–93.
32. Yin G, Chen R, Alvero AB, Fu HH, Holmberg J, Glackin C, et al. TWISTing stemness, inflammation and proliferation of epithelial ovarian cancer cells though MIR199A2/214. Oncogene 2010;29:3545–53.
33. Henry JC, Park JK, Jiang J, Kim JH, Nagorney DM, Roberts LR, et al. miR-199a*-3p targets CD44 and reduces proliferation of CD44 positive hepatocellular carcinoma cell lines. Biochem Biophys Res Commun 2010;403:120–5.
34. Sun L, Xie H, Mori MA, Alexander R, Yuan B, Hattangadi SM, et al. Mir193b-365 is essential for brown fat differentiation. Nat Cell Biol 2011;13:958–65.
35. Uesugi A, Kozaki K, Tsuruta T, Furuta M, Morita K, Imoto I, et al. The tumor suppressive microRNA miR-218 targets the mTOR component Rictor and inhibits AKT phosphorylation in oral cancer. Cancer Res 2011;71:5765–78.
36. Fujita Y, Kojima K, Ohhashi R, Hamada N, Nozawa Y, Kitamoto A, et al. MiR-148a attenuates paclitaxel resistance of hormone-refractory, drug-resistant prostate cancer PC3 cells by regulating MSK1 expression. J Biol Chem 2010;285:19076–84.
37. Visone R, Veronese A, Rassenti LZ, Balatti V, Pearl DK, Acunzo M, et al. miR-181b is a biomarker of disease progression in chronic lymphocytic leukemia. Blood 2011;118:3072–9.
38. Yi R, Poy MN, Stoffel M, Fuchs E. A skin microRNA promotes differentiation by repressing 'stemness'. Nature 2008;452:225–9.
39. Shimono Y, Zabala M, Cho RW, Lobo N, Dalerba P, Qian D, et al. Downregulation of miRNA-200c links breast cancer stem cells with normal stem cells. Cell 2009;138:592–603.
40. Lal A, Navarro F, Maher CA, Maliszewski LE, Yan N, O'Day E, et al. miR-24 Inhibits cell proliferation by targeting E2F2, MYC, and other cell-cycle genes via binding to "seedless" 3′UTR microRNA recognition elements. Mol Cell 2009;35:610–25.
41. Tavazoie SF, Alarcon C, Oskarsson T, Padua D, Wang Q, Bos PD, et al. Endogenous human microRNAs that suppress breast cancer metastasis. Nature 2008;451:147–52.
42. Papadopoulos GL, Alexiou P, Maragkakis M, Reczko M, Hatzigeorgiou AG. DIANA-mirPath: integrating human and mouse microRNAs in pathways. Bioinformatics 2009;25:1991–3.
43. Murata T, Takayama K, Katayama S, Urano T, Horie-Inoue K, Ikeda K, et al. miR-148a is an androgen-responsive microRNA that promotes LNCaP prostate cell growth by repressing its target CAND1 expression. Prostate Cancer Prostatic Dis 2010;13:356–61.
44. Waltering KK, Porkka KP, Jalava SE, Urbanucci A, Kohonen PJ, Latonen LM, et al. Androgen regulation of micro-RNAs in prostate cancer. Prostate 2011;71:604–14.
45. Medina PP, Nolde M, Slack FJ. OncomiR addiction in an *in vivo* model of microRNA-21-induced pre-B-cell lymphoma. Nature 2010;467:86–90.
46. Bitarte N, Bandres E, Boni V, Zarate R, Rodriguez J, Gonzales-Huarriz M, et al. MicroRNA-451 is involved in the self-renewal, tumorigenicity, and chemoresistance of colorectal cancer stem cells. Stem Cells 2011;29:1661–71.
47. Navarro F, Gutman D, Meire E, Caceres M, Rigoutsos I, Bentwich Z, et al. miR-34a contributes to megakaryocytic differentiation of K562 cells independently of p53. Blood 2009;114:2181–92.
48. Chang TC, Zeitels LR, Hwang HW, Chivukula RR, Wentzel Ea, Dews M, et al. Lin-28B transactivation is necessary for Myc-mediated let-7 repression and proliferation. Proc Natl Acad Sci U S A 2009;106:3384–9.
49. Ribas J, Ni X, Haffner M, Wentzel EA, Salmasi AH, Chowdhury WH, et al. miR-21: an androgen receptor-regulated microRNA that promotes hormone-dependent and hormone-independent prostate cancer growth. Cancer Res 2009;69:7165–9.
50. Shi W, Gerster K, Alajez NM, Tsang J, Waldron L, Pintilie M, et al. MicroRNA-301 mediates proliferation and invasion in human breast cancer. Cancer Res 2011;71:2926–37.

Supplementary Materials & Methods:

PCa cell purification.

We first purified human PCa cells out of LAPC9, LAPC4, or Du145 xenografts by depleting murine cells. $CD44^+$ and $CD44^-$ cells were further purified from these xenograft-derived cells (or from cultures) using fluorescence-activated cell sorting (FACS) with the purities of both populations being >98% (6,7). $CD133^+$ and $CD133^-$ LAPC4 cells were purified using biotinylated monoclonal antibody to CD133 (AC133) and the magnetic beads (MACS) by following the manufacturer's instructions (Miltenyi Biotech). Post-sort analysis revealed purities of both populations being >95%. We purified the side population (SP) of LAPC9 cells by FACS as previously described (12).

Primary human prostate tumors (HPCa) were obtained with the patients' consent from robotic surgery (see Supplementary Table S1 for tumor information). All work with HPCa samples was approved by the M.D. Anderson Cancer Center Institutional Review Board (IRB LAB04-0498). We purified epithelial HPCa cells through a multi-step process and by depleting lineage-positive hematopoietic, stromal, and endothelial cells (22,25,26). We then purified Lin^-CD44^+ and Lin^-D44^- HPCa cells using MACS or FACS (22).

Quantitative RT-PCR.

miRNA levels were quantified using TaqMan MicroRNA Assays (Applied Biosystems). Briefly, total RNA was isolated from unsorted LAPC9, LAPC4 and Du145 xenograft cells using the mirVANA PARIS miRNA Isolation Kit (Ambion, Austin, TX), and was used to measure the levels of a library of 310 sequence-validated human miRNAs (see Supplementary Table S2 for the list). Then 136 miRNAs (see Supplementary Table S3) that were expressed at reliably detectable levels were further measured in purified marker-positive vs. marker-negative cell populations. Finally, 57

miRNAs (Supplementary Table S4) were measured in the SP and non-SP LAPC9 cells due to limited numbers of cells. Quantitative miRNA expression data were normalized to internal 'housekeeping' miRNAs, i.e. miR-24 and miR-103, and difference between the positive population and that of the negative population, i.e., dd*C*t values, for each of the miRNAs were converted to percentage of expression using the formula 2^{-ddCt} (22).

Tumor transplantation experiments.

Basic procedures for subcutaneous (s.c) and orthotopic (i.e., dorsal prostate or DP) tumor transplantations can be found in our earlier publications (6,7,12,22,24-26). PCa cells from maintenance tumors were harvested and transfected with oligos or infected with lentiviral vectors. 48 h later, cells were implanted, in 50% Matrigel, s.c or in the DP of intact male NOD/SCID mice.

Clonal, and sphere-formation assays.

For clonal assays (22), cultured PCa cells were plated at a clonal density (i.e., 100 cells/well) in a 6-well dish. The number of holoclones or all types of clones (24) was enumerated at several days to 2 weeks after plating. For sphere-formation assays (22), cells were plated (5,000–20,000 cells/well) in serum-free prostate epithelial basal medium (PrEBM) supplemented with 4 μg/ml insulin, B27 (Invitrogen), and 20 ng/ml EGF and bFGF in Matrigel ultra-low attachment (ULA) plates (22). Spheres that arose in 1–2 weeks were counted. For all these experiments, a minimum of triplicate wells was run for each condition and repeat experiments were performed when necessary and feasible.

BrdU incorporation assays, SA-βgal staining, Western blotting, and cell-cycle analysis.

All these procedures were detailed in our recent publication (22).

Luciferase assays.

Du145 cells were plated (100,000 cells/well) in 24 well plate and cultured overnight. Next day, cells were transfected with pGL3-Kras (wild-type) or pGL3-Kras mLCS6 (mutant) luciferase reporter vectors together with let-7b or NC oligos (30 nM) using Lipofectamine 2000. 48 h after transfection, cells were washed with PBS and directly lysed in the well in lysis buffer and then luciferase activity was detected using the Dual Luciferase Reporter Assay Kit (Promega) as described (22). Each condition was in 6 replicates.

Supplementary Figure legends:

Supplementary Figure S1. The miRNA expression profiling scheme.

Three major steps were indicated.

Supplementary Figure S2. miRNA expression profiles in 3 $CD44^+$ PCa cell populations.

Shown are the relative miRNA expression levels in $CD44^+$ LAPC4 (A), LAPC9 (B), and Du145 (C) compared to their corresponding $CD44^-$ cell populations. The top 10 over- and under-expressed miRNAs are listed on the right. Note that in both LAPC4 and LAPC9, the $CD44^+$ cells showed more under-expressed miRNAs and the magnitude of under-expression was also more pronounced than that of over-expression. In contrast, the Du145 $CD44^+$ and $CD44^-$ cells showed very similar numbers of overexpressed and under-expressed miRNAs and similar levels of over-expression and under-expression.

Supplementary Figure S3. Venn diagrams showing unique or common miRNAs in each xenograft model. Shown are the unique and shared miRNAs that are over-expressed (left panels) or under-expressed (right panels) in the indicated cell populations.

Supplementary Figure S4. Heatmap of 55 miRNA expression in 6 marker-positive PCa cell populations and validation of differentially expressed miRNAs in $CD44^+$ HPCa cells.

A. Heatmap of 55 miRNA expression in 6 marker positive populations (indicated below). Note the common under-expression of miR-34a and common over-expression of miR-452 (top two rows).

B-C. miR-106a expression in tumorigenic populations from xenografts (B) or in purified $CD44^+$ HPCa cells (C).

D-E. miR-452 expression in tumorigenic populations in xenografts (D) or in $CD44^+$ HPCa cells (E). Presented are the mean values of relative expression of the indicated miRNAs in marker-positive over the marker-negative cells.

Supplementary Figure S5. Effects of lentiviral-delivered let-7a on Du145 cells in vitro.

A. Clonal assays. Du145 cells were first infected with the pLL3.7 or pLL3.7-let7a lentiviral vectors (MOI 20). 48 h later, 250 cells/well in 6-well plate were plated in RPMI-1640 medium and the three different types of clones were enumerated on day 7. Each condition was run in triplicate and presented are the mean ± S.D. Note that both holoclone and the total clone numbers are significantly reduced in the pLL3.7-let7a groups compared to the pLL3.7 groups (P values indicated).

B-C. Sphere formation assays. Du145 cells were infected (similar to above) and plated (500 cells/well) in 6-well ULA plate in either RPMI-1640 (B) or PrEBM/B27 (C) medium. The spheres were counted on day 9. Each condition was in triplicate and presented are the mean ± S.D. Note that in both culture conditions, the pLL3.7-let7a significantly inhibited sphere formation in Du145 cells.

Supplementary Figure S6. Effects of let-7b oligos on PPC-1 cells in vitro.

A. Let-7b oligo transfection inhibits PPC-1 cell growth. Cells (50,000) transfected with let-7b, miR-34a or NC oligos (30 nM; 24 h) were plated in triplicate in 6-well culture plates. Live cells were enumerated by Trypan blue exclusion assays on the days indicated.

B. Clonal analysis in PPC-1 cells. Cells transfected as above were plated in triplicate at 100 cells/well in 6-well culture plates. Three types of clones (i.e., holoclone, meroclone, paraclone)

were counted 10 days after plating. *P = 0.0001 and $^{\#}P$ = 0.0003 when compared with the NC group.

C. Sphere analysis in PPC-1 cells. Cells were transfected and plated in triplicate at 1000 cells/well in 6-well ultra-low attachment plates. Spheres were counted 10 days after plating. *P <0.05 when compared with the NC group.

D. Senescence-associated β-gal staining. Shown are representative images of PPC-1 cells treated with the indicated oligos for 1 week. Arrows indicate SA-βgal^{+} cells.

Supplementary Figure S7. Effects of let-7b overexpression on tumor regeneration.

A. Over-expression of let-7b by oligo transfection inhibited A549 (non-small cell lung cancer cell) tumor growth. A549 cells were transfected with 30 nM of miR-NC or let-7b oligonucleotides (oligos) and 48 h later, injected (at 500,000 or 1,000,000 cells) subcutaneously (s.c) into NOD/SCID mice. Tumor incidence, harvest time, tumor weight (mean ± S.D) and the P values (for tumor weight comparisons; Student *t*-test) were indicated on the right.

B-C. Two sets of tumor experiments of let-7b overexpression by oligo transfection in Du145 cells. The experiments were performed similar to above except in two experiments Du145 cells were implanted in the dorsal prostate (DP). Neither experiment showed inhibitory effects of let-7b overexpression on Du145 tumor regeneration.

D. Let-7b oligo transfection in LAPC9 cells failed to inhibit tumor development. LAPC9 cells were freshly purified from maintenance xenografts, transfected with NC or let-7b oligos (30 nM; 48 h), and then implanted s.c into NOD/SCID mice. Tumors were harvested in ~1 month.

Supplementary Figure S8. Luciferase assays.

Luciferase assays were performed in Du145 cells as described in the Methods (above). Presented is the relative luciferase activity (mean ± S.D; n=6 for each condition). Kras refers to the luciferase reporter construct that harbors the wild-type K-Ras 3'-UTR with intact let-7 binding sites whereas Kras mLCS6 is the luciferase reporter construct with K-Ras 3'-UTR mutated at the let-7 binding sites. Note that the co-transfected let-7b oligos significantly reduced the luciferase activity compared to the NC oligos. In contrast, mutation of the let-7 binding sites at the K-Ras 3'-UTR partially abrogated let-7b-induced suppression of luciferase activity (P value is at the borderline, i.e., 0.044). These results, together with the Western blotting data (Fig. 4I), confirm K-Ras as a direct downstream target of let-7 in PCa cells.

Supplementary Figure S9. Lack of apparent biological effects of miR-301 on Du145 cells

A-D. Manipulating miR-301 levels in PCa cells did not affect clonal growth of Du145 cells. A and C. FACS-purified $CD44^-$ Du145 cells were transfected with miR-NC or miR-301 oligos (30 nM each) and sphere formation (A) or clonal (C) experiments were performed as for let-7. B and D. Purified $CD44^+$ Du145 cells were transfected with anti-NC or anti-miR-301 antagomirs (30 nM each) and then used in sphere formation (B) or clonal (D) experiments.

E. miR-301 mRNA levels measured by qRT-PCR in purified $CD44^+$ Du145 cells freshly transfected with anti-NC or anti-miR-301 (30 nM; 48 h) or in $CD44^-$ Du145 cells freshly transfected with miR-NC or miR-301 (30 nM; 48 h). Shown are the expression levels (fold; log scale) relative to the corresponding NC (or anti-NC) control.

F-I. Tumor development was not affected by manipulating miR-301 levels. Over-expressing miR-301 by transfecting miR-301 oligos in $CD44^-$ Du145 cells (500,000 cells per s.c injection) did not affect tumor growth (F & H). Conversely, Knocking down miR-301 by transfecting anti-sense miR-301 oligos in $CD44^+$ Du145 cells (100,000 cells per s.c injection) did not inhibit tumor development (G & I). Shown in F and G are tumor images with mean weight and incidence. Shown in H and I are bar graphs of mean tumor weights.

Supplementary Figure S10. Differential biological effects of miR-301 on PC3 and LAPC9 cells

A-C. Effects of miR-301 knockdown on PC3 cells in vitro (A-B) and in vivo (C). A. Knocking down miR-301 using anti-sense oligos did not affect PC3 cell clonal expansion (A). B-C. Knocking down miR-301 did not affect tumor regeneration of PC3 cells. Shown in B are the tumor weights (mean ± S.D) and in C the tumor images with mean tumor weight and incidence.

D-E miR-301 positively regulates LAPC9 clonal and sphere-forming activity. D. Clonal assays of freshly purified LAPC9 cells transfected with the indicated oligos and plated in 96-well plates (10,000 cells per well) on Swiss 3T3 fibroblast feeder layer. Colonies were counted 8 days after plating. Presented are the mean ± S.D from triplicate wells. **P<0.01. E. Sphere assays in LAPC9 cells. The experiments were conducted similarly to the clonal assays except that the transfected cells were plated in Ultra Low Attachment plates. Spheres were enumerated 11 days after plating. *P<0.05.

Supplementary Figure S11. *miR-34a* mRNA levels in purified $CD44^+$ HPCa cells are not correlated with *p53* or *c-Myc* mRNA levels.

The mRNA levels of mature miR-34a (A), p53 (B), and c-Myc (C) were quantified by qPCR analysis in $CD44^+$/$CD44^-$ cell fractions purified from 14 HPCa samples (see Supplementary Table 1). The results were relative expression levels in $CD44^+$ over $CD44^-$ HPCa cells.

Step I

Measure 310 miRNA expression in bulk cells:

- LAPC9
- LAPC4
- DU145

Identification

136 miRNAs were expressed at detectable levels

Step II

Measure 136 miRNAs in:

LAPC9: CD44+/CD44-
LAPC4: CD44+/CD44-; CD133+/CD133-
DU145: CD44+/CD44-; α2β1+/α2β1-

Identification

6 miRNAs were differentially expressed in 5 marker-positive populations

Step III

Measure 57 miRNAs in:

LAPC9: SP/non-SP

Identification

2 miRNAs were differentially expressed in all 6 marker-positive populations

Supplementary Fig. S1

A

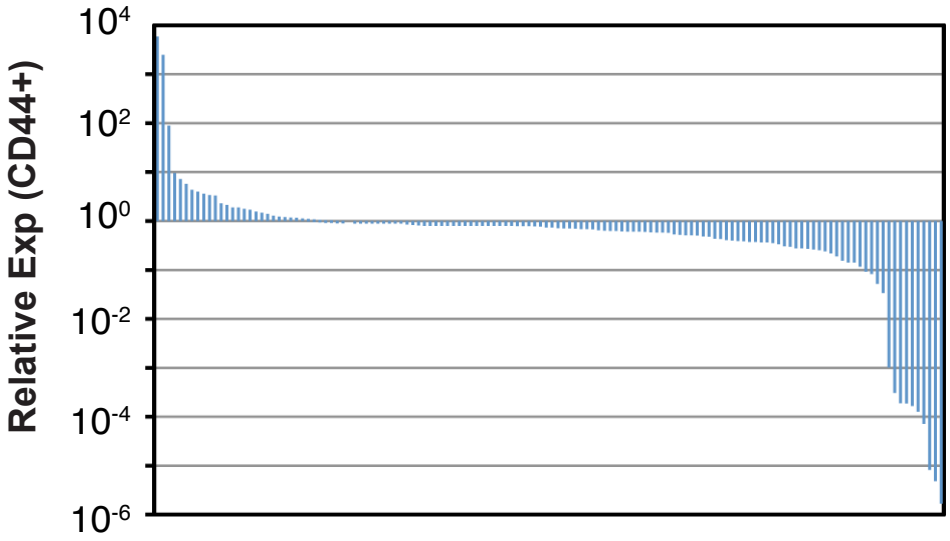

LAPC4 CD44⁺ population

Top up-regulated	Top down-regulated
miR-190	miR-375
miR-142-5p	miR-429
miR-10b	miR-10a
miR-23b	miR-423
miR-127	miR-15a
miR-361	miR-18a
let-7d	miR-199a*
miR-130b	miR-96
miR-22	miR-422a
miR-328	miR-486
	miR-34a

B

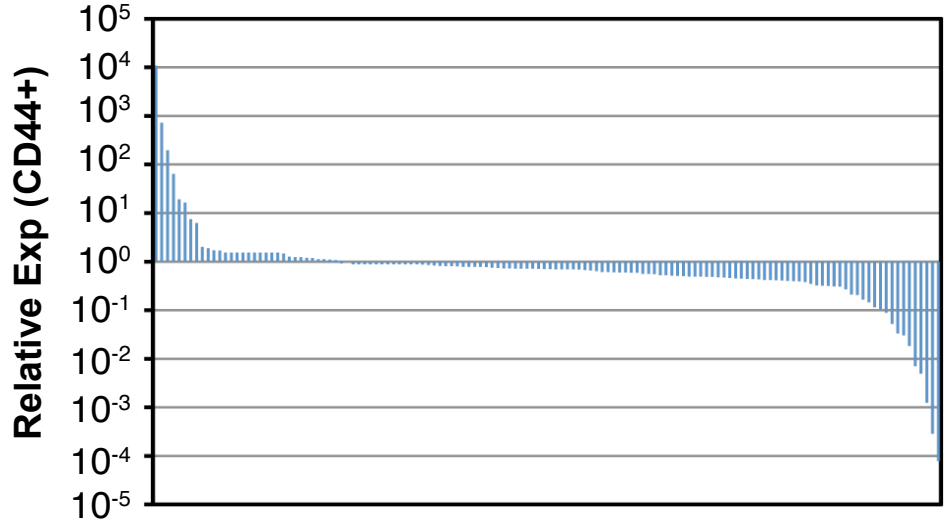

LAPC9 CD44⁺ population

Top up-regulated	Top down-regulated
let-7i	miR-127
miR-133a	miR-34a
miR-33	miR-142-5p
miR-147	miR-422a
miR-433	miR-18a*
miR-486	miR-378
miR-452	miR-10b
miR-19a	miR-422b
miR-133b	miR-199a*
miR-9*	miR-218

C

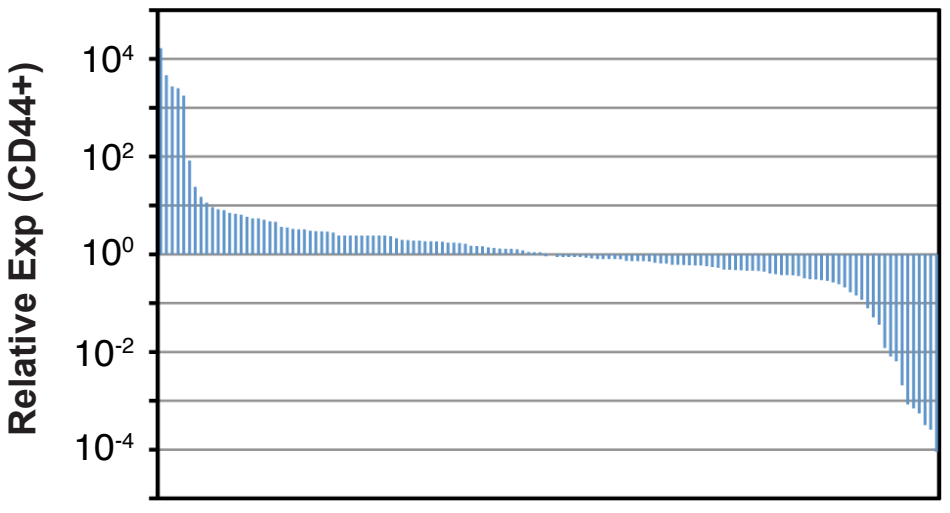

Du145 CD44⁺ population

Top up-regulated	Top down-regulated
miR-451	miR-193a
miR-500	miR-9*
miR-205	miR-127
miR-452	miR-433
miR-142-5p	miR-147
miR-100	miR-378
miR-21	miR-10b
miR-142-3p	miR-203
miR-20b	miR-218
miR-196b	miR-34a

A LAPC4 (LN metastasis)

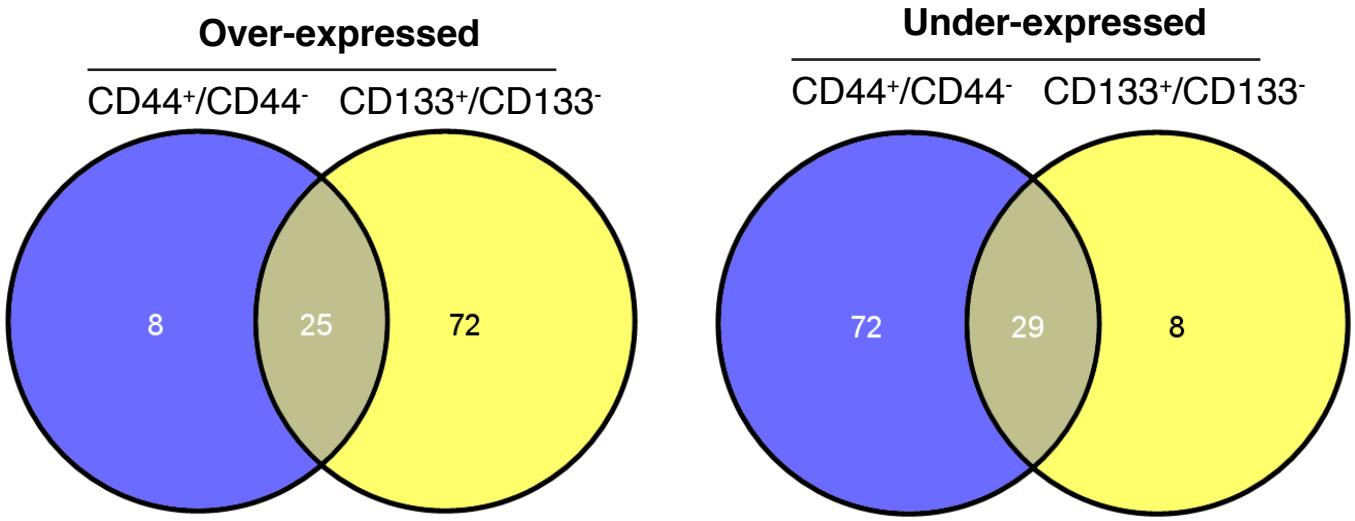

B LAPC9 (bone marrow metastasis)

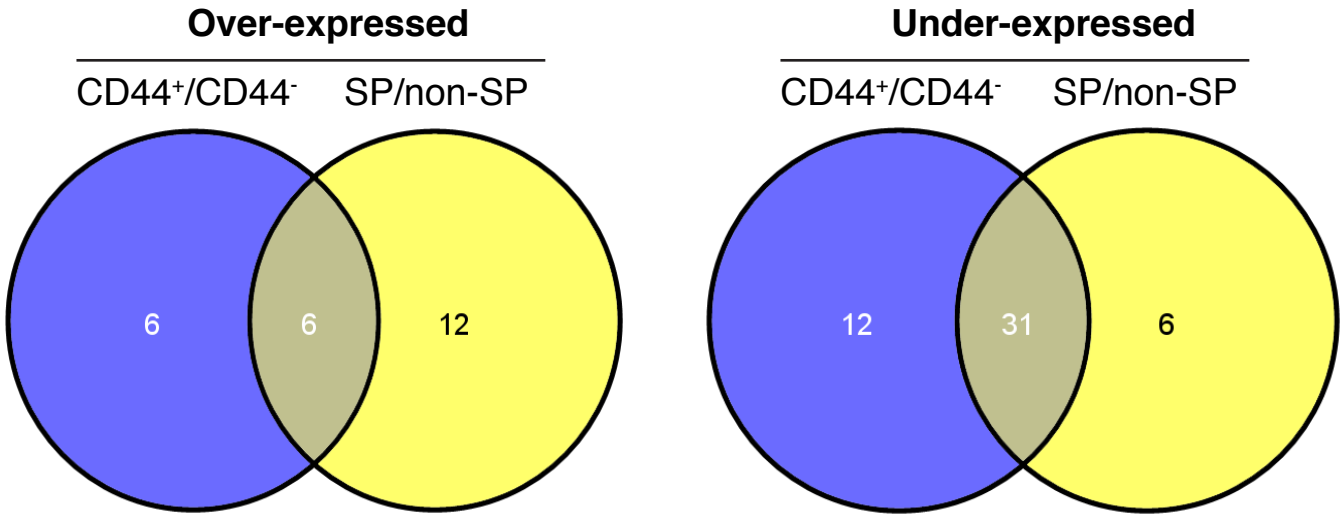

C Du145 (brain metastasis)

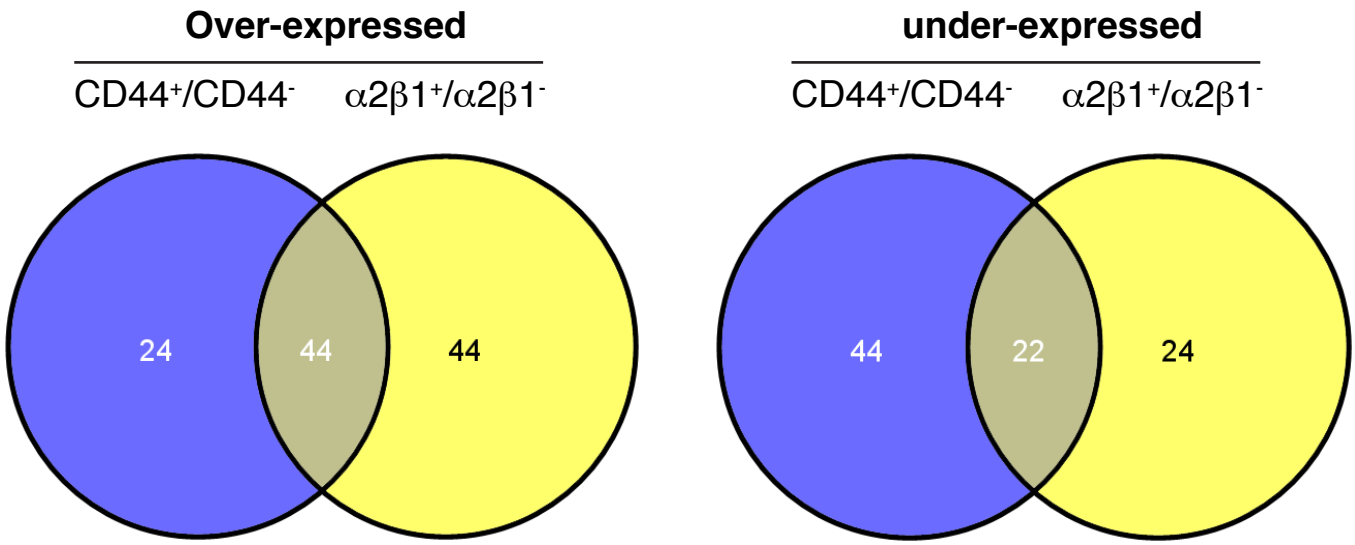

Supplementary Fig. S3

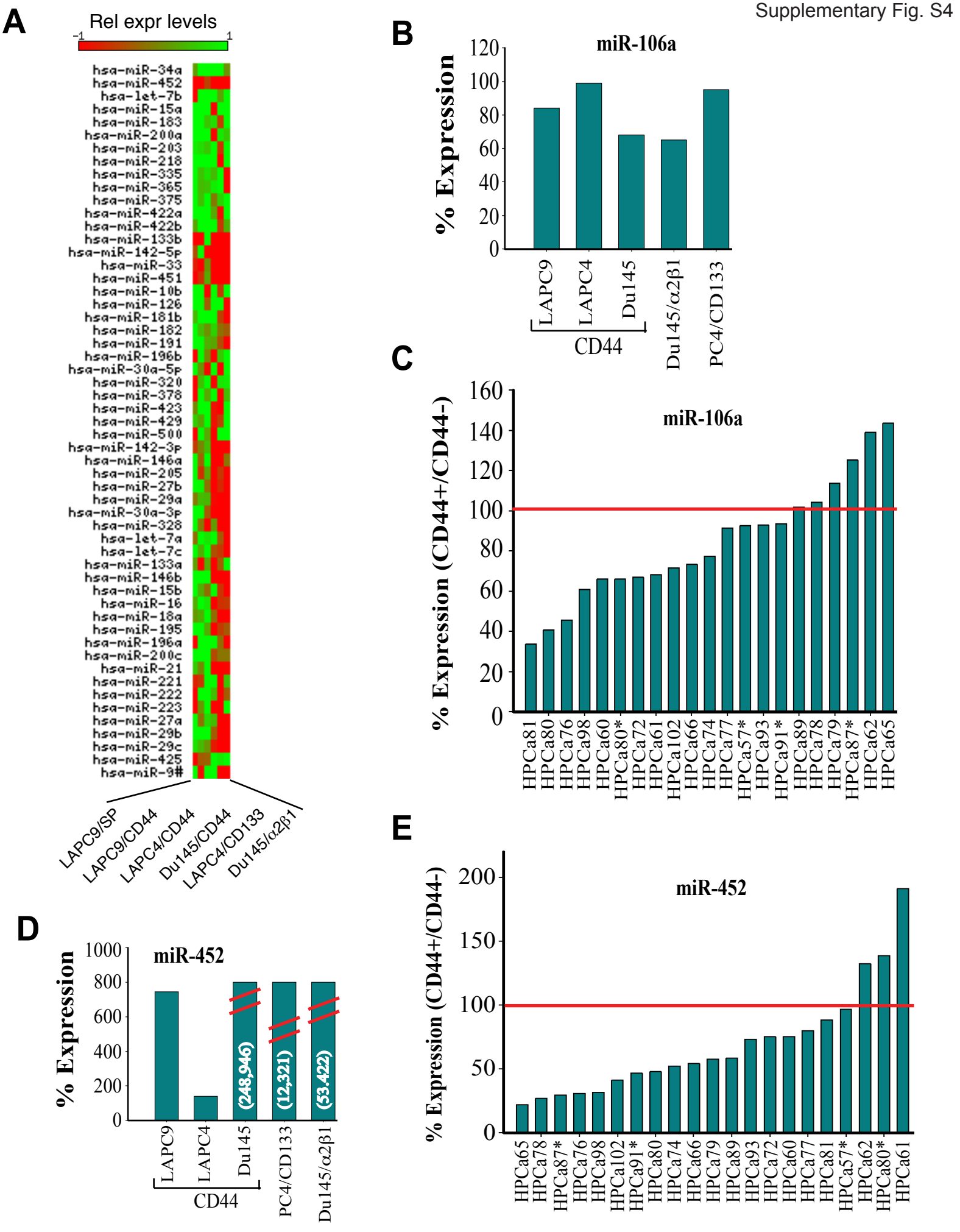
A
Rel expr levels
-1
1
hsa-miR-34a
hsa-miR-452
hsa-let-7b
hsa-miR-15a
hsa-miR-183
hsa-miR-200a
hsa-miR-203
hsa-miR-218
hsa-miR-335
hsa-miR-365
hsa-miR-375
hsa-miR-422a
hsa-miR-422b
hsa-miR-133b
hsa-miR-142-5p
hsa-miR-33
hsa-miR-451
hsa-miR-10b
hsa-miR-126
hsa-miR-181b
hsa-miR-182
hsa-miR-191
hsa-miR-196b
hsa-miR-30a-5p
hsa-miR-320
hsa-miR-378
hsa-miR-423
hsa-miR-429
hsa-miR-500
hsa-miR-142-3p
hsa-miR-146a
hsa-miR-205
hsa-miR-27b
hsa-miR-29a
hsa-miR-30a-3p
hsa-miR-328
hsa-let-7a
hsa-let-7c
hsa-miR-133a
hsa-miR-146b
hsa-miR-15b
hsa-miR-16
hsa-miR-18a
hsa-miR-195
hsa-miR-196a
hsa-miR-200c
hsa-miR-21
hsa-miR-221
hsa-miR-222
hsa-miR-223
hsa-miR-27a
hsa-miR-29b
hsa-miR-29c
hsa-miR-425
hsa-miR-9#
LAPC9/SP
LAPC9/CD44
LAPC4/CD44
Du145/CD44
LAPC4/CD133
Du145/α2β1
B
miR-106a
% Expression
120
100
80
60
40
20
0
LAPC9
LAPC4
Du145
CD44
Du145/α2β1
PC4/CD133
C
miR-106a
% Expression (CD44+/CD44-)
160
140
120
100
80
60
40
20
0
HPCa81
HPCa80
HPCa76
HPCa98
HPCa60
HPCa80*
HPCa72
HPCa61
HPCa102
HPCa66
HPCa74
HPCa77
HPCa57*
HPCa93
HPCa91*
HPCa89
HPCa78
HPCa79
HPCa87*
HPCa62
HPCa65
D
miR-452
% Expression
1000
800
600
400
200
0
(248,946)
(12,321)
(53.422)
LAPC9
LAPC4
Du145
CD44
PC4/CD133
Du145/α2β1
E
miR-452
% Expression (CD44+/CD44-)
200
150
100
50
0
HPCa65
HPCa78
HPCa87*
HPCa76
HPCa98
HPCa102
HPCa91*
HPCa80
HPCa74
HPCa66
HPCa79
HPCa89
HPCa93
HPCa72
HPCa60
HPCa77
HPCa81
HPCa57*
HPCa62
HPCa80*
HPCa61

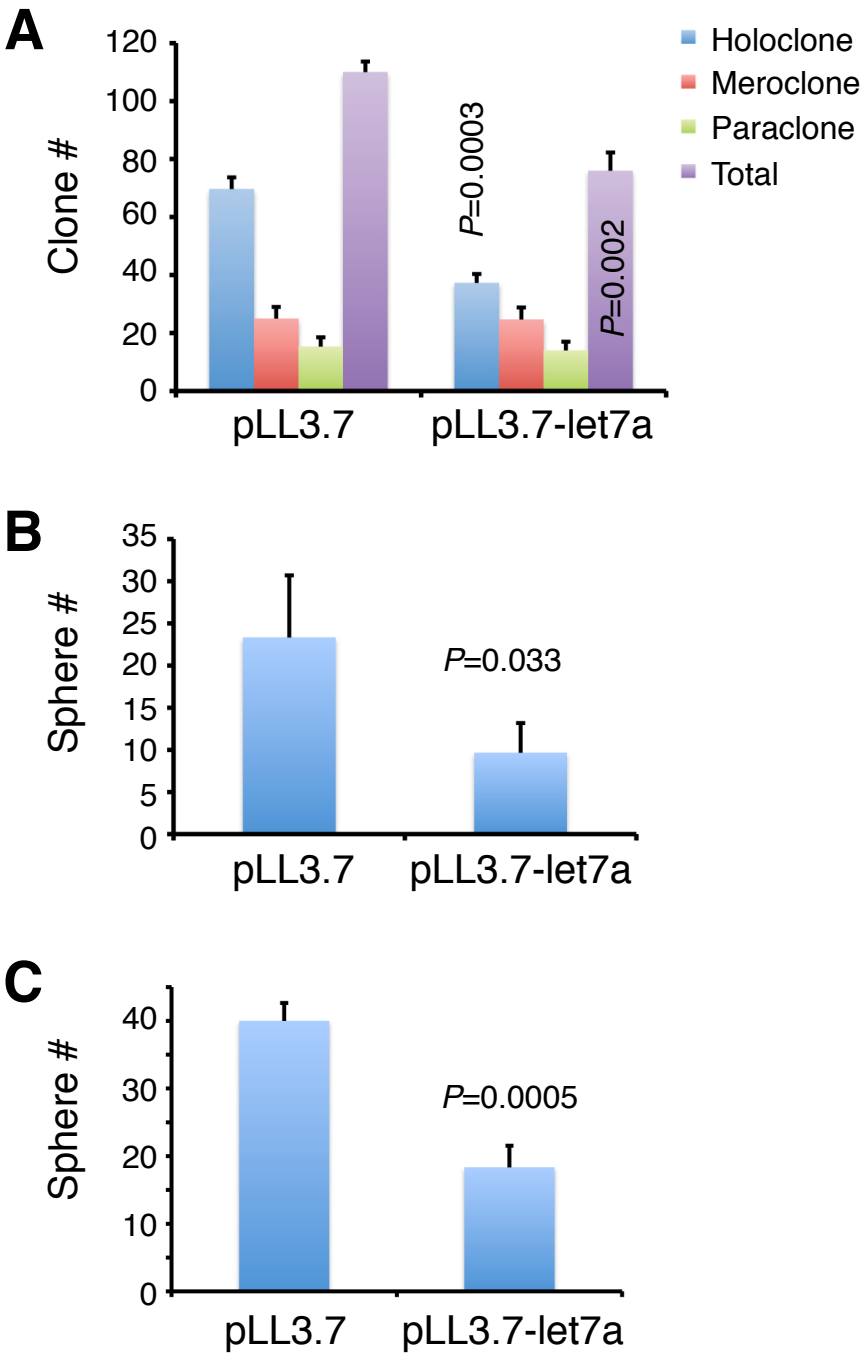

Supplementary Fig. S5

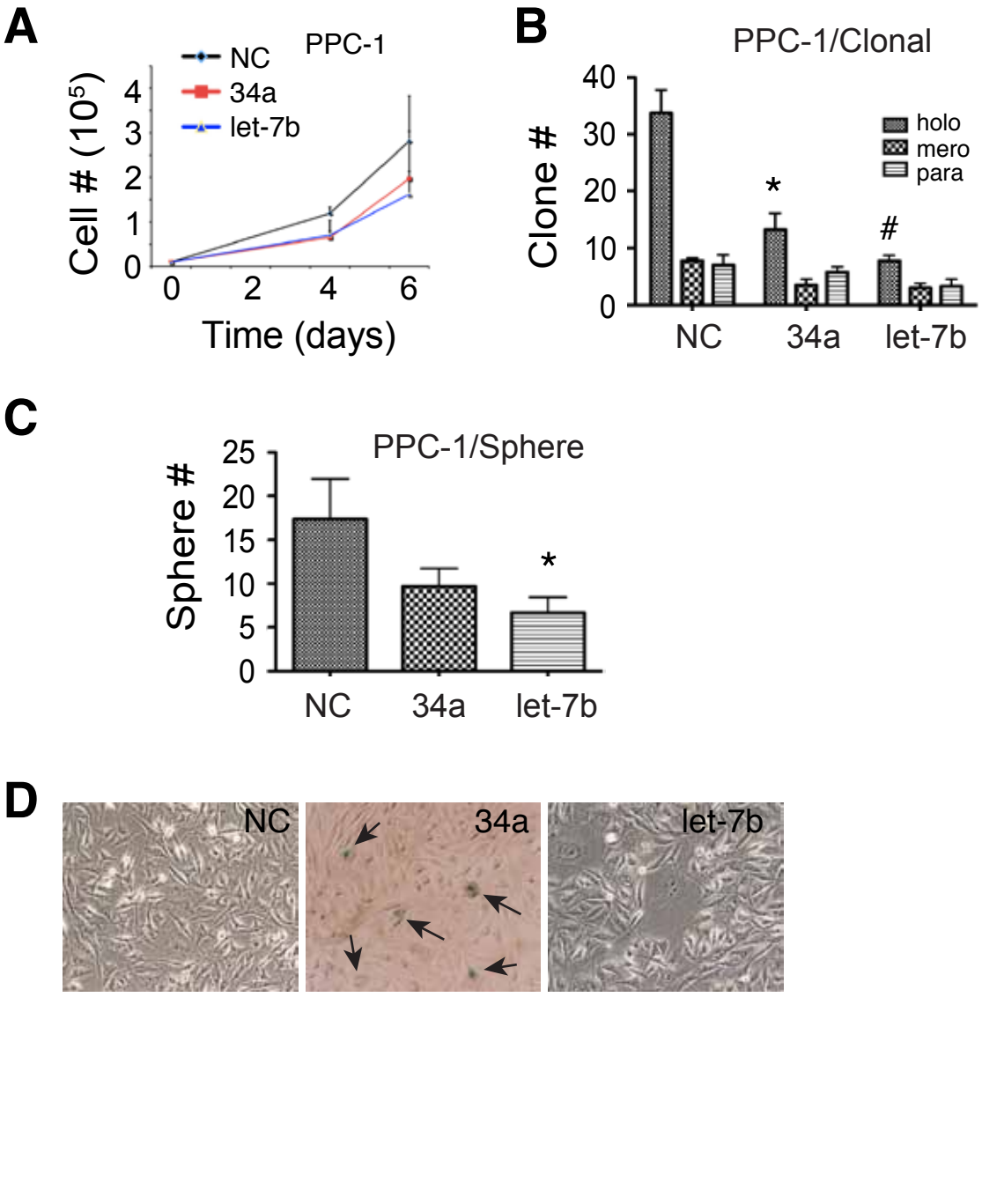

Supplementary Fig. S6

		Incidence	Harvest	Weight (g)	P value
A					
A549 (500,000 cells/s.c inj.)					
	NC	3/3 (100%)	52 d	0.37 ± 0.14	
	let-7b	3/3 (100%)	52 d	0.16 ± 0.09	0.05
A549 (1,000,000 cells/s.c inj.)					
	NC	7/7 (100%)	42 d	0.29 ± 0.05	
	let-7b	6/7 (86%)	42 d	0.12 ± 0.33	0.007
B					
Du145 (100,000 cells/s.c inj.)					
	NC	2/6 (33.3%)	57 d	0.17 ± 0.16	
	let-7b	6/6 (100%)	57 d	0.18 ± 0.13	0.49
Du145 (100,000 cells/DP inj.)					
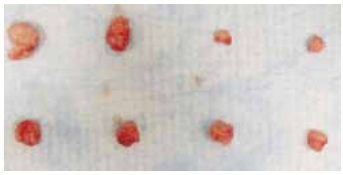	NC	4/6 (66.7%)	57 d	0.40 ± 0.34	
	let-7b	4/6 (66.7%)	57 d	0.46 ± 0.38	0.38
C					
Du145 (100,000 cells/s.c inj.)					
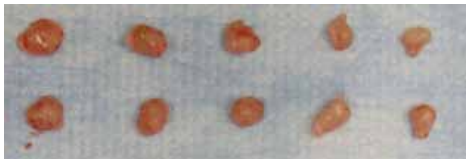	NC	5/6 (83.3%)	46 d	0.60 ± 0.26	
	let-7b	5/6 (83.3%)	46 d	0.60 ± 0.1	0.49
Du145 (100,000 cells/DP inj.)					
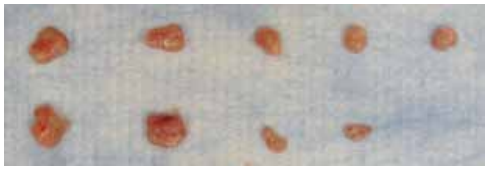	NC	5/6 (83.3%)	46 d	0.35 ± 0.16	
	let-7b	4/6 (66.7%)	46 d	0.41 ± 0.32	0.4
D					
LAPC9 (1,000,000 cells/s.c inj.)					
	NC	7/10 (70%)	33 d	0.42 ± 0.17	
	let-7b	10/10 (100%)	33 d	0.56 ± 0.18	0.29

Supplementary Fig. S7

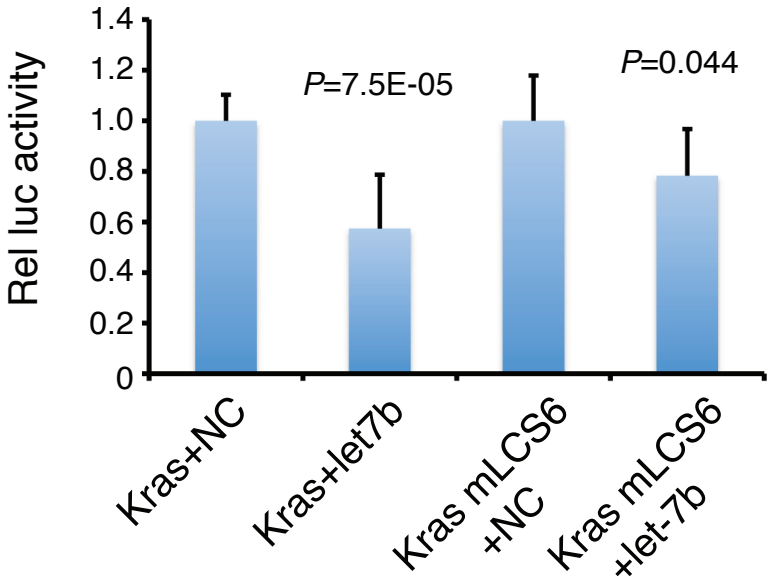

Supplementary Fig. S8

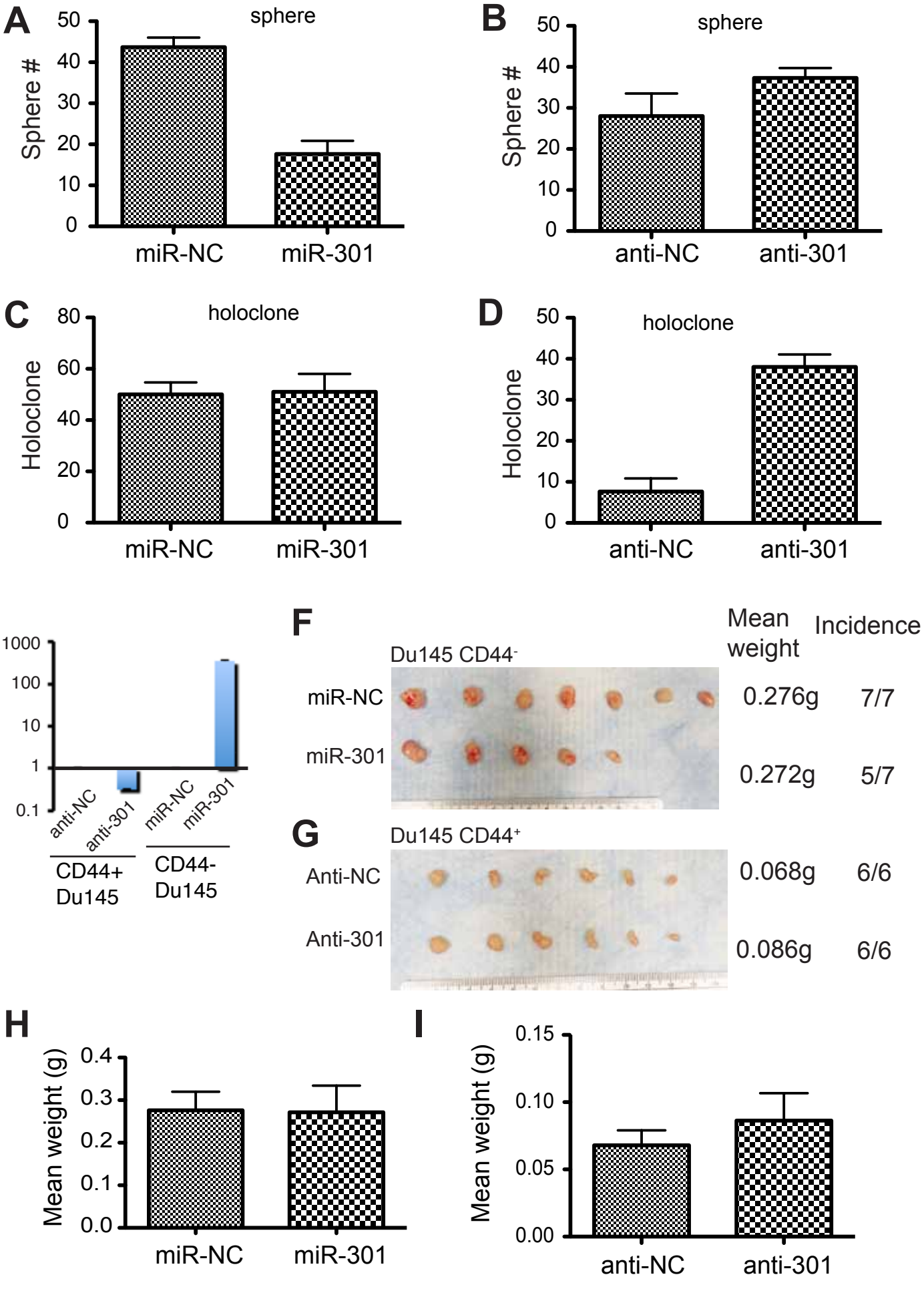

Supplementary Fig. S9

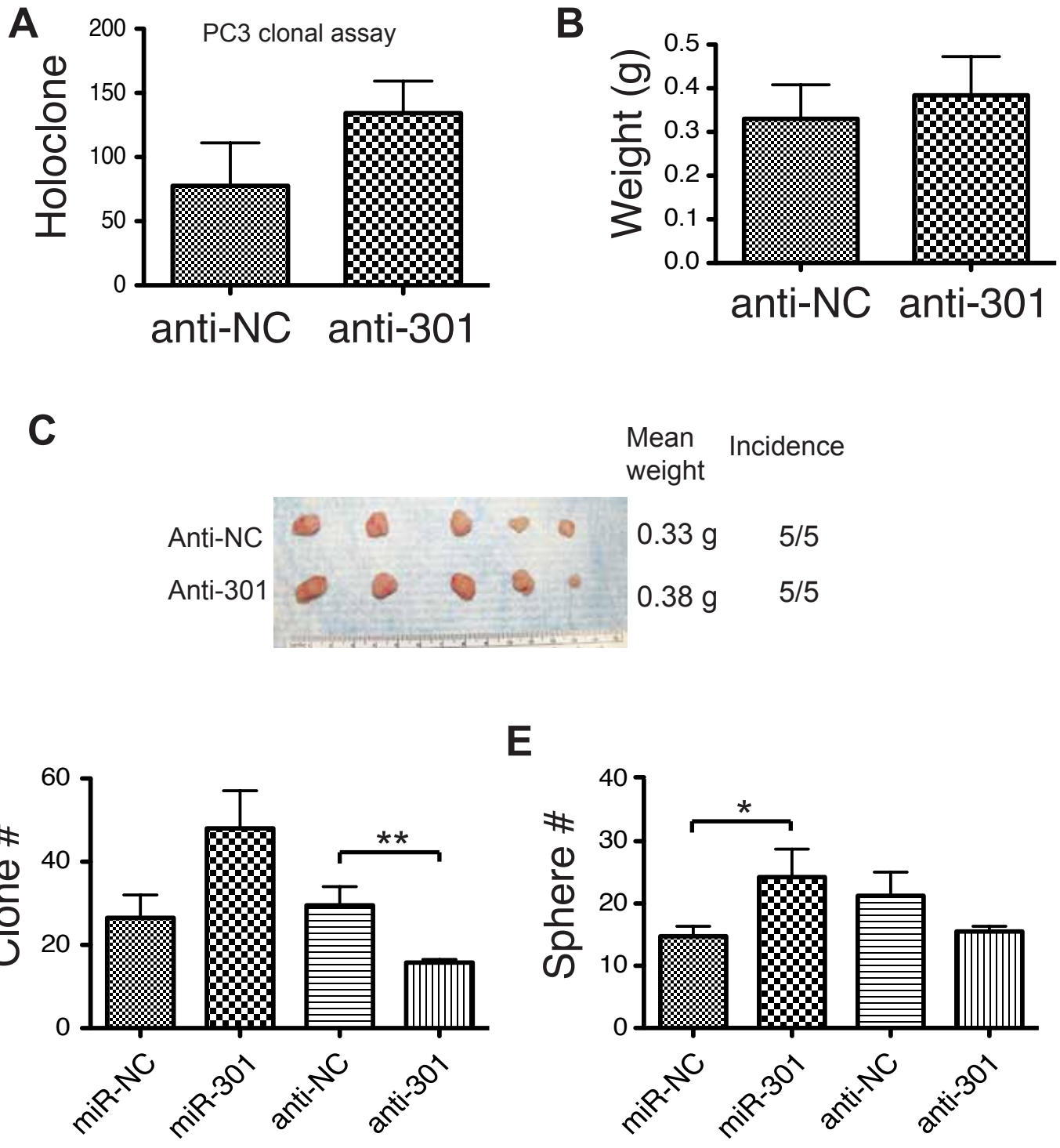

Supplementary Fig. S10

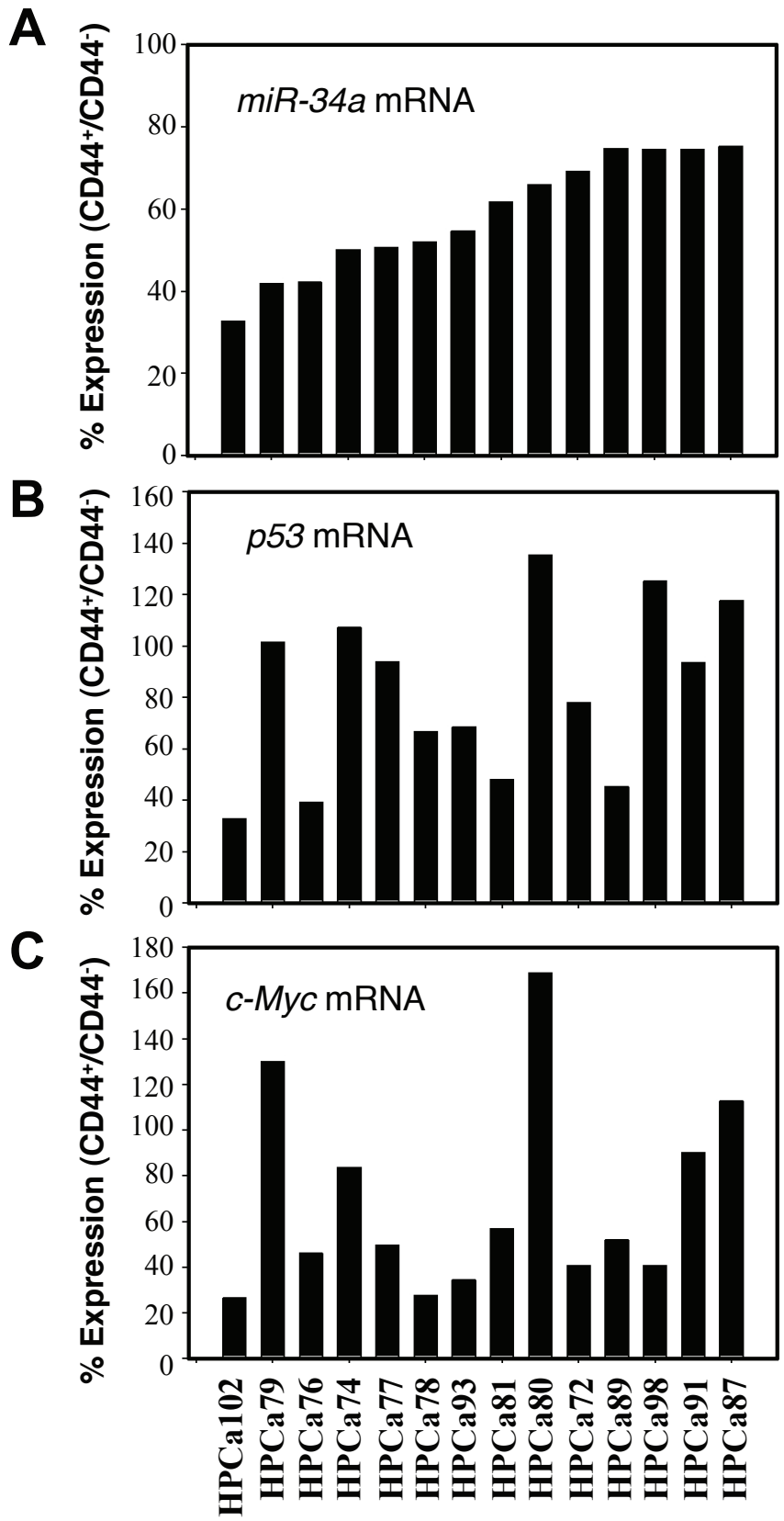

Supplementary Fig. S11

Supplementary Table S1. HPCa information

HPCa Samples	Age	Gleason
HPCa57*	53	7 (3+4)
HPCa60	54	8 (3+5)
HPCa61	56	6 (3+3)
HPCa62	59	7 (4+3)
HPCa65	59	7 (4+3)
HPCa66	58	6 (3+3)
HPCa72	58	7 (3+4)
HPCa74	59	7 (3+4)
HPCa76	64	7 (4+3)
HPCa77	46	6 (3+3)
HPCa78	64	7 (3+4)
HPCa79	67	7 (4+3)
HPCa80	65	9 (5+4)
HPCa80*	65	9 (5+4)
HPCa81	54	7 (3+4)
HPCa87*	57	9 (4+5)
HPCa89	55	9 (4+5)
HPCa91*	60	8 (3+5)
HPCa93	58	7 (4+3)
HPCa98	64	8 (4+4)
HPCa102	55	7 (3+4)

HPCa samples were patient tumors obtained from the robotic (Da Vinci) surgery. The patient age and Gleason score of each tumor were indicated.
*These were first-generation xenograft tumors established in our lab and used to purify the $CD44^{+}/CD44^{-}$ cells

Table S2. 310 miRNAs initially measured in LAPC9, LAPC4, and Du145 cells

hsa-let-7a
hsa-let-7b
hsa-let-7c
hsa-let-7d
hsa-let-7e
hsa-let-7f
hsa-let-7g
hsa-let-7i
hsa-miR-1
hsa-miR-100
hsa-miR-101
hsa-miR-103
hsa-miR-105
hsa-miR-106a
hsa-miR-106b
hsa-miR-107
hsa-miR-10a
hsa-miR-10b
hsa-miR-122a
hsa-miR-124a
hsa-miR-125a
hsa-miR-125b
hsa-miR-126
hsa-miR-126*
hsa-miR-127
hsa-miR-128a
hsa-miR-128b
hsa-miR-129
hsa-miR-130a
hsa-miR-130b
hsa-miR-132
hsa-miR-133a
hsa-miR-133b
hsa-miR-134
hsa-miR-135a
hsa-miR-135b
hsa-miR-136
hsa-miR-137
hsa-miR-138
hsa-miR-139
hsa-miR-140
hsa-miR-141
hsa-miR-142-3p
hsa-miR-142-5p
hsa-miR-143
hsa-miR-145
hsa-miR-146a

hsa-miR-146b
hsa-miR-147
hsa-miR-148a
hsa-miR-148b
hsa-miR-149
hsa-miR-150
hsa-miR-151
hsa-miR-152
hsa-miR-153
hsa-miR-154
hsa-miR-154*
hsa-miR-155
hsa-miR-15a
hsa-miR-15b
hsa-miR-16
hsa-miR-17-3p
hsa-miR-17-5p
hsa-miR-181a
hsa-miR-181b
hsa-miR-181c
hsa-miR-181d
hsa-miR-182
hsa-miR-182*
hsa-miR-183
hsa-miR-184
hsa-miR-185
hsa-miR-186
hsa-miR-187
hsa-miR-188
hsa-miR-189
hsa-miR-18a
hsa-miR-18a*
hsa-miR-18b
hsa-miR-190
hsa-miR-191
hsa-miR-192
hsa-miR-193a
hsa-miR-193b
hsa-miR-194
hsa-miR-195
hsa-miR-196a
hsa-miR-196b
hsa-miR-198
hsa-miR-199a
hsa-miR-199a*
hsa-miR-199b
hsa-miR-19a
hsa-miR-19b

hsa-miR-200a
hsa-miR-200a*
hsa-miR-200c
hsa-miR-202
hsa-miR-202*
hsa-miR-203
hsa-miR-204
hsa-miR-205
hsa-miR-206
hsa-miR-208
hsa-miR-20a
hsa-miR-20b
hsa-miR-21
hsa-miR-210
hsa-miR-211
hsa-miR-212
hsa-miR-213
hsa-miR-214
hsa-miR-215
hsa-miR-216
hsa-miR-217
hsa-miR-218
hsa-miR-219
hsa-miR-22
hsa-miR-220
hsa-miR-221
hsa-miR-222
hsa-miR-223
hsa-miR-224
hsa-miR-23a
hsa-miR-23b
hsa-miR-24
hsa-miR-25
hsa-miR-26a
hsa-miR-26b
hsa-miR-27a
hsa-miR-27b
hsa-miR-28
hsa-miR-296
hsa-miR-299-3p
hsa-miR-299-5p
hsa-miR-29a
hsa-miR-29b
hsa-miR-29c
hsa-miR-301
hsa-miR-302a
hsa-miR-302a*
hsa-miR-302b

hsa-miR-302b*
hsa-miR-302c
hsa-miR-302c*
hsa-miR-302d
hsa-miR-30a-3p
hsa-miR-30a-5p
hsa-miR-30b
hsa-miR-30c
hsa-miR-30d
hsa-miR-30e-3p
hsa-miR-30e-5p
hsa-miR-31
hsa-miR-32
hsa-miR-320
hsa-miR-323
hsa-miR-324-3p
hsa-miR-324-5p
hsa-miR-325
hsa-miR-326
hsa-miR-328
hsa-miR-329
hsa-miR-33
hsa-miR-330
hsa-miR-331
hsa-miR-335
hsa-miR-337
hsa-miR-338
hsa-miR-339
hsa-miR-340
hsa-miR-342
hsa-miR-345
hsa-miR-346
hsa-miR-34a
hsa-miR-34b
hsa-miR-34c
hsa-miR-361
hsa-miR-362
hsa-miR-365
hsa-miR-367
hsa-miR-368
hsa-miR-369-3p
hsa-miR-369-5p
hsa-miR-370
hsa-miR-371
hsa-miR-372
hsa-miR-373
hsa-miR-373*
hsa-miR-374

hsa-miR-375
hsa-miR-376a
hsa-miR-376a*
hsa-miR-376b
hsa-miR-377
hsa-miR-378
hsa-miR-379
hsa-miR-380-3p
hsa-miR-380-5p
hsa-miR-381
hsa-miR-382
hsa-miR-383
hsa-miR-409-5p
hsa-miR-410
hsa-miR-412
hsa-miR-422a
hsa-miR-422b
hsa-miR-423
hsa-miR-424
hsa-miR-425
hsa-miR-429
hsa-miR-432
hsa-miR-432*
hsa-miR-433
hsa-miR-448
hsa-miR-449
hsa-miR-450
hsa-miR-451
hsa-miR-452
hsa-miR-452*
hsa-miR-453
hsa-miR-455
hsa-miR-483
hsa-miR-485-3p
hsa-miR-485-5p
hsa-miR-486
hsa-miR-487a
hsa-miR-487b
hsa-miR-488
hsa-miR-489
hsa-miR-490
hsa-miR-491
hsa-miR-492
hsa-miR-493
hsa-miR-493-3p
hsa-miR-494
hsa-miR-495
hsa-miR-496

hsa-miR-497
hsa-miR-498
hsa-miR-499
hsa-miR-500
hsa-miR-501
hsa-miR-502
hsa-miR-503
hsa-miR-504
hsa-miR-505
hsa-miR-506
hsa-miR-507
hsa-miR-508
hsa-miR-509
hsa-miR-510
hsa-miR-511
hsa-miR-512-5p
hsa-miR-513
hsa-miR-514
hsa-miR-515-3p
hsa-miR-515-5p
hsa-miR-516-3p
hsa-miR-516-5p
hsa-miR-517*
hsa-miR-517a
hsa-miR-517b
hsa-miR-517c
hsa-miR-518a
hsa-miR-518b
hsa-miR-518c
hsa-miR-518c*
hsa-miR-518d
hsa-miR-518e
hsa-miR-518f
hsa-miR-519a
hsa-miR-519b
hsa-miR-519c
hsa-miR-519d
hsa-miR-519e
hsa-miR-519e*
hsa-miR-520a
hsa-miR-520a*
hsa-miR-520b
hsa-miR-520c
hsa-miR-520d
hsa-miR-520d*
hsa-miR-520e
hsa-miR-520f
hsa-miR-520g

hsa-miR-520h
hsa-miR-521
hsa-miR-522
hsa-miR-523
hsa-miR-525
hsa-miR-525*
hsa-miR-526a
hsa-miR-526b
hsa-miR-526b*
hsa-miR-527
hsa-miR-539
hsa-miR-542-3p
hsa-miR-542-5p
hsa-miR-7
hsa-miR-9
hsa-miR-9#
hsa-miR-92
hsa-miR-93
hsa-miR-95
hsa-miR-96
hsa-miR-98
hsa-miR-99a
hsa-miR-99b

Table S3. 136 miRNAs list used to measure marker sorted populations in LAPC9, LAPC4, and Du145, listed are mean ddCt values comparing marker positive and marker negative.

Sample Name	LAPC9 CD44 ddCt pos-neg	LAPC4 CD44 ddCt pos-neg	DU145 CD44 ddCt pos-neg	LAPC4 CD133 ddCt pos-neg	DU145 a2b1 ddCt pos-neg
hsa-let-7a	1.15	0.76	1.79	-0.28	-6.55
hsa-let-7b	1.40	1.75	1.46	0.31	1.75
hsa-let-7c	0.35	1.05	-0.37	-0.56	-1.32
hsa-let-7d	0.42	-2.11	0.75	0.20	-1.15
hsa-let-7e	0.83	0.54	0.70	-0.52	1.31
hsa-let-7f	0.75	0.66	1.41	0.13	-0.55
hsa-let-7g	0.06	0.62	-1.56	0.15	-0.28
hsa-let-7i	-13.39	0.00	3.10	0.56	7.55
hsa-miR-100	0.09	0.17	-6.37	-0.19	-3.26
hsa-miR-101	-0.30	0.29	0.75	-0.75	-2.77
hsa-miR-103	0.00	0.00	0.00	0.00	0.00
hsa-miR-105	-0.61	1.42	-1.27	-1.79	-4.48
hsa-miR-106a	0.26	0.02	0.57	0.07	0.61
hsa-miR-106b	0.09	0.48	-0.13	-0.12	-0.83
hsa-miR-10a	0.96	16.90	1.12	-0.53	-0.84
hsa-miR-10b	5.04	-6.47	8.91	-0.56	7.12
hsa-miR-124a	-0.61	0.33	-1.27	1.32	-4.48
hsa-miR-125a	1.04	-0.02	-0.38	-0.70	-0.35
hsa-miR-125b	-0.61	0.33	-1.27	-6.94	-4.48
hsa-miR-126	2.29	-0.27	1.62	2.26	-2.19
hsa-miR-127	13.63	-2.85	11.62	-1.08	-4.48
hsa-miR-130b	3.12	-1.99	0.46	0.07	-0.65
hsa-miR-132	0.92	0.72	0.61	-0.27	-0.62
hsa-miR-133a	-9.49	0.33	-1.27	5.45	4.39
hsa-miR-133b	-1.01	1.93	-2.81	-1.85	-1.47
hsa-miR-135a	2.24	0.04	-0.92	-0.49	-4.48
hsa-miR-140	1.31	1.19	-1.59	-1.24	0.00
hsa-miR-141	1.03	0.38	2.80	0.21	8.58
hsa-miR-142-3	0.04	0.49	-3.90	-6.49	-3.77
hsa-miR-142-5	9.65	-11.28	-10.79	-8.64	-4.97
hsa-miR-145	-0.61	0.33	4.78	-2.53	-4.48
hsa-miR-146a	-0.23	1.22	-1.55	-6.32	-0.08
hsa-miR-146b	1.65	1.45	-1.68	-3.07	-1.95
hsa-miR-147	-6.00	0.33	10.47	-6.94	-4.48
hsa-miR-148a	1.69	-0.04	0.46	-1.00	0.67
hsa-miR-148b	1.62	1.45	0.90	-0.60	-2.01
hsa-miR-149	0.76	0.96	-0.13	0.10	-1.24
hsa-miR-151	0.73	0.67	1.03	-0.14	-1.30
hsa-miR-152	-0.26	0.13	-2.43	0.64	10.44
hsa-miR-15a	2.78	12.94	-1.52	1.33	9.95
hsa-miR-15b	0.35	-0.13	2.03	-0.57	-2.28
hsa-miR-16	1.51	0.79	-2.54	-0.61	-0.56
hsa-miR-17-5p	1.15	-0.36	-1.26	0.14	-3.88

hsa-miR-181a	-0.61	0.33	-1.27	-6.94	-4.48
hsa-miR-181b	1.19	1.37	1.07	-0.48	-2.00
hsa-miR-181d	-0.61	0.33	-1.27	-6.94	-4.48
hsa-miR-182	0.48	0.14	0.64	-0.12	-0.31
hsa-miR-183	1.08	0.54	0.73	-0.53	1.25
hsa-miR-186	1.20	1.71	-0.54	0.17	-0.23
hsa-miR-18a	0.35	12.55	-0.14	0.04	-1.07
hsa-miR-18a*	7.15	-1.20	-1.22	-1.82	0.60
hsa-miR-190	1.34	-12.52	1.75	-2.04	-5.86
hsa-miR-191	1.12	0.36	0.31	-0.38	-1.13
hsa-miR-192	1.26	-0.91	1.08	-0.81	-1.65
hsa-miR-193a	1.65	-1.73	13.43	0.28	-0.30
hsa-miR-193b	0.42	1.50	0.16	-0.65	-1.75
hsa-miR-195	1.28	0.35	-1.47	-0.52	-0.29
hsa-miR-196a	0.99	2.69	2.57	-0.14	-6.11
hsa-miR-196b	1.33	0.07	-3.19	0.53	1.34
hsa-miR-199a*	4.25	12.39	3.67	-0.43	-1.89
hsa-miR-19a	-2.63	-0.17	-0.71	-0.67	2.14
hsa-miR-19b	0.37	0.23	0.12	-0.76	-1.60
hsa-miR-200a	1.01	1.35	-1.69	0.84	0.57
hsa-miR-200a*	-0.77	2.82	-3.06	0.03	-3.23
hsa-miR-200c	1.02	1.05	-0.42	-0.07	-0.08
hsa-miR-203	0.74	0.56	7.27	-0.62	8.34
hsa-miR-205	-0.61	0.33	-11.42	-0.55	-4.48
hsa-miR-20a	0.36	0.91	-2.24	0.10	0.13
hsa-miR-20b	0.64	1.30	-3.51	-0.10	-4.32
hsa-miR-21	0.09	3.09	-4.58	-26.46	-0.97
hsa-miR-210	0.52	1.85	-0.56	0.06	-1.42
hsa-miR-214	3.25	1.97	0.32	-0.94	-1.79
hsa-miR-218	3.49	3.60	6.94	-2.39	6.88
hsa-miR-22	0.18	-1.85	0.06	0.77	-1.84
hsa-miR-221	-0.55	4.26	1.42	-1.42	0.53
hsa-miR-222	0.98	2.19	0.49	-1.86	-0.28
hsa-miR-223	0.17	2.06	-2.44	-6.94	8.42
hsa-miR-23b	0.60	-3.25	-0.97	-0.34	-2.86
hsa-miR-24	0.71	0.73	0.33	-0.78	-0.64
hsa-miR-25	-0.16	1.85	1.05	-0.65	0.31
hsa-miR-26a	0.52	0.35	-0.36	-0.45	2.89
hsa-miR-26b	1.03	0.49	-1.85	-0.54	-0.22
hsa-miR-27a	-0.10	0.68	0.45	-1.98	-1.87
hsa-miR-27b	0.93	-0.11	-2.75	-0.67	-1.35
hsa-miR-28	0.10	-0.83	1.12	-0.90	-0.25
hsa-miR-29a	0.46	0.43	-0.92	-2.88	-1.47
hsa-miR-29b	1.07	1.33	-0.26	-2.03	-1.80
hsa-miR-29c	0.45	0.17	-0.79	-1.24	-2.04
hsa-miR-301	-0.76	-1.09	-0.76	-0.35	-1.86
hsa-miR-30a-3	0.54	0.33	1.18	-1.16	-1.29
hsa-miR-30a-5	0.30	0.98	0.74	-0.97	-8.45

hsa-miR-30b	0.53	0.43	-0.96	-0.51	0.46
hsa-miR-30c	0.30	0.34	0.31	-1.00	-1.30
hsa-miR-30d	-0.34	0.70	-0.33	-0.81	-2.77
hsa-miR-30e-3	1.89	-0.30	-2.20	-0.15	-1.91
hsa-miR-30e-5	0.15	-0.92	1.70	-1.46	2.97
hsa-miR-32	-0.16	-0.64	0.71	-0.73	9.52
hsa-miR-320	0.50	2.40	-1.72	0.80	0.86
hsa-miR-324-3	0.16	-0.76	1.12	-0.64	-0.16
hsa-miR-324-5	0.00	3.45	0.27	-1.21	-1.81
hsa-miR-328	-0.05	-1.76	0.23	-3.10	-1.35
hsa-miR-33	-7.61	0.14	-1.27	-2.12	-4.48
hsa-miR-331	0.22	-0.22	1.35	-0.71	-1.36
hsa-miR-335	0.52	0.77	0.44	13.68	-1.80
hsa-miR-338	-0.61	0.33	-1.27	-6.94	-4.48
hsa-miR-339	-0.14	0.96	-0.55	-2.03	-0.98
hsa-miR-340	0.51	0.33	1.41	0.76	-1.47
hsa-miR-342	1.17	2.81	0.04	0.00	0.03
hsa-miR-345	0.75	-0.08	1.69	-0.72	-0.16
hsa-miR-34a	11.76	4.88	6.37	6.15	0.13
hsa-miR-361	0.84	-2.51	-2.69	-1.17	5.43
hsa-miR-362	2.59	0.77	-1.81	0.80	-0.85
hsa-miR-365	0.47	0.51	0.87	18.80	-1.52
hsa-miR-374	0.31	-0.04	-2.99	-1.11	2.97
hsa-miR-375	0.49	19.18	-0.04	0.63	9.22
hsa-miR-378	5.77	0.33	10.22	-1.23	0.49
hsa-miR-422a	7.66	11.67	0.33	-0.90	9.60
hsa-miR-422b	4.90	1.88	1.29	-0.56	0.40
hsa-miR-423	1.24	13.77	-0.87	-2.14	12.94
hsa-miR-425	-0.31	-0.24	4.28	0.82	5.69
hsa-miR-429	0.31	17.66	-0.86	-0.50	12.65
hsa-miR-433	-4.26	1.42	10.82	-2.26	1.34
hsa-miR-451	-0.61	0.33	-14.00	-6.50	-4.48
hsa-miR-452	-2.90	-0.48	-11.28	-6.94	-9.06
hsa-miR-486	-4.04	9.94	-0.88	-0.08	8.50
hsa-miR-500	1.26	0.33	-12.18	12.57	4.27
hsa-miR-501	0.20	0.33	-0.84	-0.59	12.52
hsa-miR-7	0.48	-0.01	1.90	0.15	1.18
hsa-miR-9	-0.61	-0.56	2.25	-0.37	-1.12
hsa-miR-9*	-0.90	0.94	11.93	-1.93	-1.92
hsa-miR-92	0.13	0.72	0.79	0.56	-0.26
hsa-miR-93	0.47	1.57	-0.45	0.65	1.65
hsa-miR-96	1.70	12.37	-2.34	-1.79	9.38
hsa-miR-98	0.56	0.33	-0.78	0.56	12.04
hsa-miR-99a	0.85	0.71	-1.09	-0.04	-17.51
hsa-miR-99b	0.70	0.26	0.06	-0.35	-1.41

red represents overexpression in marker positive populations

green represents underexpression in marker positive populations

Table S4. 57 miRNAs measured in marker-sorted populations in LAPC9, LAPC4, and Du145 cells (Listed are mean ddCt values by comparing marker-positive vs. marker-

	LAPC9 SP ddCt pos-neg	LAPC9 CD44 ddCt pos-neg	LAPC4 CD44 ddCt pos-neg	DU145 CD44 ddCt pos-neg	LAPC4 CD133 ddCt pos-neg	DU145 a2b1 ddCt pos-neg
hsa-let-7a	-0.132	1.15	0.76	1.79	-0.2824	-6.55
hsa-let-7b	-1.067	1.40	1.75	1.46	0.3123	1.75
hsa-let-7c	1.917	0.35	1.05	-0.37	-0.5581	-1.32
hsa-miR-103	10.258	0.00	0.00	0.00	0.0000	0.00
hsa-miR-10b	8.156	5.04	-6.47	8.91	-0.5592	7.12
hsa-miR-126	3.072	2.29	-0.27	1.62	2.2628	-2.19
hsa-miR-133a	0.253	-9.49	0.33	-1.27	-0.2741	4.39
hsa-miR-133b	-1.379	-1.01	1.93	-2.81	-1.8480	-1.47
hsa-miR-142-3p	-0.510	0.04	0.49	-3.90	-6.4863	-3.77
hsa-miR-142-5p	-0.405	9.65	-11.28	-10.79	-8.6407	-4.97
hsa-miR-146a	6.823	-0.23	1.22	-1.55	-6.3199	-0.08
hsa-miR-146b	6.153	1.65	1.45	-1.68	-3.0690	-1.95
hsa-miR-15a	10.643	2.78	12.94	-1.52	1.3330	9.95
hsa-miR-15b	12.112	0.35	-0.13	2.03	-0.5743	-2.28
hsa-miR-16	0.370	1.51	0.79	-2.54	-0.6147	-0.56
hsa-miR-181b	0.447	1.19	1.37	1.07	-0.4822	-2.00
hsa-miR-182	2.564	0.48	0.14	0.64	-0.1188	-0.31
hsa-miR-183	5.262	1.08	0.54	0.73	-0.5309	1.25
hsa-miR-18a	0.211	0.35	12.55	-0.14	-1.8224	-1.07
hsa-miR-191	1.136	1.12	0.36	0.31	-0.3847	-1.13
hsa-miR-195	2.977	1.28	0.35	-1.47	-0.5163	-0.29
hsa-miR-196a	-1.835	0.99	2.69	2.57	-0.1439	-6.11
hsa-miR-196b	-1.515	1.33	0.07	-3.19	0.5323	1.34
hsa-miR-200a	1.539	1.01	1.35	-1.69	0.8372	0.57
hsa-miR-200c	0.940	1.02	1.05	-0.42	-0.0681	-0.08
hsa-miR-203	0.874	0.74	0.56	7.27	-0.6154	8.34
hsa-miR-205	9.035	-0.61	0.33	-11.42	-0.5496	-4.48
hsa-miR-21	0.581	0.09	3.09	-4.58	-26.4581	-0.97
hsa-miR-218	1.087	3.49	3.60	6.94	-2.3908	6.88
hsa-miR-221	-0.728	-0.55	4.26	1.42	-1.4197	0.53
hsa-miR-222	-1.018	0.98	2.19	0.49	-1.8574	-0.28
hsa-miR-223	-1.375	0.17	2.06	-2.44	-6.9422	8.42
hsa-miR-24	0.000	0.71	0.73	0.33	-0.7757	-0.64
hsa-miR-27a	1.095	-0.10	0.68	0.45	-1.9827	-1.87
hsa-miR-27b	5.645	0.93	-0.11	-2.75	-0.6736	-1.35
hsa-miR-29a	-0.036	0.46	0.43	-0.92	-2.8784	-1.47

hsa-miR-29b	2.434	1.07	1.33	-0.26	-2.0327	-1.80
hsa-miR-29c	0.780	0.45	0.17	-0.79	-1.2433	-2.04
hsa-miR-30a-3p	1.018	1.89	-0.30	-2.20	-1.1645	-1.91
hsa-miR-30a-5p	2.218	0.15	-0.92	1.70	-0.9717	2.97
hsa-miR-320	-1.896	0.50	2.40	-1.72	0.8032	0.86
hsa-miR-328	9.581	-0.05	-1.76	0.23	-3.0956	-1.35
hsa-miR-33	-0.753	-7.61	0.14	-1.27	-2.1178	-4.48
hsa-miR-335	10.701	0.52	0.77	0.44	13.6781	-1.80
hsa-miR-34a	0.250	11.76	4.88	6.37	6.1466	0.13
hsa-miR-365	0.959	0.47	0.51	0.87	18.7994	-1.52
hsa-miR-375	1.338	0.49	19.18	-0.04	0.6335	9.22
hsa-miR-378	-1.941	5.77	0.33	10.22	-1.2293	0.49
hsa-miR-422a	3.121	7.66	11.67	0.33	-0.9040	9.60
hsa-miR-422b	0.312	4.90	1.88	1.29	-0.5609	0.40
hsa-miR-423	0.042	1.24	13.77	-0.87	-2.1380	12.94
hsa-miR-425	-1.485	-0.31	-0.24	4.28	0.8198	5.69
hsa-miR-429	0.608	0.31	17.66	-0.86	-0.4966	12.65
hsa-miR-451	-7.575	-0.61	0.33	-14.00	-6.4959	-4.48
hsa-miR-452	-3.483	-2.90	-0.48	-11.28	-6.9450	-9.06
hsa-miR-500	-5.137	1.26	0.33	-12.18	12.5725	4.27
hsa-miR-9*	1.216	-0.90	0.94	11.93	-1.9282	-1.92

red represents overexpression in marker positive populations

green represents underexpression in marker positive populations

Published OnlineFirst September 13, 2011; DOI:10.1158/0008-5472.CAN-11-1035

Cancer Research

MicroRNA Regulation of Cancer Stem Cells

Can Liu and Dean G. Tang

Cancer Res 2011;71:5950-5954. Published OnlineFirst September 13, 2011.

Published OnlineFirst September 13, 2011; DOI:10.1158/0008-5472.CAN-11-1035

Review

Cancer Research

MicroRNA Regulation of Cancer Stem Cells

Can Liu[1,2] and Dean G. Tang[1,2,3]

Abstract

Cancer stem cells (CSC), or cancer cells with stem cell properties, have been reported in many human tumors and are thought to be responsible for tumor initiation, therapy resistance, progression, relapse, and metastasis. Despite their potential clinical importance, how CSCs are regulated at the molecular level is not well understood. MicroRNAs (miRNA), small noncoding RNAs that play critical roles in normal stem cell functions during development, have emerged as important regulators of CSCs as well. In this review, we summarize the current major findings of miRNA regulation of various CSCs and discuss our recent findings that miR-34a suppresses prostate CSCs and metastasis by directly repressing CD44. This recent progress has important implications for understanding how CSCs are intricately regulated by networks of miRNAs and for developing novel mechanism-based miRNA therapeutics that specifically target CSCs. *Cancer Res; 71(18); 5950–4. ©2011 AACR.*

Introduction

Research in the past decade suggests the presence of cancer stem cells (CSC) that can both regenerate themselves and differentiate into a spectrum of maturing daughter cells, which create the cellular heterogeneity of cancer. CSCs were first discovered in acute myeloid leukemia and, since 2003, have also been reported in most solid tumors (1). Emerging evidence indicates that CSCs may be involved in tumor maintenance, therapy resistance, tumor progression, and distant metastasis. Despite their potential clinical significance, how intrinsic CSC properties are regulated at the molecular level is poorly understood. Recent discoveries of microRNAs (miRNA) have provided a new avenue in understanding the regulatory mechanisms in CSCs.

miRNAs are 21- to 25-nucleotide (nt)–long, noncoding RNAs that induce the target mRNA degradation or repress mRNA translation by imperfect binding to their 3′-untranslated region (2). The miRNA gene is first transcribed by RNA polymerase II into primary transcript (pri-miRNA) in the nucleus, where the hairpin stem-loop structure is processed into precursor miRNA (pre-miRNA) by a microprocessing complex, including Drosha and DGCR8. The ∼70-nt-long pre-miRNA is then exported into cytoplasm, where it undergoes a second processing by Dicer, in which one strand of the hairpin is incorporated into the ribonucleoprotein complex called miRNA-induced silencing complex (2). A single miRNA may target dozens of mRNAs, and one mRNA can be regulated by multiple miRNAs. Although small, miRNAs play a powerful role in biological processes including development, proliferation, and apoptosis. Early studies have linked miRNAs to controlling the self-renewal and differentiation of embryonic stem cells (ESC), and later, aberrant expression and/or functions of miRNAs are implicated in tumorigenesis (3). More recent studies suggest that miRNAs may also regulate CSC properties.

miRNA Regulation of Development and Embryonic Stem Cells

The first 2 miRNAs, *lin-4* and *let-7*, were both discovered during *Caenorhabditis elegans* development. Since then, miRNAs have emerged as important regulators of embryonic development and stem cell functions in mammals. The overall roles of miRNAs in both mouse and human ESCs have been evaluated by analyzing the phenotypes of *Dicer* and *DGCR8* mutants. Deletion of *Dicer* in mouse causes embryonic lethality (4), and *Dicer*-deficient mouse ESCs exhibit defects in differentiation and G_1 cell-cycle arrest (5). Similarly, *DGCR8*-deficient mouse ESCs show problems in cell-cycle progression and differentiation, evidenced by failing to silence self-renewal genes, such as *OCT4*, *REX1*, *NANOG*, and *SOX2*, as well as delayed expression of differentiation markers (6). Other studies have also revealed specific expression and functions of individual miRNAs in ESCs (7).

A regulatory circuitry between miRNAs and "pluripotency" genes required for maintaining ESC stemness has been identified. On one hand, the master regulators of stem cell pluripotency, including OCT-4, NANOG, SOX2, and TCF3, all

Authors' Affiliations: [1]Department of Molecular Carcinogenesis, University of Texas MD Anderson Cancer Center, Smithville; [2]Program in Molecular Carcinogenesis, University of Texas Graduate School of Biomedical Sciences (GSBS); [3]Centers for Cancer Epigenetics, Stem Cell and Developmental Biology, RNA Interference and Non-Coding RNAs, and Molecular Carcinogenesis, University of Texas MD Anderson Cancer Center, Houston, Texas

Corresponding Author: Dean G. Tang, Department of Molecular Carcinogenesis, the University of Texas MD Anderson Cancer Center, 1808 Park Rd. 1C, Smithville, TX 78957. Phone: 512-237-9575; Fax: 512-237-2475; E-mail: dtang@mdanderson.org

doi: 10.1158/0008-5472.CAN-11-1035

Published OnlineFirst September 13, 2011; DOI:10.1158/0008-5472.CAN-11-1035

directly regulate ESC-specific miRNAs by binding to their promoter regions (8). On the other hand, some of these pluripotency genes are also regulated by miRNAs at the posttranscriptional level. Thus, miR-134, miR-296, and miR-470 suppress the expression of NANOG, OCT4, and SOX2 by binding to their coding regions (9). Lin-28, a marker of undifferentiated ESCs that is used to generate induced pluripotent stem cells, also forms a negative feedback loop with the let-7 family miRNAs to precisely control each other's levels. Lin-28 regulates the expression of let-7 by binding to the precursors and blocking their maturation, whereas in differentiated cells where let-7 levels are increased, let-7 miRNAs, in turn, target the Lin-28 mRNA (10).

miRNA Regulation of Cancer and Cancer Stem Cells

Interestingly, the miRNA expression patterns in tumor cells often bear resemblance to those in ESCs. Let-7, for instance, is excluded in ESCs and often lost in cancers, including breast, lung, and ovarian cancers. Such cancer-specific miRNA expression signature(s) may become very informative for diagnostic and prognostic purposes. Functional studies of the dysregulated miRNAs indicate that they regulate molecular pathways in cancer via targeting different oncogenes and/or tumor suppressors. More recent evidence suggests that miRNAs may also be involved in tumor development by critically regulating CSCs. Here, we discuss the major findings of some recent studies highlighting the roles of certain "CSC-specific" miRNAs in several representative cancer types. From these discussions, we present an emerging theme that several miRNAs may distinctively and concertedly (coordinately) regulate the key biological properties of CSCs.

Differential expression of miRNAs in cancer stem cells

Yu and colleagues were the first to examine the miRNA expression in breast CSCs (BCSC; ref. 11). The authors enriched BCSCs by consecutively passaging breast cancer cell SKBR3 in mice treated with chemotherapy. The tumors were shown to contain a high percentage of $CD44^+CD24^{-/lo}$ cells and high ability to form mammospheres *in vitro* and tumors *in vivo*. Importantly, the BCSC-enriched cells expressed much lower levels of let-7 as well as a number of other miRNAs, including miR-16, miR-107, miR-128, and miR-20b, than the parental cells and the *in vitro* differentiated progeny (11). Later, Shimono and colleagues identified 37 miRNAs to be differentially expressed in $CD44^+CD24^{-/lo}$ BCSCs, in which 3 clusters, miR-200c-141, miR-200b-200a-429, and miR-183-96-182, were significantly downregulated (12). Notably, these miRNAs were markedly reduced in normal mammary stem and/or progenitor cells as well. In glioblastoma multiforme (GBM), some miRNAs, including miR-451, miR-486, miR-425, miR-16, miR-107, and miR-185, were decreased in the $CD133^+$ population (13). In hepatocellular carcinoma (HCC), $EpCAM^+AFP^+$ CSCs expressed a unique miRNA signature with upregulation of miR-181 family members and several miR-17-92 cluster members (14). Through unbiased miRNA expression profiling, our group recently showed that prostate cancer stem and/or progenitor cell populations enriched with surface markers CD44, CD133, or $\alpha2\beta1$ prominently and commonly underexpress miR-34a and let-7b (15).

Breast cancer stem cells

BCSCs were the first CSCs to be reported and are among the best characterized of all CSCs in solid tumors. BCSCs are most commonly enriched using the $CD44^+CD24^{-/lo}$ marker profile (12) or Aldefluor assays (16). Because of the early discovery and better understanding of BCSCs, miRNA studies in these cells are also more advanced than in other CSCs. On the basis of profiling results that let-7 was significantly reduced in BCSCs (11), Yu and colleagues further unraveled that let-7 regulated the stem cell properties, that is, self-renewal and differentiation. Lentiviral-mediated overexpression of let-7a inhibited cell proliferation, mammosphere formation, tumor formation, and metastasis in nonobese diabetic (NOD)/severe combined immunodeficient mice (SCID) mice and reduced the proportion of undifferentiated cells *in vitro*. In contrast, antagonizing let-7 by antisense oligonucleotides enhanced *in vitro* propagation of non-CSCs. H-RAS and HMGA2 were identified as the direct downstream targets that partially mediated the let-7 effects (11).

Interestingly, a recent study from the same group suggested that miRNAs besides let-7 might also play a role in regulating BCSCs because overexpression of let-7 alone was not sufficient to completely block the tumor formation and progression (17). Subsequently, miR-30 was found to be one of the miRNAs markedly reduced in BCSCs and to negatively modulate the stemness of BCSCs. Overexpression of miR-30 in BCSCs not only diminished their self-renewal ability but also reduced anoikis resistance and increased apoptosis by directly targeting ubiquitin-conjugating enzyme 9 (UBC9) and integrin $\beta3$ (ITGB3). Conversely, knocking down endogenous miR-30 with antagomirs enhanced self-renewal, tumor regeneration, and metastasis in differentiated breast cancer cells. Impressively, a more complete inhibition of self-renewal and mammospheres in BCSCs was observed when both let-7 and miR-30 were introduced at the same time, compared with transfecting either miRNA alone (17). The synergistic BCSC-inhibitory effects of let-7 and miR-30 on BCSC self-renewal suggest that multiple miRNAs may distinctively and concertedly regulate CSC properties (Fig. 1A).

miRNA expression profiling in purified $CD44^+CD24^{-/lo}$ BCSCs identified 37 miRNAs to be differentially expressed in these cells with miR-200 family significantly downregulated in both BCSCs and normal mammary stem and/or progenitor cells (12). Functional studies showed that overexpression of miR-200c reduced the clonogenic and tumor-initiation activities in BCSCs and suppressed formation of mammary ducts by normal mammary stem cells. The stem cell factor BMI-1 was directly modulated by miR-200c. This work (12), thus, provides a molecular link between normal breast stem cells and BCSCs.

Recently, aldehyde dehydrogenase (ALDH) has emerged as a functional marker for both normal and malignant stem and/or progenitor cell populations in various tissues,

Published OnlineFirst September 13, 2011; DOI:10.1158/0008-5472.CAN-11-1035

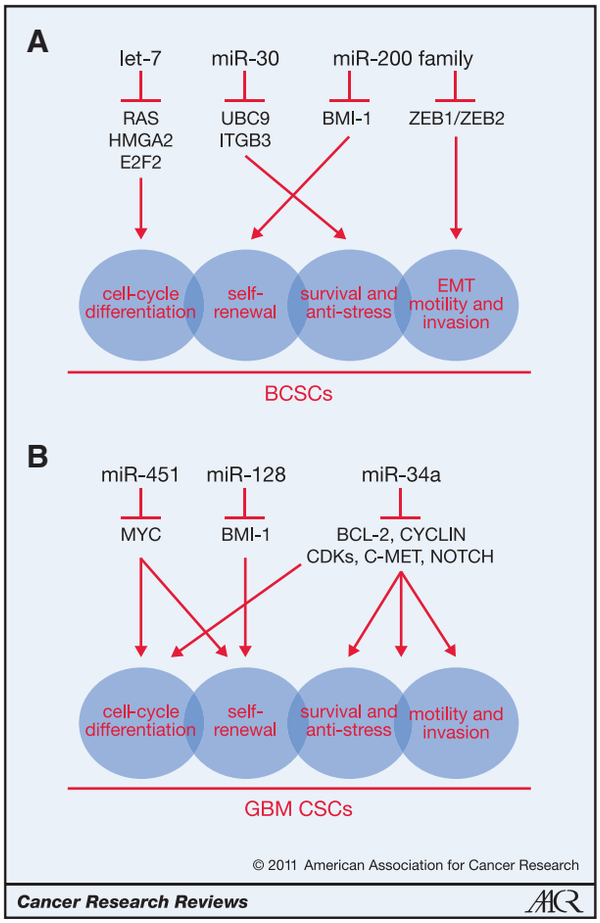

Figure 1. miRNAs distinctively and concertedly regulate key properties of CSCs. A, let-7, miR-30, and miR-200 family miRNAs, via targeting critical downstream signaling molecules, regulate several fundamental properties of BCSCs, including cell-cycle exit and differentiation, self-renewal, EMT, migration and invasion, and cell survival (represented by 4 shaded circles that overlap with each other). B, miR-451, miR-128, and miR-34a distinctively and concertedly regulate the key biological properties of CSCs in GBM. A and B, representative miRNAs that are underexpressed in tumorigenic subpopulations.

including human (16) and mouse (18) mammary gland. In human mammary epithelial cells, for example, $ALDH^+$ cells were shown to possess high-proliferative and broad-lineage differentiation potential and were able to regenerate mammary ductal structures *in vivo*. Likewise, breast cancer cells with high ALDH activity were capable of self-renewal and generating tumors in mouse models (16). miRNA expression profiling revealed that miR-205 and miR-22 were most abundant, whereas let-7 family members and miR-93 were depleted in $ALDH^+$, $Sca\text{-}1^+$ mouse mammary epithelial cells (18). Interestingly, although miR-205 was most abundant in $ALDH^+$ normal mouse mammary progenitor cells, its expression in breast cancer cells remains heterogeneous, varying in different subtypes of breast cancer and at different stages of tumor progression. One group reported high levels of miR-205 in $ER^+PR^+Her2^+$ breast cancers, whereas others reported both high miR-205 expression in triple-negative tumors and low miR-205 levels in metastatic breast cancer cell lines and clinical samples (19).

CSCs are morphologically and phenotypically plastic and possess high migratory and invasive capacities. Several groups have observed that miR-205 and miR-200 family members regulate epithelial–mesenchymal transition (EMT), a process thought to be critical in the metastatic cascade. For example, miR-200 miRNAs and miR-205 are significantly downregulated in cancer cells undergoing EMT and in metastatic breast cancer specimens (20, 21). Overexpression of miR-200 miRNAs prevents TGFβ-induced EMT by negatively regulating the expression of EMT activator ZEB1 (also known as TCF8) and ZEB2 (also known as ZFXH1B and SMAD interacting protein 1 or SIP1). Interestingly, ZEB1 and ZEB2 can also transcriptionally repress the expression of miR-200 miRNAs by binding to their promoter regions, leading to strong activation of EMT. These findings (20, 21) establish a double-negative feedback loop between ZEB1/ZEB2 and miR-200 family miRNAs that, together, regulate an important biological process in tumor development and cancer metastasis.

The studies on miRNAs and BCSCs suggest an emerging theme that may also be applicable to understanding how miRNAs regulate other CSCs. BCSCs possess several fundamental biological properties, including self-renewal, quiescence associated with slow cell-cycle kinetics or differentiation associated with cell-cycle exit, prosurvival and antistress mechanisms (e.g., resistance to anoikis), and high capacities to undergo EMT and to invade, all of which likely contribute to their resistance to anticancer therapies and enhanced tumor-initiating and metastatic potential (Fig. 1A). Distinct miRNAs, via their respective downstream targets, distinctively and concertedly regulate these critical CSC properties. Thus, let-7 mainly restricts cell-cycle progression by targeting RAS, HMGA2, and E2F2; miR-30 may preferentially be involved in modulating the survival and stress responses; miR-200 miRNAs negatively regulate the self-renewal by targeting molecules such as BMI-1; and miR-200 (and miR-205) may regulate EMT, migration, and invasiveness in BCSCs (Fig. 1A).

Glioblastoma multiforme and other brain cancer stem cells

Specific miRNA dysregulation in GBM and other brain CSCs has recently been reported in several studies. By comparing miRNA expression in $CD133^+$ versus $CD133^-$ GBM cells, one group reported underexpression of tumor-suppressor miR-451 in the $CD133^+$ population (13). miR-451 is well known to repress Myc expression. Another miRNA expression profiling in human GBM specimens revealed a significant reduction of miR-128 compared with adjacent normal brain tissue (22). Subsequently, miR-128 was shown to inhibit glioma stem cell proliferation *in vitro* and glioma xenograft growth *in vivo*. Overexpression of miR-128 significantly blocked glioma CSC self-renewal by directly targeting BMI-1 (22). Finally, miR-34a was found to be downregulated in human glioblastomas (23). Transfection of miR-34a into bulk GBM cells or GBM CSCs caused cell-cycle arrest or apoptosis and also inhibited xenograft growth, mediated by downregulation of multiple

Published OnlineFirst September 13, 2011; DOI:10.1158/0008-5472.CAN-11-1035

oncogenic targets, including c-MET, Notch-1/2, and CDK6 (23). These studies in GBM (13, 22, 23) support the concept that several major miRNAs may distinctively and concertedly act together to restrict the key GBM CSC properties (Fig. 1B).

miR-199-5p was downregulated in medulloblastoma, and overexpression of miR-199-5p inhibited proliferation and anchorage-independent growth of medulloblastoma cells by targeting HES-1 (24), a transcription factor of the Notch signaling pathway. Significantly, overexpression of miR-199-5p decreased the $CD133^+$ subpopulation of cells and inhibited tumor development of medulloblastoma cells.

Prostate cancer stem cells

Our group was the first to profile miRNA expression in prostate cancer stem and/or progenitor cells (15). Prostate CSCs (PCSC) with high tumor-initiating and metastatic potential are enriched in the side population (25), $CD44^+$ (26), and $CD44^+\alpha2\beta1^+$ (27) subpopulations. Prostate cancer cells with $CD133^+CD44^+\alpha2\beta1^+$ phenotype also show enhanced clonogenic potential *in vitro* (28). Through an unbiased miRNA expression profiling in 5 PCSC and/or progenitor cell populations purified from prostate cancer xenografts, including 3 $CD44^+$ populations from the LAPC9, LAPC4, and Du145 tumors, $CD133^+$ cells from LAPC4 tumors, and $\alpha2\beta1^+$ cells from Du145 tumors, we identified miR-34a, together with let-7b, to be commonly underexpressed in all marker-positive cell populations (15). The underexpression of miR-34a was subsequently corroborated in $CD44^+$ prostate cancer cells purified from ~20 patient prostate tumors. Overexpression of miR-34a in bulk prostate cancer cells or purified $CD44^+$ cells by transfecting with mature oligonucleotide mimics or infecting with lentiviral vectors encoding pre–miR-34a exerted pronounced inhibitory effects on tumor growth and metastasis *in vivo*. In contrast, neutralizing endogenous miR-34a using antagomirs in bulk or $CD44^-$ prostate cancer cells promoted tumor regeneration and metastasis. Strikingly, delivery of miR-34a oligos systemically through tail vein inhibited metastasis to the lung and other organs and prolonged the survival of animals bearing orthotopic human prostate cancer, indicating the therapeutic potential of this miRNA. Mechanistically, miR-34a suppressed PCSC properties as it inhibited prostasphere establishment, migration and invasiveness of $CD44^+$ prostate cancer cells, and serial prostasphere passaging and serial tumor transplantation. Of significance, we showed that CD44 itself represented a direct and relevant downstream target of miR-34a. Hence, the CD44 protein levels decreased in cells overexpressing miR-34a, and knocking down of CD44 functionally phenocopied the miR-34a effects in inhibiting tumor development and metastasis. Our findings (15) shed new light on the mechanisms of miRNA regulation of PCSCs.

Other cancer stem cells

Interestingly, miR-34, a transcriptional target of p53, not only inhibits the GBM CSCs (23) and PCSCs (15) but also restrains the biological properties of pancreatic and gastric CSCs (29, 30). Restoration of miR-34 expression in these latter CSCs inhibits sphere formation *in vitro* and tumor regeneration *in vivo* (29, 30). HCC CSCs identified by $EpCAM^+AFP^+$ marker profile overexpressed the miR-181 family and several miR-17-92 cluster members (14). Inhibition of miR-181 led to a reduction in the number of $EpCAM^+$ HCC cells and in tumor-initiating ability, whereas overexpression of miR-181 increased the $EpCAM^+$ cells. The biological effects of miR-181 might be mediated via targeting caudal type homeobox transcription factor 2 (CDX2), GATA6, and nemo-like kinase (NLK), a Wnt/β-catenin pathway inhibitor (14).

Therapeutic Implications and Perspectives

Dysregulation of miRNAs has been intimately implicated in tumor development, and miRNAs may regulate tumorigenesis via modulating CSC properties. Thus, let-7 miRNAs control the cell-cycle and differentiation properties of BCSCs, miR-200c modulates the self-renewal of BCSCs by targeting Bmi-1, and miR-34a restricts the migratory and invasive properties of PCSCs by directly repressing CD44. The new findings discussed above better our understanding of CSC regulation and provide novel insight on developing new strategies to target therapy-resistant cancer cells. Given that CSCs seem to be involved in multiple steps of tumorigenesis, including tumor initiation, tumor maintenance, metastasis, and therapy resistance, and that miRNAs exert a broad regulatory role on tumor development, miRNA-based therapeutics that specifically target CSCs may add novel firepower to the anticancer arsenal, as exemplified by our recent demonstrations of the impressive therapeutic efficacies of systemically delivered miR-34a on preestablished human prostate cancers. As distinct miRNAs seem to distinctively and concertedly regulate key and interconnected biological properties of CSCs (Fig. 1), complete eradication of CSCs and residual tumors may entail manipulations or targeting of multiple miRNAs. In addition to developing miRNAs as anti-CSC therapeutics, miRNA expression profiling in CSCs or specific subtypes of cancer and at various clinical stages may have diagnostic and prognostic values.

Disclosure of Potential Conflict of Interest

No potential conflicts of interest were disclosed.

Acknowledgments

The authors apologize to colleagues whose original work could not be cited due to space constraint.

Grant Support

Work in the authors' laboratory was supported in part by grants from the NIH (R01-ES015888, R21-ES015893, and R21-CA150009), U.S. Department of Defense (W81XWH-08-1-0472), Elsa Pardee Foundation (D.G. Tang), and MD Anderson Cancer Center grants (CCSG-5 P30 CA016672-34 and ES007784). C. Liu was supported in part by a predoctoral fellowship from the U.S. Department of Defense.

Received March 25, 2011; revised May 23, 2011; accepted May 25, 2011; published OnlineFirst September 13, 2011.

Published OnlineFirst September 13, 2011; DOI:10.1158/0008-5472.CAN-11-1035

References

1. Visvader JE, Lindeman GJ. Cancer stem cells in solid tumours: accumulating evidence and unresolved questions. Nat Rev Cancer 2008;8:755–68.
2. Bartel DP. MicroRNAs: genomics, biogenesis, mechanism, and function. Cell 2004;116:281–97.
3. Calin GA, Croce CM. MicroRNA signatures in human cancers. Nat Rev Cancer 2006;6:857–66.
4. Bernstein E, Kim SY, Carmell MA, Murchison EP, Alcorn H, Li MZ, et al. Dicer is essential for mouse development. Nat Genet 2003;35:215–7.
5. Kanellopoulou C, Muljo SA, Kung AL, Ganesan S, Drapkin R, Jenuwein T, et al. Dicer-deficient mouse embryonic stem cells are defective in differentiation and centromeric silencing. Genes Dev 2005;19:489–501.
6. Wang Y, Medvid R, Melton C, Jaenisch R, Blelloch R. DGCR8 is essential for microRNA biogenesis and silencing of embryonic stem cell self-renewal. Nat Genet 2007;39:380–5.
7. Calabrese JM, Seila AC, Yeo GW, Sharp PA. RNA sequence analysis defines Dicer's role in mouse embryonic stem cells. Proc Natl Acad Sci U S A 2007;104:18097–102.
8. Marson A, Levine SS, Cole MF, Frampton GM, Brambrink T, Johnstone S, et al. Connecting microRNA genes to the core transcriptional regulatory circuitry of embryonic stem cells. Cell 2008;134:521–33.
9. Tay Y, Zhang J, Thomson AM, Lim B, Rigoutsos I. MicroRNAs to Nanog, Oct4 and Sox2 coding regions modulate embryonic stem cell differentiation. Nature 2008;455:1124–8.
10. Peter ME. Let-7 and miR-200 microRNAs: guardians against pluripotency and cancer progression. Cell Cycle 2009;8:843–52.
11. Yu F, Yao H, Zhu P, Zhang X, Pan Q, Gong C, et al. let-7 regulates self renewal and tumorigenicity of breast cancer cells. Cell 2007;131:1109–23.
12. Shimono Y, Zabala M, Cho RW, Lobo N, Dalerba P, Qian D, et al. Downregulation of miRNA-200c links breast cancer stem cells with normal stem cells. Cell 2009;138:592–603.
13. Gal H, Pandi G, Kanner AA, Ram Z, Lithwick-Yanai G, Amariglio N, et al. MIR-451 and Imatinib mesylate inhibit tumor growth of Glioblastoma stem cells. Biochem Biophys Res Commun 2008;376:86–90.
14. Ji J, Yamashita T, Budhu A, Forgues M, Jia HL, Li C, et al. Identification of microRNA-181 by genome-wide screening as a critical player in EpCAM-positive hepatic cancer stem cells. Hepatology 2009;50:472–80.
15. Liu C, Kelnar K, Liu B, Chen X, Calhoun-Davis T, Li H, et al. The microRNA miR-34a inhibits prostate cancer stem cells and metastasis by directly repressing CD44. Nat Med 2011;17:211–5.
16. Ginestier C, Hur MH, Charafe-Jauffret E, Monville F, Dutcher J, Brown M, et al. ALDH1 is a marker of normal and malignant human mammary stem cells and a predictor of poor clinical outcome. Cell Stem Cell 2007;1:555–67.
17. Yu F, Deng H, Yao H, Liu Q, Su F, Song E. Mir-30 reduction maintains self-renewal and inhibits apoptosis in breast tumor-initiating cells. Oncogene 2010;29:4194–204.
18. Ibarra I, Erlich Y, Muthuswamy SK, Sachidanandam R, Hannon GJ. A role for microRNAs in maintenance of mouse mammary epithelial progenitor cells. Genes Dev 2007;21:3238–43.
19. Greene SB, Herschkowitz JI, Rosen JM. The ups and downs of miR-205: identifying the roles of miR-205 in mammary gland development and breast cancer. RNA Biol 2010;7:300–4.
20. Gregory PA, Bert AG, Paterson EL, Barry SC, Tsykin A, Farshid G, et al. The miR-200 family and miR-205 regulate epithelial to mesenchymal transition by targeting ZEB1 and SIP1. Nat Cell Biol 2008;10:593–601.
21. Park SM, Gaur AB, Lengyel E, Peter ME. The miR-200 family determines the epithelial phenotype of cancer cells by targeting the E-cadherin repressors ZEB1 and ZEB2. Genes Dev 2008;22:894–907.
22. Godlewski J, Nowicki MO, Bronisz A, Williams S, Otsuki A, Nuovo G, et al. Targeting of the Bmi-1 oncogene/stem cell renewal factor by microRNA-128 inhibits glioma proliferation and self-renewal. Cancer Res 2008;68:9125–30.
23. Li Y, Guessous F, Zhang Y, Dipierro C, Kefas B, Johnson E, et al. MicroRNA-34a inhibits glioblastoma growth by targeting multiple oncogenes. Cancer Res 2009;69:7569–76.
24. Garzia L, Andolfo I, Cusanelli E, Marino N, Petrosino G, De Martino D, et al. MicroRNA-199b-5p impairs cancer stem cells through negative regulation of HES1 in medulloblastoma. PLoS ONE 2009;4:e4998.
25. Patrawala L, Calhoun T, Schneider-Broussard R, Zhou J, Claypool K, Tang DG. Side population is enriched in tumorigenic, stem-like cancer cells, whereas ABCG2$^+$ and ABCG2$^-$ cancer cells are similarly tumorigenic. Cancer Res 2005;65:6207–19.
26. Patrawala L, Calhoun T, Schneider-Broussard R, Li H, Bhatia B, Tang S, et al. Highly purified CD44$^+$ prostate cancer cells from xenograft human tumors are enriched in tumorigenic and metastatic progenitor cells. Oncogene 2006;25:1696–708.
27. Patrawala L, Calhoun-Davis T, Schneider-Broussard R, Tang DG. Hierarchical organization of prostate cancer cells in xenograft tumors: the CD44$^+\alpha2\beta1^+$ cell population is enriched in tumor-initiating cells. Cancer Res 2007;67:6796–805.
28. Collins AT, Berry PA, Hyde C, Stower MJ, Maitland NJ. Prospective identification of tumorigenic prostate cancer stem cells. Cancer Res 2005;65:10946–51.
29. Ji Q, Hao X, Meng Y, Zhang M, Desano J, Fan D, et al. Restoration of tumor suppressor miR-34 inhibits human p53-mutant gastric cancer tumorspheres. BMC Cancer 2008;8:266.
30. Ji Q, Hao X, Zhang M, Tang W, Yang M, Li L, et al. MicroRNA miR-34 inhibits human pancreatic cancer tumor-initiating cells. PLoS ONE 2009;4:e6816.